MRI in rectal cancer : prediction of the risk factors for a local recurrence

MRI in rectal cancer

Prediction of the risk factors for a local recurrence

ISBN 9789071382949

DESIGN AND LAY-OUT

Max Jef Lahaye

PRINTING AGENCY

Gildeprint B.V.

MRI in rectal cancer

Prediction of the risk factors for a local recurrence

Proefschrift

ter verkrijging van de graad van doctor aan de Universiteit Maastricht,
op gezag van de Rector Magnificus, Prof. mr. G.P.M.F. Mols,
volgens het besluit van het College van Decanen
in het openbaar te verdedigen op vrijdag 27 maart 2009 om 12:00 uur

door

Max Jef Lahaye
geboren op 12 april 1979, te Ede

PROMOTORES

Prof. dr. R.G.H. Beets-Tan
Prof. dr. J.M.A. van Engelshoven

CO-PROMOTOR

Dr. G.L. Beets

BEOORDELINGSCOMMISSIE

Prof. dr. J.T. Wilmink (voorzitter)
Prof. dr. C.G.M.I. Baeten
Prof. dr. J.O. Barentz (Universitair Medisch Centrum St. Radboud)
Prof. dr. M.J.H.M. Jacobs
Dr. G. Lammering

Financial support by the Dutch Cancer Society for the publication of this thesis is gratefully acknowledged.

Additional financial support was generously provided by: Guerbet Nederland, Boema Smeets-Limpens, Bayer Schering Pharma, Amgen BV (manufacturer of Vectibix), Roche Nederland BV and Raadsheeren BV.

CONTENTS

GENERAL INTRODUCTION

1

General introduction

Colorectal cancer is one of the leading causes of cancer-related deaths in the Western world [1-3]. In one third of the colorectal cancer patients the tumor is located in the rectum. Additional to the risk for distant metastases, rectal cancer carries a marked risk for local recurrence (3-32%) [4]. Although local recurrences have only a small impact on the survival, they have a profound impact on the quality of life. A local recurrence is often debilitating causing severe pain, a continuous urge, immobility and prolonged and multiple hospital visits for surgery, radiation- and chemotherapy.

Several treatment strategies have been developed to obtain a better local control: optimal surgical techniques and neoadjuvant (chemo)radiotherapy. Heald's total mesorectal excision (TME) produces the best local control by removing en bloc the rectum and surrounding mesorectal fat by sharp dissection along the mesorectal fascia [5]. Histology of these resection specimens has shown that the local recurrence rate greatly decreases when a tumor-free circumferential resection margin (CRM) of more than 1 mm can be obtained. In addition, to TME surgery, the Dutch TME trial showed that preoperative 5 x 5 Gy radiotherapy significantly reduced local recurrence compared to TME alone [6]. Especially in N+ patients preoperative radiotherapy significantly reduced the local recurrence rate from 21.5 to 11.2% at 5 years. However, in patients with Stage I disease (T1/T2N0) preoperative radiotherapy had a negligible effect on the local recurrence rate (surgery only: 1.7% versus radiation plus surgery: 0.4%), so preoperative radiotherapy could be omitted in this group. On the other hand, for more locally advanced tumors with a close or involved CRM this short-term radiotherapy is not adequate enough to reduce the local recurrence rate. Fortunately, other studies demonstrated improved results in patients with an involved mesorectal fascia using neoadjuvant chemoradiation [7, 8]. Chemoradiation downsizes the tumor and sometimes-even downstages locally advanced tumors and their nodes. However, the best studies available suggest that preoperative radiation- and chemotherapy is associated with significant functional morbidity.

This wide variety of available therapeutic options entail that clinicians would like to tailor the treatment to the individual patient, varying from minimal invasive surgery to extensive surgery combined with neoadjuvant chemoradiation. This optimal

treatment combines the best possible local control with as low as possible treatment related morbidity. Preoperative accurate identification of Stage I (T1-2N0) disease for instance could help to select patients who do not require preoperative short course radiotherapy, while patients with a close or involved CRM would benefit from a long course of chemoradiation. This implies that the radiologists must able to accurately identify CRM+, tumors limited to the bowel wall and N0 patients in order to select patients who could benefit from neoadjuvant chemo and/or radiotherapy. In addition, new emerging therapeutic techniques such as a transanal endoscopic microsurgery (TEM) for early tumors (T1N0) or downstaged tumors after chemoradiation emphasize the need for an accurate N0 prediction, also after chemoradiation.

At present several studies have demonstrated good results for MR prediction of the CRM, and this was again confirmed in the European multicenter study (MERCURY) [9]. Thus MRI has in many centers become part of the standard diagnostic work up for selecting high-risk patients. Until now, the available evidence on MR prediction of CRM has not been summarized in a review.

Accurate prediction of nodal disease, however, remains more problematic for the radiologist. In rectal cancer many involved nodes are small and as a consequence non-invasive conventional imaging methods using size criteria are not reliable. Radiologists are therefore continuously trying to improve the accuracy in predicting nodal disease with modern imaging techniques. A recent meta-analysis has shown that a new lymph node specific MR agent, ultrasmall superparamagnetic iron oxide (USPIO), is promising in differentiating benign from malignant nodes in cancer patients. No studies so far were conducted with rectal cancer patients.

The objectives of this thesis are:

Objective 1

To evaluate USPIO enhanced MRI in rectal cancer patients for prediction of the nodal status, both in a university setting and a general radiological practice setting.

Objective 2

To identify the most important predictive criteria on USPIO enhanced MRI for distinction between benign and malignant lymph nodes in rectal cancer patients both in the primary staging and in the restaging after chemoradiation.

Outline of this thesis

Chapter two describes the relevant MR anatomy of the rectum and mesorectum for radiologists, surgeons and radiation oncologists involved in the multidisciplinary approach of rectal cancer.
Chapter three gives an overview of the present status of modern imaging techniques for identifying nodal disease in high-risk patients focusing on colorectal cancer by non-invasive imaging techniques.
Chapter four is a meta-analysis of English literature on the accuracy of preoperative imaging in predicting the two most important risk factors for local recurrence in rectal cancer, the circumferential resection margin and the nodal status using endoluminal ultrasound (EUS), computed tomography (CT) or magnetic resonance imaging (MRI).
Chapter five evaluates the diagnostic performance of MRI (with USPIO) for CRM, T-stage and the nodal status for early and non locally advanced rectal cancer in general setting and compare it with that in a university setting with histology or MR follow-up as the reference standard.
Chapter six and seven describe the most important predictive criteria on USPIO enhanced MRI for distinction between benign and malignant lymph nodes both in primary (chapter six) and post chemoradiation restaging (chapter seven) of rectal cancer patients.
In chapter eight our studies are discussed within the present knowledge concerning diagnosis and treatment in rectal cancer. The clinical relevance of our findings and recommendations for clinical practice are given as well as future directions in rectal cancer imaging.

References

1. *Jemal A, Tiwari RC, Murray T, et al. Cancer statistics, 2004. CA Cancer J Clin 2004; 54:8-29.*
2. *Boyle P, Ferlay J. Cancer incidence and mortality in Europe, 2004. Ann Oncol 2005; 16:481-488.*
3. *Parkin DM, Bray F, Ferlay J, Pisani P. Estimating the world cancer burden: Globocan 2000. Int J Cancer 2001; 94:153-156.*
4. *Sagar PM, Pemberton JH. Surgical management of locally recurrent rectal cancer. Br J Surg 1996; 83:293-304.*
5. *Heald RJ. A new approach to rectal cancer. Br J Hosp Med 1979; 22:277-281.*
6. *Kapiteijn E, Marijnen CA, Nagtegaal ID, et al. Preoperative radiotherapy combined with total mesorectal excision for resectable rectal cancer. N Engl J Med 2001; 345:638-646.*
7. *Sauer R, Becker H, Hohenberger W, et al. Preoperative versus postoperative chemoradiotherapy for rectal cancer. N Engl J Med 2004; 351:1731-1740.*
8. *Minsky BD, Cohen AM, Kemeny N, et al. Combined modality therapy of rectal cancer: decreased acute toxicity with the preoperative approach. J Clin Oncol 1992; 10:1218-1224.*
9. *Brown G, Daniels IR. Preoperative staging of rectal cancer: the MERCURY research project. Recent Results Cancer Res 2005; 165:58-74.*

MR ANATOMY OF THE RECTUM AND MESORECTUM

MODIFIED VERSION PUBLISHED IN TEXTBOOK *BENIGN ANORECTAL DISEASES*, ED. G.A. SANTORO & G. DI FALCO

2

M.J. LAHAYE

W.H. LAMERS

G.L. BEETS

AND R.G.H. BEETS-TAN

Introduction

Magnetic resonance imaging (MRI) of rectal cancer is gradually becoming more important in the management of this disease. Knowledge of relevant MR anatomy of the rectum and mesorectum is important for radiologists, surgeons, and radiation oncologists involved in the multidisciplinary approach of rectal cancer.

Total mesorectal excision (TME), first described by Heald in 1979 [1], has become the standard surgical procedure for curative resection of rectal cancer. Previously, surgeons often bluntly worked their way through the fat surrounding the rectal wall, with a considerable likelihood of leaving tumor tissue behind in the fat. With a TME, the rectum is removed en bloc with the complete mesorectal compartment, including the surrounding mesorectal fat and lymph nodes. The mesorectal fascia forms the border of this compartment. In a TME procedure, this fascia constitutes the ideal resection plane to remove, through sharp dissection, the complete mesorectal compartment within its fascia (see Figure 2.1).

The distance of the tumor to the circumferential resection margin (CRM) is an important prognostic variable: the closer the tumor, the higher the risk for a local recurrence [2]. A preoperative pelvic MRI can visualize the rectal tumor, the mesorectum, and the surrounding mesorectal fascia [3]. By understanding the MR pelvic anatomy, the distance of the tumor to the mesorectal fascia can be accurately identified [4], and an involved or close circumferential resection margin of a standard TME specimen can be anticipated. Rather than proceeding with a standard resection and putting the patient at risk for a local recurrence, the clinician can choose for neoadjuvant (chemo)radiotherapy and/or a more extensive resection.

Techniques

Imaging sequences

MRI of the rectum were performed at 3.0 Tesla (T) (Intera Achieva 3.0T Release 1.2.1.3. Quasar Dual, maximum gradient strength 30 mT/m, maximum slew rate 200 T/m/s, Philips Medical System, Best, The Netherlands). The male and female volunteers were positioned supine, in feet-first position, and a six element synergy

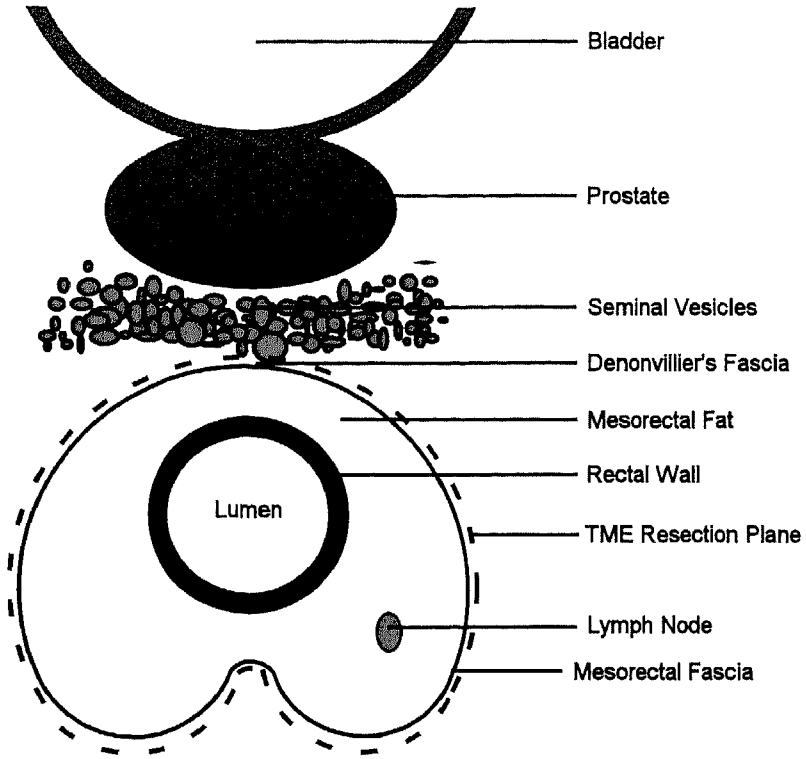

Figure 2.1. A TME radically removes en bloc the tumor-bearing part of the rectum together with the associated mesorectal compartment, including surrounding mesorectal fat, mesorectal lymph nodes and its border, the mesorectal fascia. The mesorectal fascia is used as the resection plane during the TME procedure.

phased array coil was used. Sequences used were a sagittal T2-weighted (T2W), two-dimensional (2-D), fast spin echo (FSE) [T2W FSE: TR/TE 4,598/150 ms, 34-echo train length, 4 mm slice thickness, 0.8 mm gap, 2 signal averages, 432x272 matrix, 512 reconstruction, 0.58/0.92/4.00-voxel MPS (mm), 250 mm FOV, 5:13 min acquisition time]. An axial T2W, 2-D, FSE [T2W FSE: TR/TE 5,312/150 ms, 28-echo train length, 4 mm slice thickness, 0.80 gap, 2 signal averages, 384x235 matrix, 512 reconstruction, 0.65/1.06/4.00-voxel MPS (mm), 250 mm FOV, 5:19 min acquisition time].

A coronal T2W FSE [T2W FSE: TR/TE 5,952/150 ms, 29-echo train length, 4 mm slice thickness, 0.80 gap, 2 signal averages, 416x281 matrix, 512 reconstruction, 0.67/1.07/4.00-voxel MPS (mm), 280 mm FOV, 5:39 min acquisition time]. Volunteers did not receive bowel preparation or intravenous or intrarectal MRI contrast agents.

Anatomical preparations

Male and female human hemipelvic preparations were obtained from the collection of the Department of Anatomy and Embryology, Maastricht University. Images of axial sections of the pelvis were acquired from the male and female specimens of the Visible Human Data Set. These anatomical data sets were developed under a contract from the National Library of Medicine by the Departments of Cellular and Structural Biology, and Radiology, University of Colorado School of Medicine, Denver, USA.

MR anatomy of the rectum and the rectal wall

The rectum

The rectum extends from the anorectal junction to the rectosigmoid junction. For practical purposes, the rectosigmoid junction is arbitrarily defined, most often, as 15 cm from the anal verge. Other definitions use a length of 12 cm or the dentate line or anorectal junction as a starting point. The most common definition of 15 cm from the anal verge corresponds to the level of the third sacral vertebrae (Figure 2.2A & B), which is lower than often thought. At the anorectal junction, the rectum bends sharply posterior and caudal into the anal canal (Figure 2.2A & B). The rectum, when distended, has a clear reservoir function, anatomically referred to as rectal ampulla (see Figure 2.2A & B).

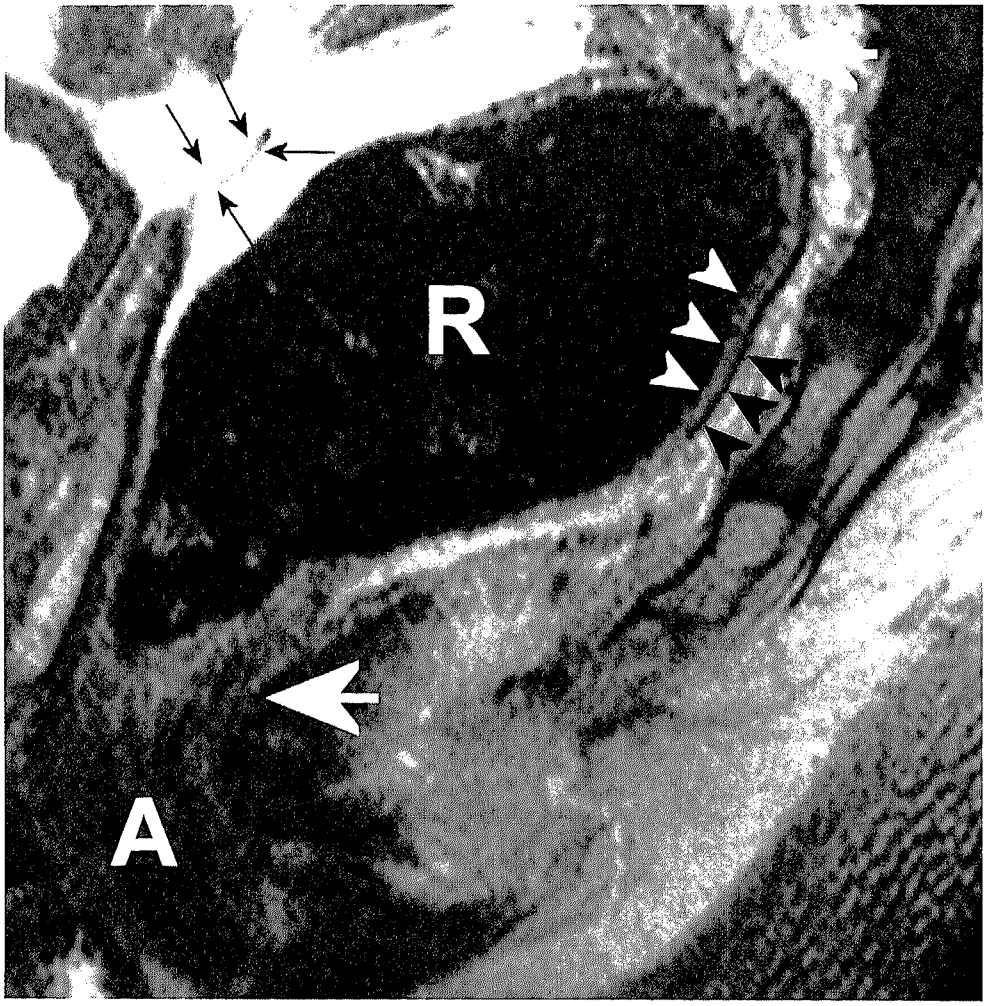

Figure 2.2A. Sagittal T2W FSE (TR/TE 4598/150 msec) MR image of a healthy male volunteer shows the rectosigmoid transition and end of the rectum (white arrows) in the anal canal (A). The rectal ampulla (R) is evident. The inner layer of the rectal wall can be visualized as a line of intermediate signal intensity relative to muscle tissue representing the mucosa (white arrowheads). The outside layer of the rectal wall, a hypo-intense line, corresponds to the muscularis propria recti (black arrowheads). The peritoneal reflection appears as a low signal intensity V-shaped structure ("seagull sign", black arrows).

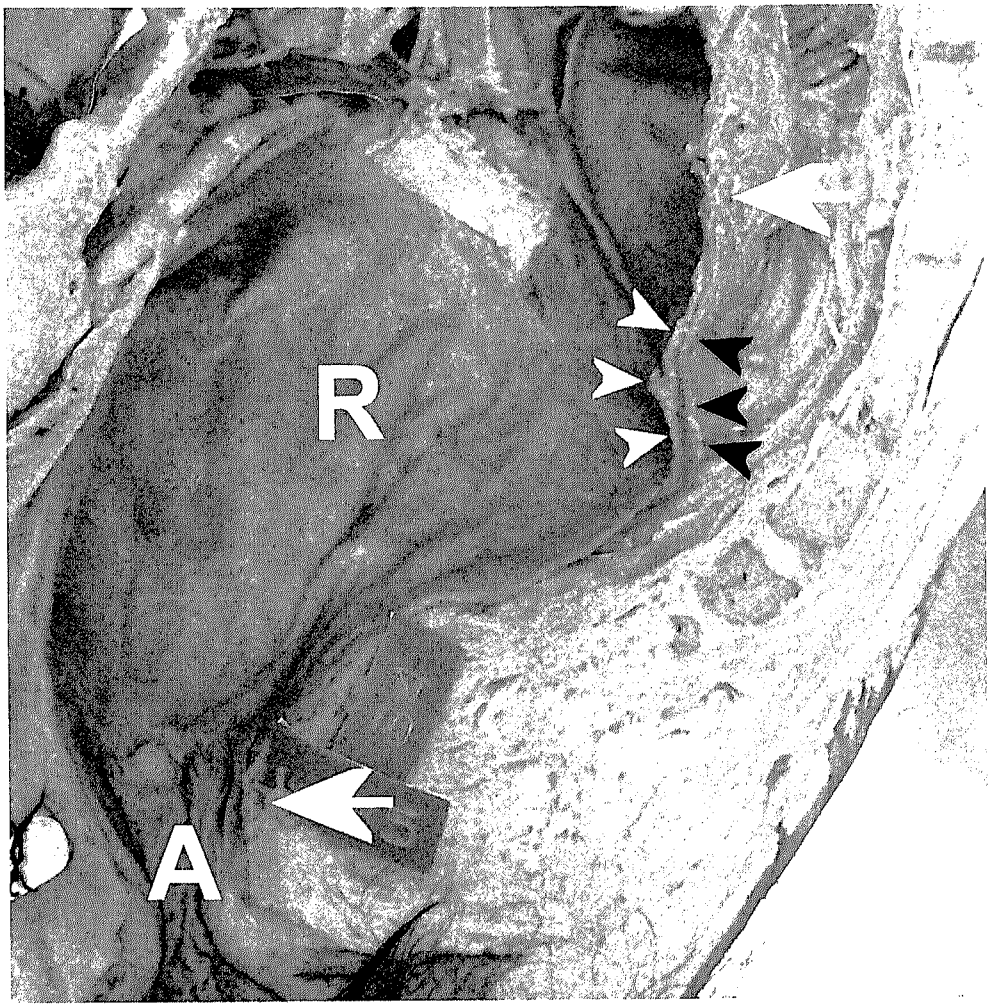

Figure 2.2B. Midsagittal rectum seen from left of the male pelvis in shows the whole rectum (between the white arrows); rectal ampulla (R), anal canal (A), mucosae (white arrowheads) and muscularis propria (black arrowheads).

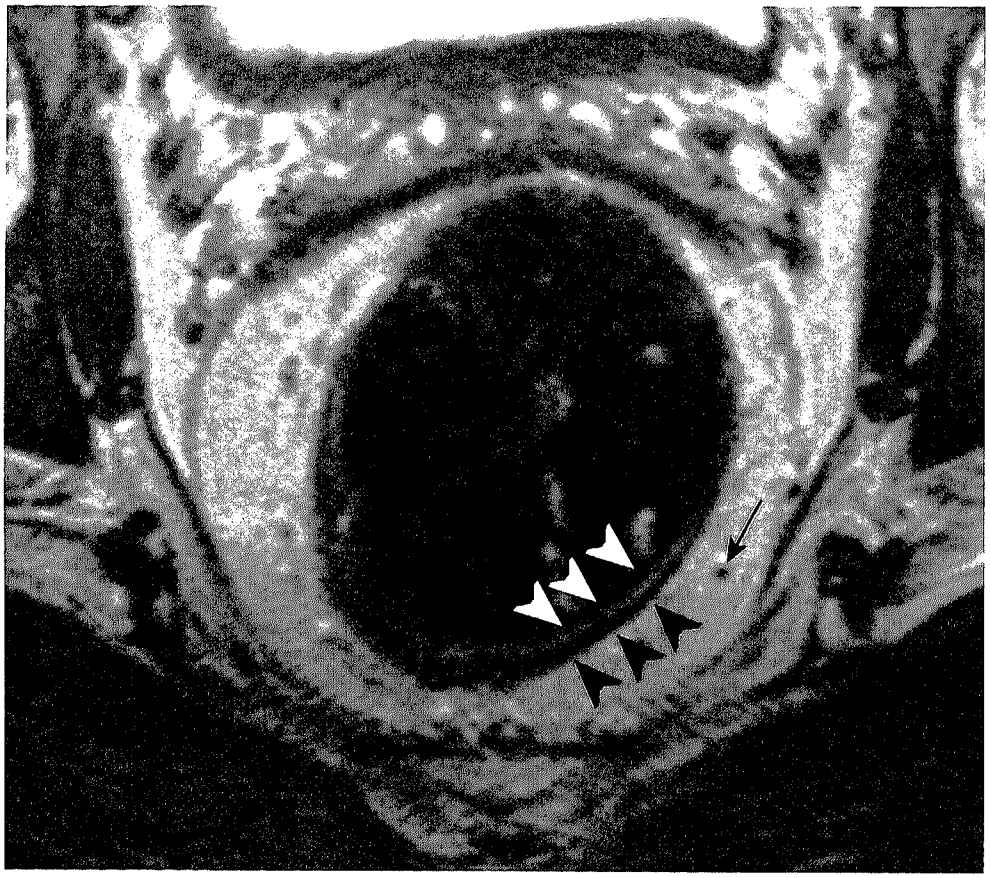

Figure 2.3A. Axial T2W FSE (TR/TE 5312/150 msec) MR image shows the inner layer of the rectal wall, as a line of intermediate signal intensity relative to muscle tissue representing the mucosa (white arrowheads). The outside layer of the rectal wall, a hypo-intensity line, corresponds to the muscularis propria recti (black arrowheads). A small lymph node is visible as low intensity round structure (black arrow).

Figure 2.3B. Axial section of the male pelvis shows the inner layer of the rectal wall, the mucosa (white arrowheads) and the outside layer of the rectal wall, the muscularis propria recti (black arrowheads). A small lymph node is also visible (black arrow).

The rectal wall

On T2W images, the normal rectal wall shows two separate layers. The innermost layer is a line of intermediate signal intensity relative to muscle tissue representing the mucosa, that is, epithelium, lamina propria, and muscularis mucosae. The hypointense outermost layer corresponds to the muscularis propria recti (in anatomical literature also referred to as muscularis externa (see Figure 2.2A & B)).

The total thickness of a normal rectal wall on a phased array MRI should not be more than 1-3 mm (see Figure 2.3A & B). If the bowel wall has become edematous (i.e., inflammatory conditions), a third layer of high signal intensity corresponding to the thickened submucosal layer appears in between the inner and outer layers (see Figure 2.4).

Figure 2.4.
Sagittal T2W FSE (TR/TE 3427/150 msec) MR image of a male patient with rectal cancer shows a layer of high signal intensity (white arrowheads) corresponding to the edematous submucosal layer between the inner mucosal layer (black arrowheads) and outer layer, the muscularis propria recti (black arrows).

MR ANATOMY OF THE MESORECTUM

The mesorectum is enclosed by the mesorectal fascia and contains the rectum, mesorectal fat, blood vessels, lymphatic vessels, and lymph nodes.

THE MESORECTAL FAT

The mesorectal fat surrounds the rectal wall but is not equally thick along its entire circumference and length. On T2W MR images, mesorectal fat is seen as a high-

intensity structure surrounding the rectum. Anteriorly, the rectum is close to the genital organs; the vagina and cervix in females and the prostate and seminal vesicles in males. Anteriorly, the mesorectal fat is much thinner than on the lateral and posterior aspect (see Figure 2.5A & B).

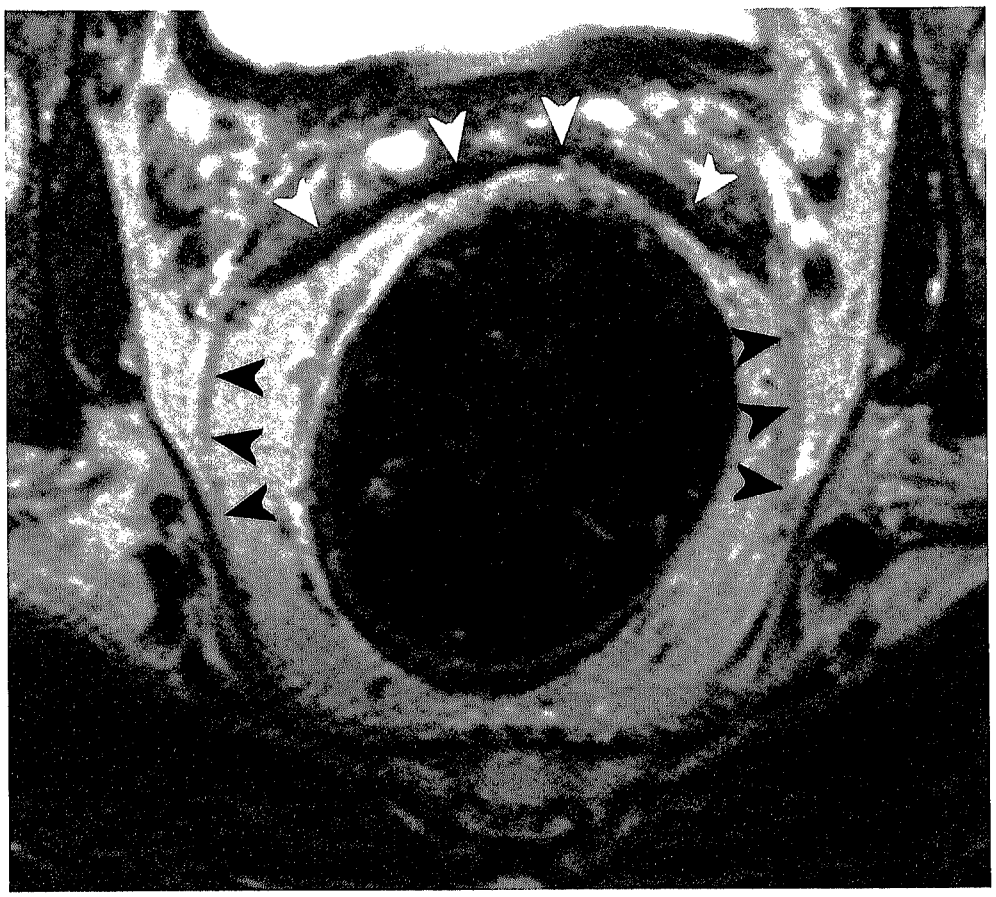

Figure 2.5A. Axial T2W FSE (TR/TE 5312/150 msec) MR image of a healthy male volunteer shows the mesorectal fascia (black arrowheads) as a fine line of low signal intensity surrounding the mesorectal fat. The Denonvilller's fascia is also visualized (white arrowheads) posterior to the seminal vesicles.

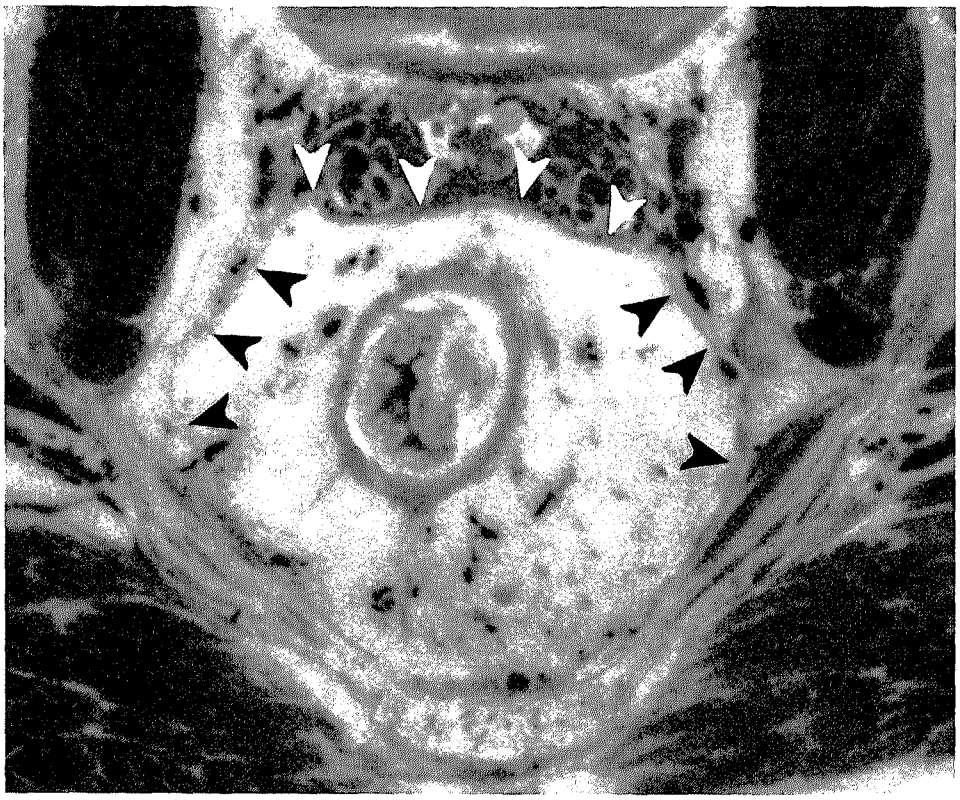

Figure 2.5B. Axial section of the male pelvis in shows the mesorectal fascia (black arrowheads). The Denonvillier's fascia is also visualized (white arrowheads) posterior to the seminal vesicles.

This results in a closer distance of the anterior rectal wall to the vagina and cervix in women and the prostate and seminal vesicles in men. A low anteriorly located rectal cancer has therefore a shorter distance to the mesorectal fascia, with a higher risk for a positive or close CRM. Furthermore, the distal tapering or coning of the mesorectum entails a close topographical relationship of the distal rectal wall and the muscles of the pelvic floor (Figure 2.6). At the anorectal junction, the mesorectal fat has all but disappeared, and the mesorectal fascia can no longer be distinguished from the pelvic floor muscles.

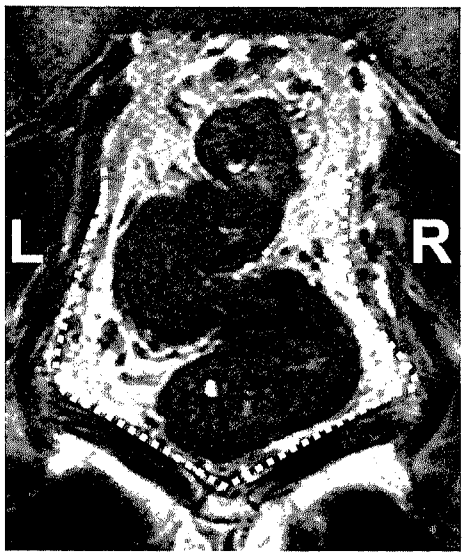

Figure 2.6.
A coronal T2W FSE (TR/TE 3427/150 msec) MR image of a patient with rectal cancer shows the distal tapering or coning of the mesorectum which entails a close topographical relationship of the distal rectal wall and the muscles of the pelvic floor (white dotted line).

The mesorectal fascia

The mesorectum is bounded by the mesorectal fascia (see Figure 2.7A & B). On both T1W and T2W MR images, the mesorectal fascia is seen as a fine line of low signal intensity surrounding the mesorectal fat. In the literature, the mesorectal fascia is also referred to as the fascia propria or the perirectal fascia. Sometimes it is erroneously described as Denonvilliers' fascia and even Waldeyer's fascia. Denonvilliers' fascia is the thickened anterior part of the mesorectal fascia that separates the mesorectal fat from the vagina or seminal vesicles. On T2W MR images, the Denonvilliers' fascia is seen as a single, hypointense, 1 to 2 mm thick anatomical structure (Figure 2.5A & B and Figure 2.7A & B) The Waldeyer's fascia is the presacral fascia [5]. This presacral fascia is located dorsal to the mesorectal fascia and is thus anatomically a separate entity. On MRI, both the dorsal mesorectal fascia and the Waldeyer's fascia are seen as a single hypointense linear structure (Figure 2.8A & B). However, during the surgical procedure, these two fascias are individually recognized, and the virtual space in between the fascias provides an optimal landmark for the resection plane.

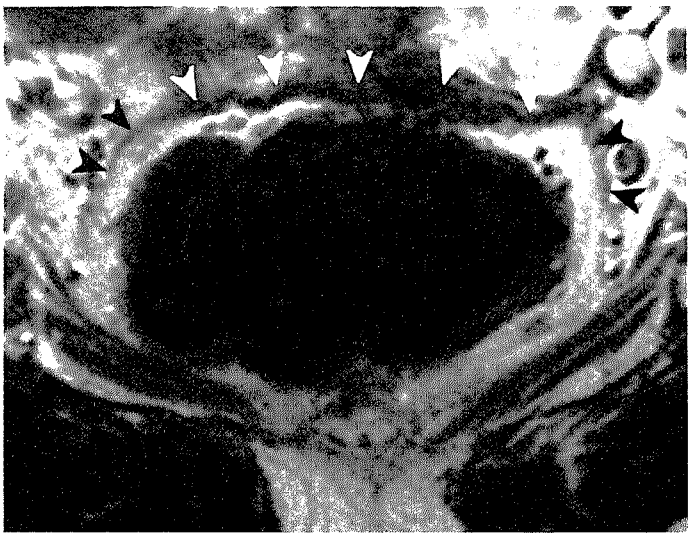

Figure 2.7A. Axial T2W FSE (TR/TE 5312/150 msec) MR image of a healthy female volunteer shows the mesorectal fascia (black arrowheads) as a fine line of low signal intensity surrounding the mesorectal fat. The Denonvilliers' fascia is also visualized (white arrowheads) posterior to the vagina.

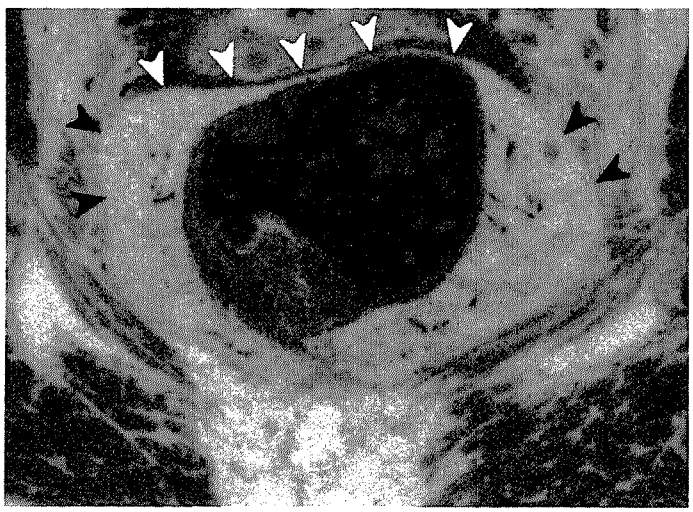

Figure 2.7B. Axial section of the female pelvis shows the mesorectal fascia (black arrowheads). The Denonvilliers' fascia is also visualized (white arrowheads) posterior to the vagina.

Figure 2.8A.
Sagittal T2W FSE (TR/TE 4598/150 msec) MR image of a healthy female volunteer shows the Waldeyer's fascia as a hypointense linear presacral structure of low signal intensity close to the sacrum (black arrowheads).

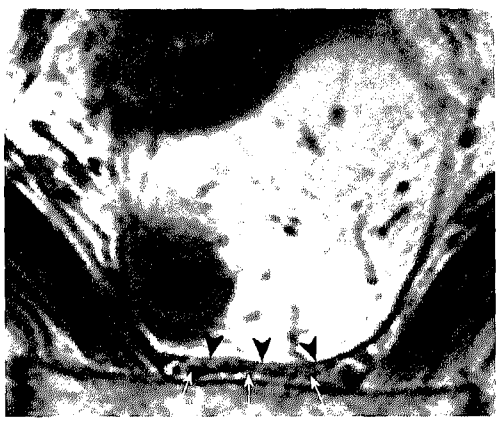

Figure 2.8B.
Axial T2W FSE (TR/TE 5312/150 msec) MR image of a healthy female volunteer shows the Waldeyer's fascia as a hypointense linear presacral structure (black arrowheads). The presacral venous plexus and the lateral sacral veins are visualized as round, tubular, structures of low signal intensity (white arrows).

The peritoneum

The parietal and visceral peritoneum envelops the mesorectum anteriorly and laterally in the upper two thirds of the rectum. At the transition of the middle and lower third of the rectum, just above the pelvic floor, the peritoneum reflects on to the seminal vesicles in males to form the rectovesical pouch and the posterior vaginal wall in females to form the rectouterine pouch (of Douglas). The height of the

rectovesical excavation is about 6.5 cm and that of the rectouterine excavation about 7.5 cm from the dentate line. The peritoneal reflection appears as a low-signal-intensity V-shaped structure ("seagull sign") on sagittal T2W MR images (see Figure 2.2A). Whereas a tumor that comes close to or invades the mesorectal fascia may lead the clinician to a change in management, a tumor that comes close to or invades the visceral peritoneum above the pouch of Douglas is less likely to do so. For anteriorly located tumors, it is therefore of importance to locate the tumor relative to the pouch of Douglas.

Neurovascular and lymphatic anatomy

Vascular supply

The hindgut, and thus the rectum, is embryologically supplied by the inferior mesenteric artery. It arises from the aorta at the level of the third lumbar vertebra (L3). One of its branches, the superior rectal artery, is the main feeding artery of the rectum. Once the superior rectal artery reaches the posterior wall of the rectum, it splits into left and right branches that feed both sides of the rectum via their fine peripheral branches. On axial T2W MR images, the superior rectal artery and its branches can be detected as low-intensity, tubular structures in the presacral region. The superior rectal vein runs on the dorsal and left side from the artery (see Figure 2.9, 2.10 and 2.11). The distal part of the rectum receives additional blood supply from the middle rectal artery, an inconsistent branch from the internal iliac artery (see Figure 2.12), accompanied by a parallel, and small, middle rectal vein. The internal iliac artery and vein course together with the ureter on the lateral pelvic sidewall close to the mesorectal fascia. The inferior rectal artery comes off the pudendal artery, a branch of the internal iliac artery. The inferior rectal artery is situated below the pelvic floor muscles, and its relevance in blood supply of the rectum is minimal (see Figure 2.13). Anastomoses between the lateral and median sacral veins, which accompany the corresponding arteries, often form the so-called "presacral venous plexus" behind Waldeyer's fascia. On T2W MR images, they are seen as low-intensity tubular structures (see Figure 2.8B). The presacral venous plexus can bleed profusely, and hemostasis may be difficult to achieve if it is accidentally injured during rectal surgery.

Figure 2.9. On a sagittal T2W FSE (TR/TE 4598/150 msec) MR image the superior rectal artery and its branches can be detected as low-intensity, tubular structures in the presacral region (white arrowheads). The superior rectal vein runs on the dorsal and left side of the artery (black arrowheads).

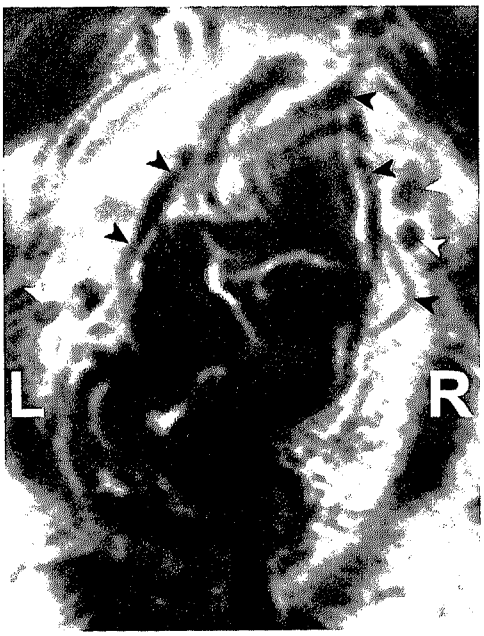

Figure 2.10 & 2.11. Coronal T2W FSE (TR/TE 3427/150 msec) MR images of a patient with rectal cancer show the superior rectal artery and its branches (black arrowheads). Also small hypointense lymph nodes are depicted (white arrowheads).

Figure 2.12.
On the coronal T2W FSE (TR/TE 3427/150 msec) MR image the common iliac artery (white arrow) and its first branch -the internal iliac artery (white arrowheads)- are depicted. Both the pudendal artery (black arrows) and the middle rectal artery (black arrowheads) originate from the internal iliac artery.

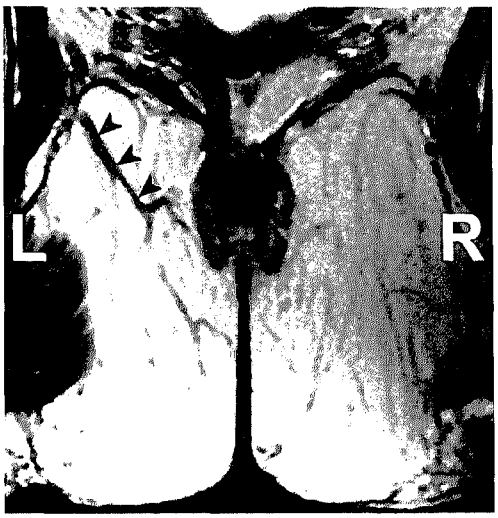

Figure 2.13.
Coronal T2W FSE (TR/TE 5952/150 msec) MR image shows the inferior rectal artery (black arrowheads). It courses through the ischiosacral fossa, under the pelvic floor towards the lower part of the rectum and anal canal.

Lymph drainage

The main lymphatic drainage of the rectum follows the superior rectal artery and vein to the inferior mesenteric vein and further up the paraaortic nodes (Figure 2.14A & B). Most of the lymph nodes in the mesorectum are situated along these vessels in the posterior and lateral part of the mesorectum [6]. Only a few lymph nodes are situated anteriorly in the mesorectum. These lymph nodes are situated inside the mesorectum. There is some controversy on the incidence and importance of lymphatic drainage of the rectum along the middle rectal artery and vein into the so-called lateral lymph pelvic nodes. These lymph nodes are situated outside the mesorectum. Through the efforts of Japanese surgeons, it is clear that lymph node metastases do occur in these lateral lymph nodes, usually in patients with distal rectal cancer and in the presence of mesorectal nodal metastases [7]. The "lateral" nodal metastases are often thought to be situated close to the obturator muscle while in reality, they most often occur at the root of the middle rectal artery situated posterolaterally in the pelvis on the lumbosacral plexus (Figures 2.10 and 2.11). On T2W MR images of healthy volunteers, small lymph nodes less than 4 mm in diameter and of hypointense signal intensity can sometimes be seen. In rectal cancer, it is known that size alone is not a good indicator for nodal metastases, as small nodes can harbor metastases [8].

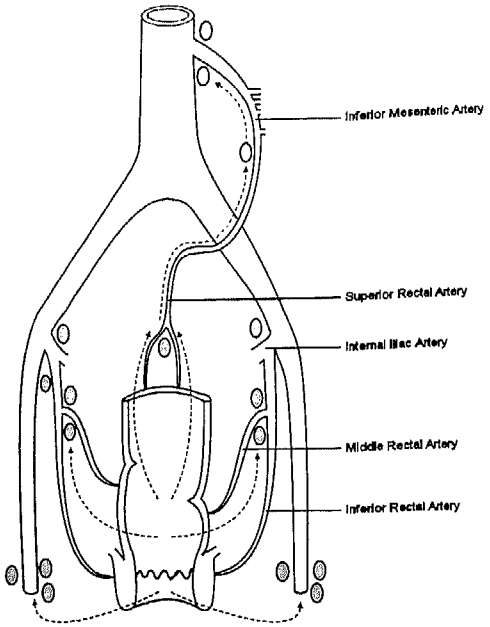

Figure 2.14A.
The main lymphatic drainage of the rectum follows the superior rectal artery and vein to the inferior mesenteric vein and further up the paraaortic nodes. Most of the lymph nodes in the mesorectum are situated along these vessels in the posterior and lateral part of the mesorectum.

Figure 2.14B.
The 'lateral' nodal metastases (black arrowheads) most often occur at the root of the middle rectal artery (white arrowheads), situated posterolaterally in the pelvis, on the lumbosacral plexus. The middle rectal vein is also depicted (black arrows).

Nerves

The relevant visceral nervous anatomy concerns sympathic and parasympathetic innervation for anorectal, urinary, and sexual functions. Because of its close relationship with the mesorectum, the nerves and plexuses can be invaded by a locally advanced tumor and easily injured when the rectum is mobilized during surgery (Figure 2.15) [9, 10]. At the level of the promontory, just below the aortic bifurcation, presacral sympathic nerve fibers form the superior hypogastric plexus.

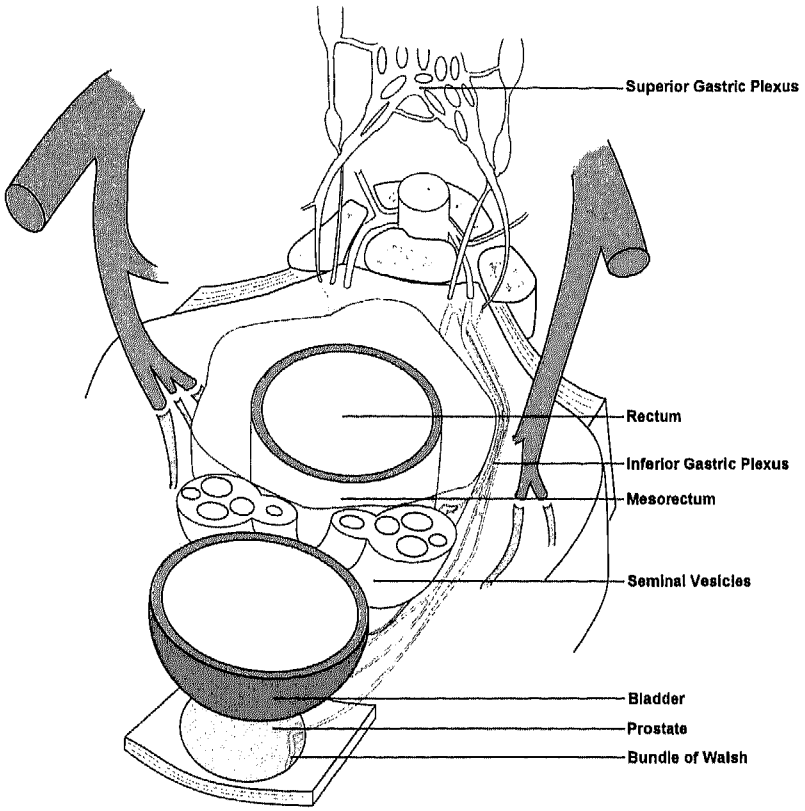

Figure 2.15. The superior hypogastric plexus splits into left and right hypogastric nerves which, at a lower level, together with the parasympathetic fibers (n. erigentes) originating from spinal segments S2-S5, clasp the mesorectum on their course to the bladder and genitals. Together they form the left and right inferior hypogastric, or pelvic plexus. The pelvic plexus is situated anterolaterally of the rectum. The pelvic plexus continues into the neurovascular bundle of Walsh which courses medially and inferiorly along the posterolateral aspect of the prostate gland [11].

The superior hypogastric plexus splits into left and right hypogastric nerves that, at a lower level, together with the parasympathetic fibers (nervi erigentes) originating from spinal segments S2–S5, clasp the mesorectum on their course to the bladder and genitals. Together they form the left and right inferior hypogastric, or pelvic plexus. The pelvic plexus is situated anterolaterally of the rectum and continues into the neurovascular bundle of Walsh, which courses medially and caudally along the posterolateral aspect of the prostate gland (see Figure 2.15). On T2W FSE MR images, the pelvic plexus cannot be discerned.

Conclusion

MRI is becoming important in the management of rectal cancer patients. Knowledge of relevant MR anatomy of the rectum and mesorectum is mandatory for radiologists, surgeons and radiation oncologists involved in the multidisciplinary approach of rectal cancer. This chapter aimed at providing detailed information on the MR anatomy of clinically relevant structures.

References

1. *Heald RJ. A new approach to rectal cancer. Br J Hosp Med 1974; 22(3):277–281.*
2. *Nagtegaal ID, Marijnen CA, Kranenbarg EK, et a.l Circumferential margin involvement is still an important predictor of local recurrence in rectal carcinoma: not one millimeter but two millimeters is the limit.Am J Surg Pathol 2002; 26(3):350–357.*
3. *Bissett IP, Fernando CC, Hough DM, et al. Identification of the fascia propria by magnetic resonance imaging and its relevance to preoperative assessment of rectal cancer. Dis Colon Rectum 2001; 44(2):259–265.*
4. *Beets-Tan RG, Beets GL, Vliegen RF, et al. Accuracy of magnetic resonance imaging in prediction of tumour-free resection margin in rectal cancer surgery. Lancet 2001; 357(9255):497–504.*
5. *Heald RJ, Moran B.J. Embryology and anatomy of the rectum. Semin Surg Oncol 1998; 15(2):66–71.*
6. *Dworak O. Morphology of lymph nodes in the resected rectum of patients with rectal carcinoma. Pathol Res Pract 1991; 187(8):1020–1024.*
7. *Moriya Y, Sugihara K, Akasu T, et al. Importance of extended lymphadenectomy with lateral node dissection for advanced lower rectal cancer. World J Surg 1997; 21(7):728–732.*
8. *Brown G, Richards CJ, Bourne MW, et al. Morphologic predictors of lymph node status in rectal cancer with use of high-spatial-resolution MR imaging with histopathologic comparison. Radiology 2003; 227(2):371–377.*
9. *Church JM, Raudkivi PJ, Hill GL. The surgical anatomy of the rectum – a review with particular relevance to the hazards of rectal mobilisation. Int J Colorectal Dis 1987; 2(3):158–166.*
10. *Havenga K, DeRuiter MC, Enker WE, et al. Anatomical basis of autonomic nerve-preserving total mesorectal excision for rectal cancer. Br J Surg 1996; 83(3):384–388.*
11. *Kockerling F, Sinnatamby Ch, Von Hagens G. Total Mesorectal Excision with the water-Jet. 2002. Science Med Dr. Sperber.*

LYMPH NODE IMAGING: PRESENT STATUS AND FUTURE DEVELOPMENT

MODIFIED VERSION PUBLISHED IN TEXTBOOK *CLINICAL BLOOD POOL MR IMAGING*; ED. T. LEINER

3

M.J. LAHAYE

R.B.J. DE BONDT

G.L. BEETS

S.M.E. ENGELEN

AND R.G.H. BEETS-TAN

Introduction

Nodal tumor spread in cancer patients is associated with a poor prognosis [1]. Multimodality treatment in cancer, combining surgery with pre and/or post operative systemic +/- radiation therapy, aims at sterilizing microscopic tumor deposits in the surgical bed and locoregional nodes as well as at sterilizing occult metastases in distant organs and distant lymph nodes. The effectiveness of multimodality treatment for the high risk groups have been shown in multiple cancer treatment trials [2]. Combined preoperative modality treatment, however, carries a considerable perioperative morbidity and mortality [3] and it is questioned whether with multimodality treatment of all cancer patients the overall increased morbidity will outweigh the clinical effectiveness. The Dutch TME trial has shown in rectal cancer surgery that in patients with involved rectal tumor nodes the local recurrence rate at 5 years was significantly lower when a standard preoperative radiation therapy was given as compared to patients who went for immediate surgery. However, this was at the expense of radiotherapy toxicity and a significant increase in perioperative morbidity in terms of perineal wound leakage [4]. Furthermore, long term complications like bowel dysfunction were also described [5]. The trial also proved that subgroups existing of patients with early stage rectal tumors without nodal involvement (Stage I) did not significantly benefit from radiotherapy in addition to surgery, because these patients were already at low risk for local failure. If these patients could be selected from the higher risk patients with bulky tumors and nodal involvement, then a more individual based stratification of a multimodality treatment regime can be introduced, restricting the more aggressive combined preoperative treatment for the "ugly" diseases and omitting preoperative irradiation in the "good" early tumors.

So far no imaging tool has been shown to be reliable for detecting nodal metastases. A recent meta-analysis of all endoluminal ultrasonography (EUS), computed tomography (CT) and magnetic resonance imaging (MRI) studies on nodal detection in rectal cancer patients has confirmed that identifying nodal disease by presently available noninvasive imaging techniques is not accurate enough for clinical decision making [6]. Distinction between malignant and benign nodes with noninvasive imaging tools has only been done using morphological criteria such as size for CT and in addition to size, border contour and heterogeneity for EUS and MRI,

consequently leaving small malignant nodes undetected. For example in rectal cancer treatment using the 9 mm size cut off for differentiating benign from malignant nodes would lead to a considerable understaging of patients with nodal involvement because more than half of the malignant rectal cancer nodes are between 2 and 5 mm in size [7].

Consequently, further research needs to be done to investigate advanced imaging techniques to improve nodal staging, should imaging want to develop into one of the most powerful predictors for confident stratification of the higher risk cancer patients into a more aggressive treatment and the lower risk cancer patients into surgery only or even a wait and see policy. In this pursuit radiologists are pushed forward by new developments in lymph node specific contrast agents. MR blood pool contrast agents, such as ultrasmall super paramagnetic iron oxide (USPIO) has in different studies (concerning lymphoma, colon, rectum, lung, breast, head and neck, prostate, uterus, endometrial, ovarian, testicles, kidney, bladder, cervical and vulval cancer) shown better sensitivities and specificities for the detection of malignant nodes. Another blood pool MR contrast agent is now on the market, approved for MR angiography, which may be promising for visualization of lymph nodes Vasovist®: Gadovosfeset Trisodium (Bayer Schering Pharma, Berlin, Germany) [8].

This chapter will describe the present status of modern imaging techniques for identifying nodal disease in high risk patients focusing on colorectal cancer and describe the upcoming role and evidence so far of promising modern imaging techniques and new contrast agents that could help radiologists to improve his/her performance for selecting oncology patients with lymph node metastases by non-invasive modern imaging techniques.

Lymph node anatomy and physiology

Knowledge of the anatomy and physiology of the lymphatic system and lymph nodes is important in order to have a basic understanding of lymph node imaging. Lymph nodes are small bean-shaped structures that are usually less than 2.5 cm in length. Lymph nodes are largely distributed in drainage areas of body sites most exposed to the external environment like limbs, gastrointestinal tract, lungs and pharynx axis.

The lymphatic system is an essential first line of defense against pathogens. The normal lymph node is separated into compartments called lymph nodules and surrounded by a connective tissue capsule (Figure 3.1). In these lymph nodules, dense masses of macrophages and lymphocytes are situated and separated by spaces called lymph sinuses. Through these lymph sinuses the lymph fluid passes, on their way from the numerous afferent lymphatic vessels towards an efferent lymphatic vessel. The efferent vessel leaves the node at a concave area called the hilum. The lymph fluid consists chyle, proteins, fat and white blood cells of which predominantly lymphocytes. The lymphatic vessels and the lymph node pattern anatomically define the lymph fluid flow to lymph nodes. Metastasis can follow this specific structured lymph flow pattern to spread to the next lymph node. Cabanas et al. demonstrated the existence of specific lymph node center, the so-called sentinel lymph node (SLN), which was the primary site of metastases from penile cancer [9]. When a biopsy of the SLN is negative for metastatic disease, the other lymph nodes downstream are likely to be also benign. Thus, a specific node can be the doorway for cancer to spread to other regional nodes. It is possible for a metastasis in a sentinel node to grow and block lymphatic flow, thus redirecting lymph and tumor cells to other, possibly not ordinarily sequential, nodes. This hypothesis of a sentinel node has been firmly established in malignancies like breast cancer, penile cancer and melanoma, but not in several other malignancies like thyroid, head and neck, gastric, colorectal, cervical, and endometrial cancers.

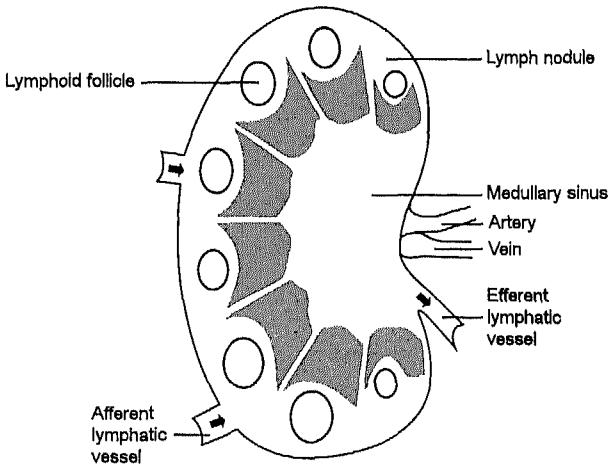

Figure 3.1. Schematic drawing of the anatomy of a normal lymph node.

EUS AND ULTRASOUND FOR LYMPH NODE STAGING

During the past decades radiologists have gained a great deal of experience in lymph node imaging by means of EUS and/or ultrasound [10, 11]. Several morphological characteristics of lymph nodes are assessed to distinguish malignant from benign lymph nodes. Those characteristics suggesting tumoral lymph node involvement are: enlargement, round shape, irregular border, loss of the central hilum and hypo-echogeneity [12].

However, none of these morphological characteristics are accurate enough in malignant node identification and therefore (E)US only, without fine needle aspiration cytology (FNAC), cannot be relied on for clinical decision making neither in gastrointestinal tract cancer staging like esophageal cancer and rectal cancer. In rectal cancer EUS, is slightly, although not significantly, better than CT or MRI in a large meta-analysis evaluating the diagnostic performance for nodal staging. However, large variation in accuracy of EUS for nodal detection (62-85%) can be found, illustrating its operator dependency [13-16]. Controversial reports on the performance of EUS-FNAC exist. Harewood et al. found no benefit from EUS-FNAC staging as compared to EUS staging only [11], while Shami et al. showed significant improvement for EUS-FNAC compared to EUS alone with a sensitivity of 93% [17].

A drawback of ultrasound in general is that the performance depends on the experience of the sonographer and in rectal cancer multicenter trials EUS staging accuracy has been shown to drop with 30% when non expert centers are doing the examination [18]. In rectal cancer EUS-FNAC has been introduced, but not yet widely adopted. First, besides that the technique is highly operator dependent and invasive, it is limited in that many nodes outside the scope of the endosonography probe go undetected. Second, if nodes adjacent to the tumor are suspected based on the EUS aspects, cytological aspiration of these nodes, which can only be done by direct penetration of the needle through the tumoral wall. This contaminates the needle with tumor cells leading to false positive results [19]. Finally there is the high chance of sampling errors especially when small nodes less then 5 mm in size have to be aspirated. In rectal cancer these nodes have 20-50% chance of harboring tumor cells.

New ultrasound techniques like Doppler-ultrasound combined with micro-bubble contrast agents or 3D EUS are being studied with promising results, although these

only involve studies in single centers. The real question is whether advanced noninvasive EUS techniques in rectal cancer will gain widespread acceptance when advanced EUS techniques will in future multicenter studies turn out to be operator dependent [20-22].

Computed tomography

Computed tomography has long been adopted as a tool for identifying malignant retroperitoneal lymph nodes in several cancers. On CT imaging, mesorectal nodes measuring > 5 mm can be identified as oval structures of soft tissue density within the fatty mesorectum [23]. Conventional single and 4-16 slice CT machines demonstrated accuracies varying between 22% and 77% for nodal staging in rectal cancer [16, 24-26]. In contrast to EUS, CT has a much larger field of view and is less reader/operator dependent. However, due to its low contrast resolution, conventional computed tomography techniques have primarily relied on size criteria, and size on its own is insufficient for a reliable distinction between malignant and benign lymph nodes, and the high frequency of malignant nodes between 2 and 5 mm size in rectal cancer patients would only further limit CT in its ability in identifying rectal nodal disease. Other criteria, such as the presence of necrosis or extra nodal tumor spread, are used but are less valuable. Necrosis is mainly seen in lymph nodes exceeding 10 mm and those lymph nodes will at first instance already be classified as malignant based on the large size. Advancement in MDCT techniques with 64 slice CT being introduced in patient clinics, could theoretically mean an upgrading of CT for nodal disease detection, but so far no studies exist on the 64 slice CT for evaluating rectal cancer nodes except for one, indeed showing an improvement with 85% accuracy [27].

FDG-PET

18Fluorodeoxyglucose (FDG) PET has proven its additional value for the search of distant metastases in a wide variety of tumor types. Cancer cells have an increased glycolytic rate compared to normal cells, which 18FDG-PET is able to detect.

Although FDG-PET has proven to be value in the search for distant extra hepatic disease in rectal cancer patients, for loco regional staging of the primary rectal tumor FDG-PET showed unsatisfactory results. The limitation of the nowadays-available human PET machine is its low resolution and consequently its inaccuracy for the detection of low-bulk tumor, requiring a size of at least 1 cm^3 tumor volume before PET can depict it. Furthermore, the uptake of 18FDG within the primary tumor and urinary bladder obscures the visualization of approximate mesorectal nodes in rectal cancer, because of the scatter artifacts. This may explain why in primary rectal cancer staging with FDG-PET more than half of the malignant nodes goes undetected with an unacceptable low sensitivity of 21-29% reported in literature [28, 29].

The introduction of hybrid techniques for whole body staging such as PET-CT, combining anatomical and functional information might lead to superior results to PET or CT only as a single staging tool, but to date no large evidence exists. So far one study has been reported with 53 rectal cancer patients showing a disappointing accuracy of 72% for nodal staging using PET-CT [30].

Magnetic resonance imaging

Conventional MR techniques with 0.5 to 1.5 Tesla powerfield systems are in general not accurate for the detection of nodal metastases in cancer patients, despite the superior contrast resolution of MR imaging as compared with all other existing conventional imaging techniques. Two meta-analyses in literature show a similar ROC curve for the detection with conventional MRI for node metastases, both showing insufficient performance for clinical decision making [6, 16, 31-37]. Most of these studies used size criteria to distinguish malignant from benign nodes. Only studies that investigated new criteria additional to size, such as a border contour and signal homogeneity, demonstrated higher sensitivities and specificities for the prediction of lymph node involvement in patients with rectal cancer. Only large metastases, over 5 mm in size, could accurately be evaluated for its border and MR signal intensity [36, 37]. The introduction of higher field MR machines into a clinical practice could improve the disappointing performance of conventional MRI. So far two studies on rectal cancer staging with 3 Tesla MRI have reported promising

accuracies of 91-95% for predicting nodal metastases in rectal cancer [38, 39], but larger studies are necessary before the role of high powerfield MR machines for staging rectal cancer can be established.

Lymph node specific MR contrast agents

During the last decade, new MR contrast agents, like ultrasmall super paramagnetic iron oxide (USPIO), Gadofluorine M and Vasovist® have been developed and in preclinical as well as clinical studies have proven to be promising for oncology patients [8, 40, 41]. Of these, USPIO is at present the only agent that has shown the largest evidence that it is effective in nodal staging of cancer patients.

Ultrasmall superparamagnetic iron oxide

USPIO is a contrast agent that undergoes phagocytosis by the reticuloendothelial system in the liver but also by macrophages located in benign lymph nodes. Uptake of USPIO within the node results in a decrease of signal intensity on T2*-weighted images due to increased susceptibility artifacts. This means that benign regions in a node appear black on T2*-weighted images (see Figure 3.2). In malignant nodes the macrophages are displaced by tumor deposits. In these regions in the node no uptake of USPIO will occur (see Figure 3.3). These regions with no uptake will be depicted as regions within the node with high signal intensity (white region). Weissleder et al. were the first to distinguish malignant from benign nodes in an animal model using USPIO [41], followed by Anzai et al. who demonstrated in a study with healthy volunteers that the uptake of USPIO reached its peak after 24 hours [42]. In the NEJM, Harisinghani et al. published the results of a study in 80 patients with prostate cancer and showed that USPIO MRI could distinguish malignant from benign nodes with 100% sensitivity and 95.7% specificity [43]. A recent meta-analysis of 19 USPIO MR studies showed that USPIO MRI has a sensitivity and specificity of 88% and 96%, respectively, for the detection of malignant nodes in various pelvic and head and neck cancers [31].

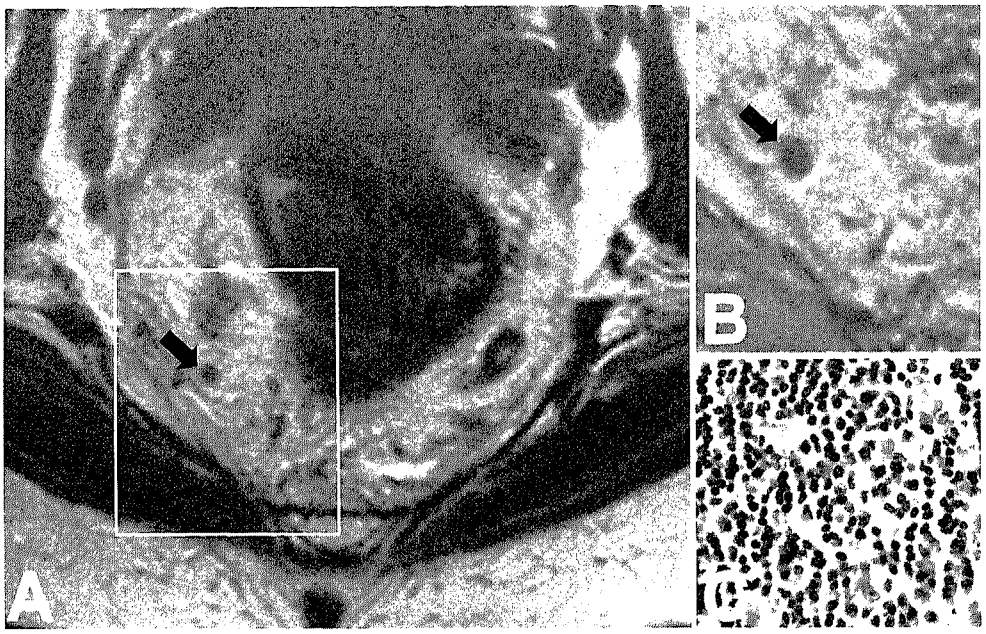

Figure 3.2. (A) T2-weighted image TSE image in the axial plane of the pelvis in a rectal cancer patient. On conventional T2-weighted images it is difficult to predict whether this 5 mm lymph node (arrow) is malignant or benign. (B) On the corresponding UPSIO enhanced T2*-weighted image the same node in more detail showed general low signal intensity, indicating a normal USPIO uptake pattern within the node. (C) At histological examination (HE stainng) this node shows a normal nodal architecture and shows no metastasis.

For rectal cancer patients the evidence so far has been through limited single center studies [44]. Therefore, an ongoing multicenter rectal cancer study in the Netherlands, investigating whether or not USPIO MRI can be used as a preoperative selection tool stratifying low, intermediate and high risk patients into a differentiated treatment, will tell us in the near future whether improved diagnostic staging will ultimately be translated into less local recurrences and increased overall survival for the whole group of rectal cancer patients.

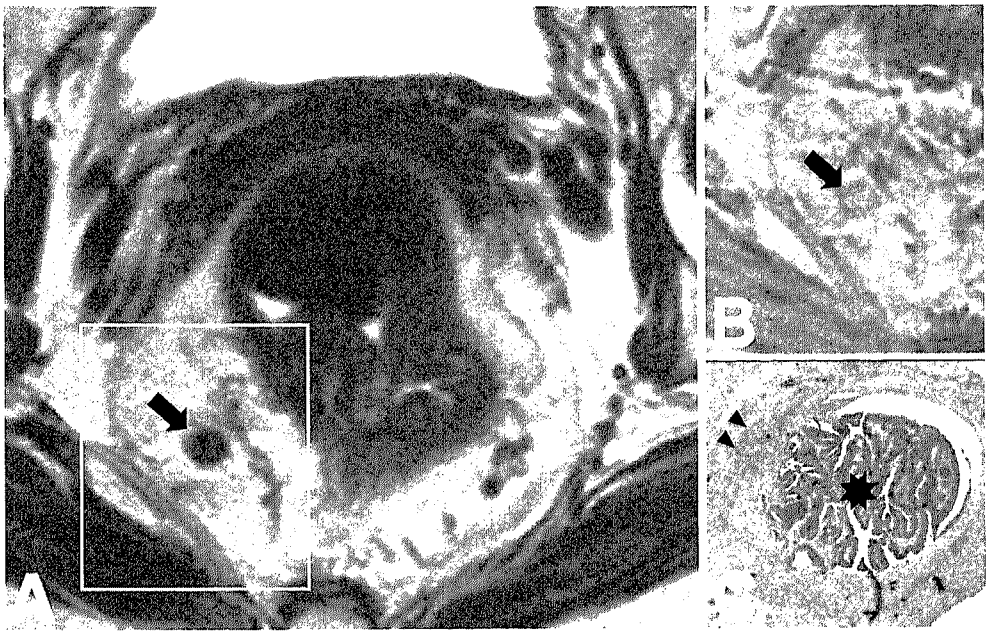

Figure 3.3. (A) T2-weighted image TSE image in the axial plane of the pelvis with a 7 mm mesorectal lymph node (arrow) in a rectal cancer patient. (B) On the corresponding UPSIO enhanced T2*-weighted image the same lymph node (arrow) showed central high signal intensity, indicating no USPIO uptake. At the border of the lymph node there is still uptake of USPIO. (C) This correlated at histological examination (HE staining) with the centrally located tumor deposit (asterisk) and the remaining surrounding normal lymphoid tissue (arrowheads).

GADOLINIUM BASED LYMPH NODE SPECIFIC MR CONTRAST AGENTS

Another type of MR contrast agents are Gadolinium based compounds, such as Gd-DTPA, Gadofluorine and MS325 (Vasovist®). Gadolinium-based contrast agents are also promising for the detection of malignant lymph nodes.

Gadolinium DTPA

Several studies have assessed the role of Gd-DTPA perfusion MR imaging for the detection malignant nodes [45]. In a series of 21 patients with squamous cell carcinomas of the head and neck, Fischbein et al. used dynamic contrast-enhanced

MRI (DCE-MRI) to assess cervical lymph nodes [46]. In contrast to head and neck and neck cancers, in breast cancer staging Kvistad et al. found that a significant signal increase of over 100% during the first pass imaging was a very good indicator for benign nodes in breast cancer patients [45]. Malignant nodes in head and neck cancer displayed a significantly longer time to peak enhancement, reduced peak enhancement, decreased slope and slower wash-out, compared to normal lymph nodes.

DCE-MR imaging acquires serial images following the intravenous injection of the contrast agent. Wash-in and wash-out curves can be derived from designated regions of interest (ROIs) for direct comparison, or pharmacokinetic models can be applied in order to derive permeability characteristics [47]. Gd-DTPA enhanced dynamic MR imaging reflects the physiology of the microcirculation, especially the microvasculature and the extravascular space. Microcirculation in tumoral nodes generally differs from that in non-tumoral, reactive nodes. Lymphoid tissue, especially in a reactive lymph node, generally has a higher blood flow, while tumor tissue in malignant nodes can be heterogeneous, slow and even retrograde. The delayed tumoral node enhancement due to a longer time to peak and lower peak enhancement is a direct reflection of the slower leakage of blood pool contrast agents from blood into the interstitial space of a tumoral node. A decreased volume of extravascular, extracellular space of metastatic tissue in lymph nodes as compared to that in reactive lymph node tissue further contributes to the slower leakage and wash out of contrast agents in malignant nodes.

A major drawback of the DCE-MRI is the region of interest analysis method, although embedded in the dynamic contrast-enhanced MR imaging literature. Liney et al. retrospectively evaluated three distinct methods of region of interest selection in lymph nodes in breast cancer patients [48]. Each method returned differing values, showing that further work in this area aiming at increasing reproducibility is obviously needed.

Gadofluorine M

Gadofluorine M (Bayer Schering Pharma, Berlin, Germany) is a MR contrast agent, still in preclinical phase, which in a rabbit models has shown to be effective for the detection of nodal metastases [40, 49]. The main mechanism of Gadofluorine uptake

in lymph nodes is assumed to be direct transcapillary passage through interendothelial junctions into the medullary sinuses [40]. Functional lymph node tissue is depicted with Gadofluorine M enhanced T1-weighted MR images with rapid and homogeneous enhancement, while metastatic tissue is depicted with little or no enhancement. This time of peak enhancement is observed between 5-30 minutes after injection of gadofluorine M [40]. The step for Gadofluorine from preclinical into clinical studies still needs to be taken and therefore, at the time of writing, its role in clinical decision-making remains unknown.

Vasovist®

Recently Vasovist® (Gadovosfeset Trisodium, Bayer Schering Pharma, Berlin, Germany) has been introduced and approved as Gd based blood pool MR contrast agent for vascular MR imaging. Gadovosfeset Trisodium Vasovist® is a formulation of a stable gadolinium diethylenetriaminepentaacetic acid (Gd-DTPA) chelate substituted with a diphenylcyclohexylphosphate group (gadofosveset trisodium and binds reversible to the human protein albumin. A recent study in a rabbit model has shown that interstitial MR lymphography was feasible using Vasovist® contrast agent [8]. Malignant nodes in this rabbit model showed a longer time to peak enhancement and reduced peak enhancement than benign nodes. So far no human studies in cancer lymph node metastases have been published. A pilot study in rectal cancer patients is presently ongoing in our center to validate the diagnostic accuracy of Vasovist® enhanced MRI for the prediction of lymph nodes (see Figure 3.4). If this study shows promising results for Vasovist®, larger multicenter, multicancer studies are needed to establish its role in lymph node imaging.

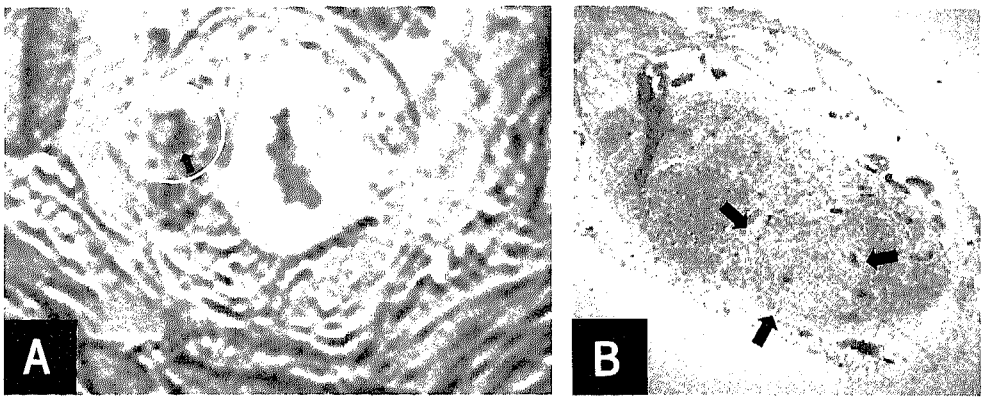

Figure 3.4. (A) 3D T1 Gradient Recalled Echo image in the axial plane of the pelvis in a rectal cancer patient. 17 Minutes after Vasovist® administration the 7 mm mesorectal lymph node (white circle) shows a heterogeneous pattern of enhancement. One region within the lymph node showed no enhancement (arrow), (B) this corresponds with tumor deposit (arrows) found at the histopathological examination (HE staining).

Conclusion

In the past two decades treatment of oncology patients has evolved from palliative into curative, from single into multimodality treatment options, the latter combining surgery with pre- or postoperative systemic and or radiotherapy. Unfortunately, a more aggressive treatment scheme in all cancer patients puts the patient at risk for increased perioperative morbidity and mortality. More individual based tailored treatment based on stratification of high risk versus low risk patients are now being adopted in rectal cancer. Preoperative selection of these patients for a tailored treatment can only be made when more reliable selection tools than the existing ones will become available.

Staging by clinical examination only does not reach a high level of accuracy for selecting these patients. The simultaneous advancement in imaging techniques during the past decade, providing morphological and functional information in one single examination, offers clinicians nowadays a promising tool to distinguish between the high risk, for whom a multimodality treatment could be the only curative option and the low risk patients for whom local and distant tumor control could be obtained with surgical excision only. This chapter aimed at describing the present

status of modern imaging techniques for identifying nodal disease in high-risk patients focusing on rectal cancer.

At present identifying nodal disease by imaging methods remains a challenge for each radiologist working in the diagnostic oncology field. Nodal prediction with the present imaging modalities, unless combined with invasive and demanding procedures such as fine needle aspiration, cannot be reliably used for clinical decision making. The hope for the future is the development of new PET tracers and new lymph node specific MR contrast agents that will enhance the accuracy of the modern planar imaging techniques and will prove its efficacy not only in expert, but also in general centers. Only then the preoperative selection by imaging methods of the low versus the high-risk oncology patients could have a tremendous effect on clinical decision-making and eventually on treatment outcome.

Take home messages

Preoperative selection of the low versus the high-risk cancer patients not only requires an accurate staging tool for local and distant tumor extent, but also for staging local and distant nodal disease. If such a tool will become available, stratification of the different risk cancer patients based on this prediction tool into a tailor made individual based treatment option might lead to a more cost effective treatment strategy with improved clinical outcome in cancer patients.

Presently available imaging methods for prediction of the N0 and N+ cancer patients are not reliable for preoperative clinical decision-making. In rectal cancer patients, evidence exists that studies are needed to further improve the resolution of modern imaging techniques such as PET or MRI by developing new tracers or contrast agents.

This chapter described some of the most promising techniques for lymph node detection and some of the most promising lymph node specific MR contrast agents such as USPIO, Gadofluorine M and Gadovosfeset Trisodium that, if in future studies will prove to be reproducible and reliable in general setting will improve the level of non-invasive imaging for the detection of nodal disease in cancer patients.

References

1. *Herrera L, Brown MT: Prognostic profile in rectal cancer. Dis Colon Rectum 1994;37:S1-5.*
2. *Sauer R: Adjuvant and neoadjuvant radiotherapy and concurrent radiochemotherapy for rectal cancer. Pathol Oncol Res 2002;8:7-17.*
3. *Valentini V, Coco C, Cellini N, et al.: Ten years of preoperative chemoradiation for extraperitoneal T3 rectal cancer: acute toxicity, tumor response, and sphincter preservation in three consecutive studies. Int J Radiat Oncol Biol Phys 2001;51:371-383.*
4. *Marijnen CA, Kapiteijn E, van de Velde CJ, et al.: Acute side effects and complications after short-term preoperative radiotherapy combined with total mesorectal excision in primary rectal cancer: report of a multicenter randomized trial. J Clin Oncol 2002;20:817-825.*
5. *Peeters KC, van de Velde CJ, Leer JW, et al.: Late side effects of short-course preoperative radiotherapy combined with total mesorectal excision for rectal cancer: increased bowel dysfunction in irradiated patients-a Dutch colorectal cancer group study. J Clin Oncol 2005;23:6199-6206.*
6. *Lahaye MJ, Engelen SM, Nelemans PJ, et al.: Imaging for predicting the risk factors--the circumferential resection margin and nodal disease-of local recurrence in rectal cancer: a meta-analysis. Semin Ultrasound CT MR 2005;26:259-268.*
7. *Monig SP, Baldus SE, Zirbes TK, et al.: Lymph node size and metastatic infiltration in colon cancer. Ann Surg Oncol 1999;6:579-581.*
8. *Herborn CU, Lauenstein TC, Vogt FM, et al.: Interstitial MR lymphography with MS-325: characterization of normal and tumor-invaded lymph nodes in a rabbit model. AJR Am J Roentgenol 2002;179:1567-1572.*
9. *Cabanas RM: An approach for the treatment of penile carcinoma. Cancer 1977;39:456-466.*
10. *Vassallo P, Wernecke K, Roos N, Peters PE: Differentiation of benign from malignant superficial lymphadenopathy: the role of high-resolution US. Radiology 1992;183:215-220.*
11. *Harewood GC, Wiersema MJ, Nelson H, et al.: A prospective, blinded assessment of the impact of preoperative staging on the management of rectal cancer. Gastroenterology 2002;123:24-32.*
12. *Tregnaghi A, De Candia A, Calderone M, et al.: Ultrasonographic evaluation of superficial lymph node metastases in melanoma. Eur J Radiol 1997;24:216-221.*
13. *Rifkin MD, Ehrlich SM, Marks G: Staging of rectal carcinoma: prospective comparison of endorectal US and CT. Radiology 1989;170:319-322.*

14. *Herzog U, von Flue M, Tondelli P, Schuppisser JP: How accurate is endorectal ultrasound in the preoperative staging of rectal cancer? Dis Colon Rectum 1993;36:127-134.*
15. *Akasu T, Sugihara K, Moriya Y, Fujita S: Limitations and pitfalls of transrectal ultrasonography for staging of rectal cancer. Dis Colon Rectum 1997;40:S10-15.*
16. *Kwok H, Bissett IP, Hill GL: Preoperative staging of rectal cancer. Int J Colorectal Dis 2000;15:9-20.*
17. *Shami VM, Parmar KS, Waxman I: Clinical impact of endoscopic ultrasound and endoscopic ultrasound-guided fine-needle aspiration in the management of rectal carcinoma. Dis Colon Rectum 2004;47:59-65.*
18. *Marusch F, Koch A, Schmidt U, et al.: Routine use of transrectal ultrasound in rectal carcinoma: results of a prospective multicenter study. Endoscopy 2002;34:385-390.*
19. *Bhutani MS: Recent developments in the role of endoscopic ultrasonography in diseases of the colon and rectum. Curr Opin Gastroenterol 2007;23:67-73.*
20. *Kim JC, Kim HC, Yu CS, et al.: Efficacy of 3-dimensional endorectal ultrasonography compared with conventional ultrasonography and computed tomography in preoperative rectal cancer staging. Am J Surg 2006;192:89-97.*
21. *Hunerbein M, Schlag PM: Three-dimensional endosonography for staging of rectal cancer. Ann Surg 1997;225:432-438.*
22. *Hünerbein, Pegios W, Rau, et al.: Prospective comparison of endorectal ultrasound, three-dimensional endorectal ultrasound, and endorectal MRI in the preoperative evaluation of rectal tumors Preliminary results. Surgical Endoscopy 2000.*
23. *Kim NK, Kim MJ, Yun SH, et al.: Comparative study of transrectal ultrasonography, pelvic computerized tomography, and magnetic resonance imaging in preoperative staging of rectal cancer. Dis Colon Rectum 1999;42:770-775.*
24. *Netri G, Coco C, Valentini V, et al.: Clinical staging of rectal cancer. Results of a prospective continuing study. Ital J Surg Sci 1985;15:169-174.*
25. *Zheng G, Johnson RJ, Eddleston B, et al.: Computed tomographic scanning in rectal carcinoma. J R Soc Med 1984;77:915-920.*
26. *Balthazar EJ, Megibow AJ, Hulnick D, Naidich DP: Carcinoma of the colon: detection and preoperative staging by CT. AJR Am J Roentgenol 1988;150:301-306.*
27. *Sinha R, Verma R, Rajesh A, Richards CJ: Diagnostic value of multidetector row CT in rectal cancer staging: comparison of multiplanar and axial images with histopathology. Clin Radiol 2006;61:924-931.*
28. *Abdel-Nabi H, Doerr RJ, Lamonica DM, et al.: Staging of primary colorectal carcinomas with fluorine-18 fluorodeoxyglucose whole-body PET: correlation with histopathologic and CT findings. Radiology 1998;206:755-760.*
29. *Llamas-Elvira JM, Rodriguez-Fernandez A, Gutierrez-Sainz J, et al.: Fluorine-18*

fluorodeoxyglucose PET in the preoperative staging of colorectal cancer. Eur J Nucl Med Mol Imaging 2007;34:859-867.

30. *Tateishi U, Maeda T, Morimoto T, et al.: Non-enhanced CT versus contrast-enhanced CT in integrated PET/CT studies for nodal staging of rectal cancer. Eur J Nucl Med Mol Imaging 2007;34:1627-1634.*
31. *Will O, Purkayastha S, Chan C, et al.: Diagnostic precision of nanoparticle-enhanced MRI for lymph-node metastases: a meta-analysis. Lancet Oncol 2006;7:52-60.*
32. *Thaler W, Watzka S, Martin F, et al.: Preoperative staging of rectal cancer by endoluminal ultrasound vs. magnetic resonance imaging. Preliminary results of a prospective, comparative study. Dis Colon Rectum 1994;37:1189-1193.*
33. *McNicholas MM, Joyce WP, Dolan J, et al.: Magnetic resonance imaging of rectal carcinoma: a prospective study. Br J Surg 1994;81:911-914.*
34. *Hodgman CG, MacCarty RL, Wolff BG, et al.: Preoperative staging of rectal carcinoma by computed tomography and 0.15T magnetic resonance imaging. Preliminary report. Dis Colon Rectum 1986;29:446-450.*
35. *Schnall M, Furth E, Rosato E, Kressel H: Rectal tumor stage: correlation of endorectal MR imaging and pathologic findings. Radiology 1994;190:709-714.*
36. *Kim JH, Beets GL, Kim MJ, et al.: High-resolution MR imaging for nodal staging in rectal cancer: are there any criteria in addition to the size? Eur J Radiol 2004;52:78-83.*
37. *Brown G, Richards CJ, Bourne MW, et al.: Morphologic Predictors of Lymph Node Status in Rectal Cancer with Use of High-Spatial-Resolution MR Imaging with Histopathologic Comparison. Radiology 2003;227:371-377.*
38. *Winter L, Bruhn H, Langrehr J, et al.: Magnetic resonance imaging in suspected rectal cancer: determining tumor localization, stage, and sphincter-saving resectability at 3-Tesla-sustained high resolution. Acta Radiol 2007;48:379-387.*
39. *Kim CK, Kim SH, Chun HK, et al.: Preoperative staging of rectal cancer: accuracy of 3-Tesla magnetic resonance imaging. Eur Radiol 2006;16:972-980.*
40. *Misselwitz B, Platzek J, Weinmann HJ: Early MR lymphography with gadofluorine M in rabbits. Radiology 2004;231:682-688.*
41. *Weissleder R, Elizondo G, Wittenberg J, et al.: Ultrasmall superparamagnetic iron oxide: an intravenous contrast agent for assessing lymph nodes with MR imaging. Radiology 1990;175:494-498.*
42. *Anzai Y, McLachlan S, Morris M, et al.: Dextran-coated superparamagnetic iron oxide, an MR contrast agent for assessing lymph nodes in the head and neck. AJNR Am J Neuroradiol 1994;15:87-94.*
43. *Harisinghani MG, Barentsz J, Hahn PF, et al.: Noninvasive detection of clinically occult lymph-node metastases in prostate cancer. N Engl J Med 2003;348:2491-2499.*
44. *Koh D-M, Brown G, Temple L, et al.: Rectal Cancer: Mesorectal Lymph Nodes at MR*

Imaging with USPIO versus Histopathologic Findings-Initial Observations. Radiology 2004;231:91-99.

45. *Kvistad KA, Rydland J, Smethurst HB, et al.: Axillary lymph node metastases in breast cancer: preoperative detection with dynamic contrast-enhanced MRI. Eur Radiol 2000;10:1464-1471.*

46. *Fischbein NJ, Noworolski SM, Henry RG, et al.: Assessment of metastatic cervical adenopathy using dynamic contrast-enhanced MR imaging. AJNR Am J Neuroradiol 2003;24:301-311.*

47. *de Lussanet QG, Backes WH, Griffioen AW, et al.: Dynamic contrast-enhanced magnetic resonance imaging of radiation therapy-induced microcirculation changes in rectal cancer. Int J Radiat Oncol Biol Phys 2005;63:1309-1315.*

48. *Liney GP, Gibbs P, Hayes C, et al.: Dynamic contrast-enhanced MRI in the differentiation of breast tumors: user-defined versus semi-automated region-of-interest analysis. J Magn Reson Imaging 1999;10:945-949.*

49. *Choi SH, Han MH, Moon WK, et al.: Cervical lymph node metastases: MR imaging of gadofluorine M and monocrystalline iron oxide nanoparticle-47 in a rabbit model of head and neck cancer. Radiology 2006;241:753-762.*

IMAGING FOR PREDICTING THE RISK FACTORS -CIRCUMFERENTIAL RESECTION MARGIN AND NODAL DISEASE- OF LOCAL RECURRENCE IN RECTAL CANCER: A META-ANALYSIS

PUBLISHED IN *SEMINARS IN US, CT & MRI 2005; VOLUME 26, ISSUE 4, PAGES 259-68*

M.J. LAHAYE

S.M.E. ENGELEN

P.J. NELEMANS

G.L. BEETS

C.J.H. VAN DE VELDE

J.M.A. VAN ENGELSHOVEN

AND R.G.H. BEETS-TAN

4

Purpose

The aim of the present study was to conduct a meta-analysis of English literature on the accuracy of preoperative imaging in predicting the two most important risk factors for local recurrence in rectal cancer, the circumferential resection margin (CRM) and the nodal status (N-status).

Materials and methods

Articles published between 1985 and August 2004 that report on the diagnostic accuracy of endoluminal ultrasound (EUS), computed tomography (CT), or magnetic resonance imaging (MRI) in the evaluation of lymph node involvement were included. A similar search was done for the assessment of the circumferential resection margin in rectal cancer in the period from January 1985 till January 2005. The inclusion criteria were as follows: (1) more than 20 patients with histological proven rectal cancer were included, (2) histology was used as the gold standard, and (3) results were given in a 2 x 2 contingency table or this table could otherwise be extracted from the article by two independent readers. Based on the results summary receiver-operating characteristic (ROC) curves were constructed.

Results

Only 7 articles matching inclusion criteria were found concerning the CRM. The meta-analysis shows that MRI is rather accurate in diagnosing a close or involved CRM. For nodal status 84 articles could be included. The diagnostic odds ratio of EUS is estimated at 8.83. For MRI and CT, the diagnostic odds ratio were 6.53 and 5.86, respectively. The results show that EUS is slightly, but not significantly, better than MRI or CT for identification of nodal disease. There is no significant difference between the different modalities with respect to staging nodal status.

Conclusion

At present, MRI is the only modality that predicts the circumferential resection margin with good accuracy, making it a good tool to identify high and low risk patients. Predicting the N-status remains a problem for the radiologist for every modality, although considering the new developments in MR imaging, this may change in the near future.

Introduction

Rectal cancer surgery has been plagued traditionally by a high and variable incidence of local recurrence (5-55%), a variability that is related to the quality and technique of the surgical procedure [1]. After the introduction of a standardized surgical technique, the so-called total mesorectal excision (TME), which completely removes the entire mesorectal compartment including the rectum, surrounding mesorectal fat, perirectal lymph nodes and its border; the mesorectal fascia, consistently low local recurrence rates of below 10% were reported [2]. Both adjuvant and neoadjuvant (chemo)radiotherapy have also been shown to reduce the local recurrence rates. However, there is accumulating evidence that (chemo)radiotherapy is more effective preoperatively than postoperatively. As a result, there is a growing need to select patients at risk for a local recurrence before the operation on a basis of imaging rather than the traditional histological examination after the operation. The two foremost important factors that influence local recurrence rates are the local tumor extent and the nodal status as illustrated in Figures 4.1 and 4.2 [3]. The local tumor extent is traditionally classified through the pathological T-staging system, with T3 and T4 tumors being considered to have a high risk for local recurrence. The actual distance of the tumor to the circumferential resection plane, the circumferential margin (CRM), has also repetitively been shown a very important predictor for local recurrence [4-6]. The T-stage does not inherently discriminate between T3 tumors that can easily be resected with a wide resection margin and T3 tumors with a close or involved CRM, which have a much higher likelihood of a positive resection margin, as illustrated in Figure 4.3. The mesorectal fascia, the resection plane of a total mesorectal excision, has never been the focus of attention of radiologists, as its importance had not been recognized and visualized until 1999 [7]. A recent meta-analysis of Bipat et al. [8] evaluates the role of endoluminal ultrasound (EUS), computed tomography (CT), and magnetic resonance imaging (MRI) in the prediction of the T-stage and the N-status. EUS was found to be the most accurate modality when compared with CT and MR imaging for evaluation of T-stage of rectal cancer. For lymph node involvement, the results of EUS, CT, and MRI were comparable, nonetheless with low sensitivity values. In this meta-analysis, the more important prognostic factor of distance of the tumor to the mesorectal fascia, or the anticipated CRM, was not evaluated.

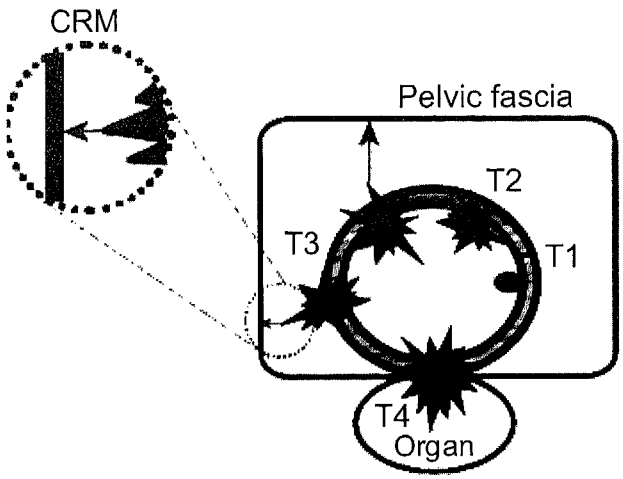

Figure 4.1. The T-stage does not inherently discriminate between T3 tumors that can easily be resected with a wide resection margin and T3 tumors with a close or involved CRM, which have a much higher likelihood of a positive resection margin.

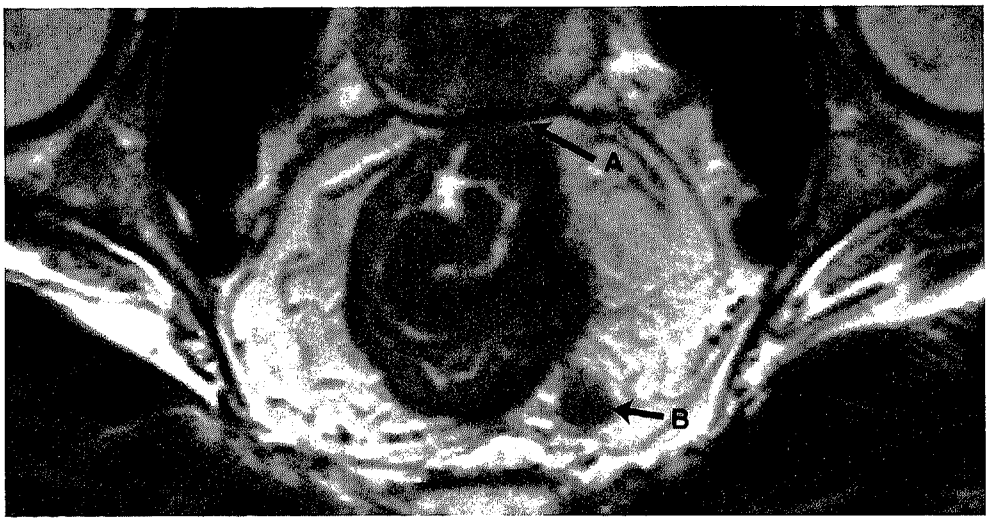

Figure 4.2. T3 rectal cancer with an involved CRM with a tumor deposit in a 44-year-old male patient. Coronal T2W FSE (TR/TE 3427/150 msec) MR image shows a tumor in the rectal wall. This figure shows both most important prognostic factors. Anteriorly the tumor minimally invades the mesorectal fascia (A). In addition, a tumor deposit is seen in the mesorectum (B).

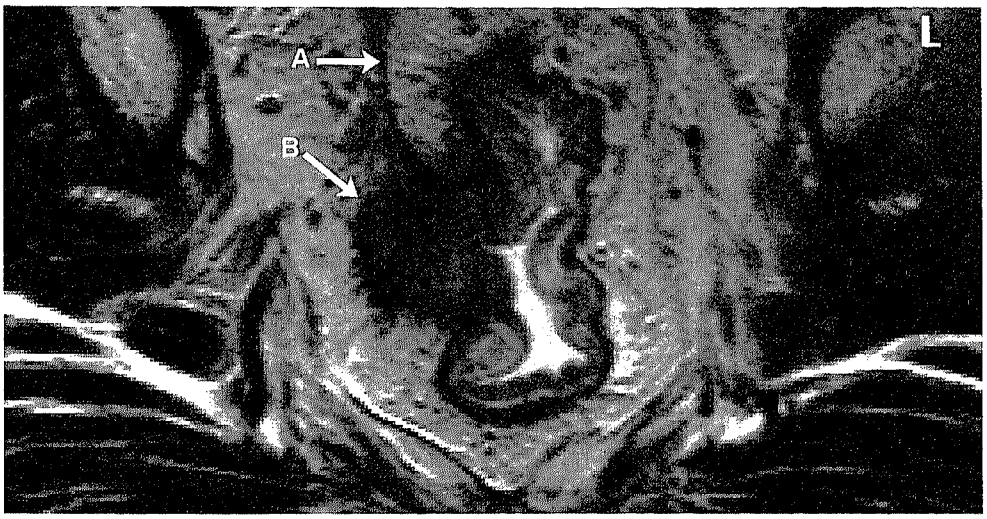

Figure 4.3. T4 rectal cancer with an obvious involved circumferential resection margin in a 45-year-old male patient. Axial T2W FSE (TR/TE 3427/150 msec) MR image shows a tumor in the rectal wall. A well visualized mesorectal fascia (A). The tumor aggressively invades the mesorectal fascia and invades deep in the extramesorectal tissue (B).

Furthermore, since the publication of the meta-analysis of Bipat et al. [8], a number of new studies on the prediction of lymph node status have been published. The aim of the present study is to conduct a meta-analysis of literature on the accuracy of preoperative imaging in predicting the two most important risk factors for local recurrence in rectal cancer; the CRM and the nodal status.

Materials and methods

Study selection

All English language articles published from January 1985 through August 2004 that report on diagnostic accuracy of EUS, CT, or MR in the evaluation of lymph node involvement, as retrieved via a MEDLINE search, were included. A similar search was done for the assessment of the circumferential resection margin in rectal cancer in the period from January 1985 till January 2005. The search terms used were: rectal

cancer, rectal neoplasms, rectal carcinoma combined with terms such as imaging, lymph node, circumferential resection margin, ultrasound, magnetic resonance imaging, tomography, and staging. Additional articles were obtained by citation tracking of all articles. Inclusion criteria were as follows: (1) more than 20 patients with histological proven rectal cancer were included, (2) histology was the gold standard and (3) results were given in a 2 x 2 contingency table or this table could otherwise be extracted from the article. Only original articles were used. If the data were published more than once, the most detailed study was used.

Data extraction

A standard form was used to extract relevant data from the retrieved studies. Recorded were modality, number of patients, study design characteristics and examination results. The examination characteristics such as type of imaging technique use of contrast agents and recruitment period (as an indication of technological advances) were documented. Important characteristics of the study design were whether patients were included consecutively, blinding versus not blinding of readers of EUS, CT, and MRI for the histology reports, prospective versus retrospective study design, and the percentage of patients with imaging results for whom histology as gold standard was available. The examination results were documented in a 2 x 2 contingency table. True positive (TP), false negative (FN), true negative (TN) and false positive (FP) test results were directly available in articles or could sometimes be derived from the marginal totals or reported sensitivity and specificity. Two investigators (M.J.L. and S.M.E.) individually documented the examination characteristics and results.

Statistical analysis

Based on the results derived from 2 x 2 contingency tables, summary receiver operating characteristic (ROC) curves were constructed according to the method described by Moses and Littenberg [9]. This method is described briefly in the Appendix. The method also allows for the calculation of diagnostic odds ratios for

EUS, CT, and MRI. The diagnostic odds ratio (DOR) is a measure for the diagnostic performance of a test, which combines sensitivity and specificity into one measure [10]. It represents the odds of a positive test result among people with the target disorder relative to the odds of a positive test result among people without the target disorder. A DOR of 1 implies that the test has no discriminatory power at all; the larger the DOR, the better the test discriminates between patients with and without the target disorder (in this chapter, lymph node involvement or CRM involvement).
It must be noted that summary ROC curves differ from ROC curves. In ROC curves, sensitivity is plotted against the corresponding false positive rate (1-specificity) for different cut-off points for a positive test result within one study. Summary ROC curves are constructed by fitting a curve through pairs of sensitivity and specificity, which are observed in different studies. Summary ROC curves have the advantage that sensitivity and specificity values reported by studies are considered jointly. Such ROC curves illustrate whether high sensitivity can be reached without too much loss of specificity. Good diagnostic tests are characterized by a ROC curve that is positioned toward the upper left corner. The method takes into account the fact that thresholds for a positive test result are likely to vary between studies. The use of implicit thresholds is very common in the interpretation of radiological imaging techniques. Radiologists may agree to use the same words in describing imaging results but may still differ in what they regard as the boundary between "abnormal" and "normal" findings [11]. If the DOR does not vary with the threshold for a positive test result, the summary ROC curve is symmetrical and test accuracy can be characterized by one odds ratio. If the DOR varies with the threshold for a positive test result, the summary ROC curve will be asymmetrical.

Results

Circumferential resection margin

Only 7 articles concerning the CRM that met the inclusion criteria were found [7, 12-17]. All these articles used MR imaging to depict the CRM. From these articles 7 datasets could be deduced. Two articles were excluded from the study since incomplete or inconclusive data were used to allow calculation of true-positive,

false-negative, true-negative, and false positive findings. Details of the 7 remaining complete datasets are shown in Table 4.1. The summary ROC curve in Figure 4.4 shows that a sensitivity of about 80% is associated with a false positive rate of about 20%, which is rather accurate.

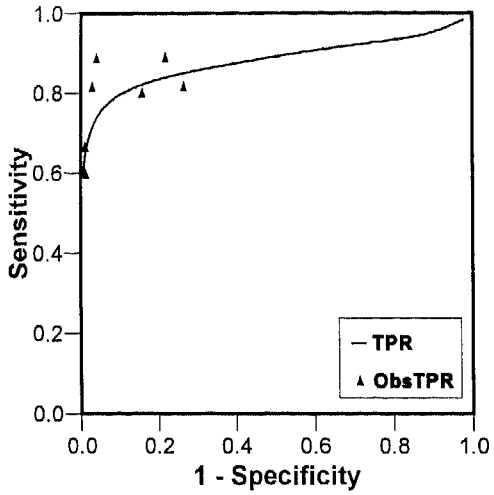

Figure 4.4.
Summary ROC curve illustrating the accuracy of magnetic resonance imaging for assessment of an involved circumferential resection margin.

Table 4.1. An overview of articles concerning the circumferential resection margin included in this meta-analysis.

	Year	N*	Prev	Sens	Spec
Vliegen	2004	83	34	88	96
Martling	2003	99	30	81	73
Mathur	2003	36	5	80	84
Brown	2003	98	5	81	97
Botteril	2001	62	6	60	100
Bisset	2001	40	21	67	100
Blomqvist	1999	26	8	88	78

*Number of patients included with available data on imaging and histology.

Lymph node involvement

Of the 115 articles retrieved 40 articles did not meet the including criteria. Of the 75 included articles 101 datasets were extracted by two independent reviewers (M.L. and S.E.). An overview of the included articles is given in Table 4.2. The diagnostic odds ratio of EUS is 8.83. For CT and MRI the diagnostic odds ratios are 5.86 and 6.53, respectively. The results show that EUS is slightly, but not significantly, better than MRI or CT for identification of nodal disease. There is no significant difference between the different modalities. The summary ROC curves for the three diagnostic modalities, in Figure 4.5, show that high sensitivity cannot be reached without unacceptable high false positive rates.

Table 4.2. An overview of articles concerning N-status staging included in this meta-analysis.

	No. of datasets	No. of patients*	References
EUS	54	3358	[1-49]
MRI	29	1235	[12, 14, 20, 37, 43, 50-69]
CT	18	773	[1, 9, 14, 16, 26, 31, 59, 70-76]

* Number of patients included with available data on imaging and histology.

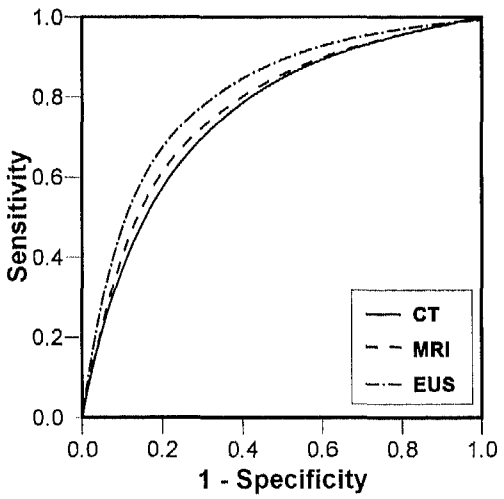

Figure 4.5.
Summary ROC curves comparing the accuracy of endoluminal ultrasound (EUS), computed tomography (CT) and magnetic resonance imaging (MRI) for prediction of N-status.

Discussion

This meta-analysis shows that MRI is rather accurate in diagnosing a close or involved CRM. Assessment of lymph node involvement, however, remains a problem for all three diagnostic modalities. None of the modalities are associated with a DOR that is acceptable from a clinical point of view. Our study shows that EUS is slightly, but not significantly, better than CT or MRI in assessing N-status.

Circumferential resection margin

Incomplete removal of the lateral spread of the tumor has been widely accepted as the cause of the majority of local recurrences [4, 18]. Multiple studies have shown that a close resection margin is a very important prognostic indicator for local recurrence [4, 18, 19]. Quirke et al. [18] have demonstrated that microscopically positive resection margins resulted in a local recurrence rate of 83%. As mentioned before, the T-staging system inherently does not discriminate between T3 tumors that can easily be resected with a wide resection margin and T3 tumors with a close or involved CRM.

So far MRI is the only modality that has been tested for the prediction of the CRM in multiple single center studies [20]. The SPICTRE (Spiral CT in Rectal Cancer) study is a Dutch multicenter study investigating the detection of the CRM with a modern CT technique; at present, however, we are still awaiting results. The present meta-analysis confirms that MRI performs reasonably well in predicting the CRM in rectal cancer surgery. From the individual studies it is unclear how often the information of MRI influenced treatment and how this was dealt with in the analysis. It is quite possible that on the basis of an involved CRM on MRI, some patients have received extensive downsizing neoadjuvant treatment and/or extensive surgery, leading to a negative resection margin on histology. As a consequence, some positive findings on MRI may have been wrongly labeled as "false positive" MR findings, implying that the real accuracy of MRI may even be higher. Whether or not the excellent MR results of single center series are applicable in routine clinical practice has been the subject of a multicenter European study (Mercury Trial). The preliminary results of the Mercury Trial show that MRI can predict the CRM status in a multicenter setting [21].

Lymph node involvement

The present meta-analysis includes 23 additional studies when compared to the study by Bipat et al., but excludes 12 studies, which were included by Bipat et al. [8]. Most of these studies were excluded, because a complete 2 x 2 contingency table could not be extracted from the published data.

Additional to the well-known and recognized risk factor that is associated with distant metastases, the N-status is a prognostic factor for local recurrence. A large multicenter study shows that nodal disease (Stage III) considerably increases the risk for local recurrence with a hazard ratio of almost 10 when compared with Stage I and a hazard ratio of almost 3 when compared to Stage II [22]. The higher the number of positive nodes, the higher the risk [23, 24].

The present study shows that assessment of lymph node involvement remains a problem for all three investigated diagnostic modalities. These findings corroborate earlier findings. Heriot et al. [25] reported in a meta-analysis that none of the imaging methods could accurately detect lymph node metastases, with endoluminal ultrasonography being the best modality. A recent meta-analysis by Bipat et al. [8] also showed no significant differences between the three modalities, EUS, CT or MRI, which were all associated with low sensitivities but with a slight, but not significant, advantage for EUS. Because of the inferior contrast resolution, CT can only rely on size criteria, and size on its own is insufficient to reliably distinguish between malignant and benign lymph nodes [26]. Inaccurate staging due to inferior contrast resolution of CT is illustrated in Figures 4.6 and 4.7. Brown et al. [27] showed that 3- or 5-mm large lymph nodes still had a prevalence of positive lymph nodes of 10% and 28%, respectively. EUS uses both size and echogenic features to determine the malignant potential of lymph nodes. This explains the slightly (and non significantly) better results for EUS in this meta-analysis. In most of the studies evaluating MR, again size was also used as the main criterion. MRI, however, has an inherent superior contrast resolution, and other criteria such as the aspect of the lymph node border and the signal intensity of the node can be used to predict lymph node involvement in patients with rectal cancer. Some studies using these additional criteria have indeed shown improved accuracy [27, 28].

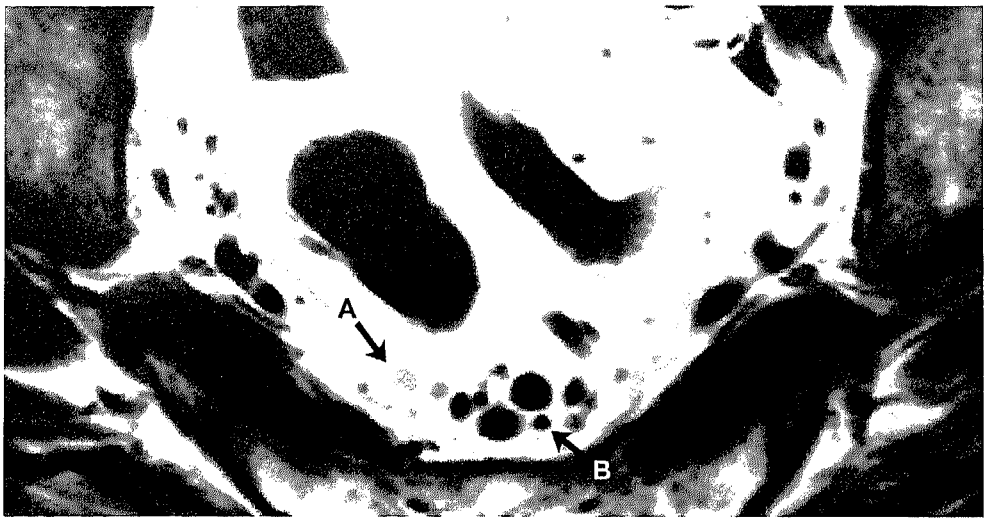

Figure 4.6A. Axial T2W FSE (TR/TE 3427/150 msec) MR image shows multiple lymph nodes, which clearly differ in signal intensity in 62-year-old female patient with rectal cancer. A large involved lymph node with a high signal intensity (A). Multiple small and large reactive lymph nodes with a low signal intensity (B). MRI is able to discriminate between metastatic and reactive lymph nodes because of the high contrast resolution.

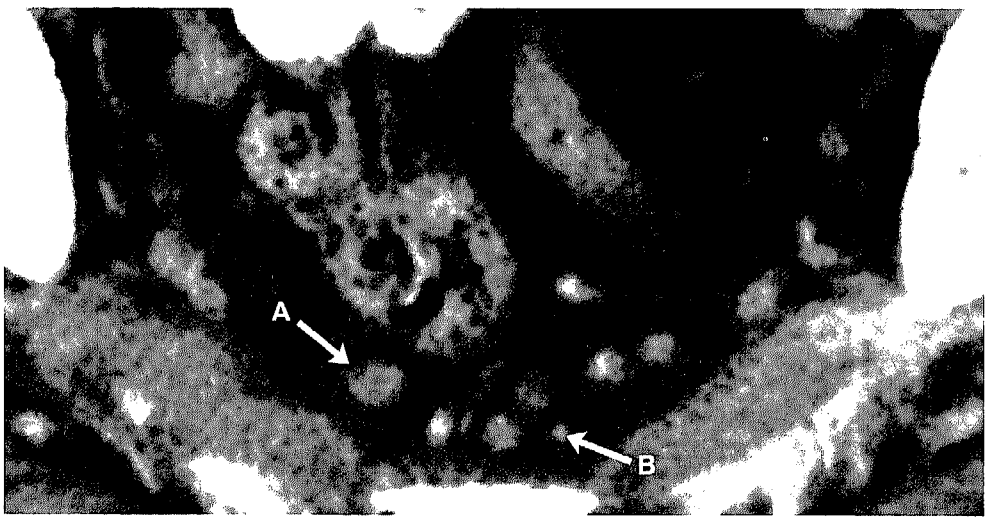

Figure 4.6B. Corresponding CT scan of the same female patient as Figure 4.6A. Discrimination between the involved lymph node (A) and the reactive lymph nodes (B) is impossible, due to lack of contrast resolution.

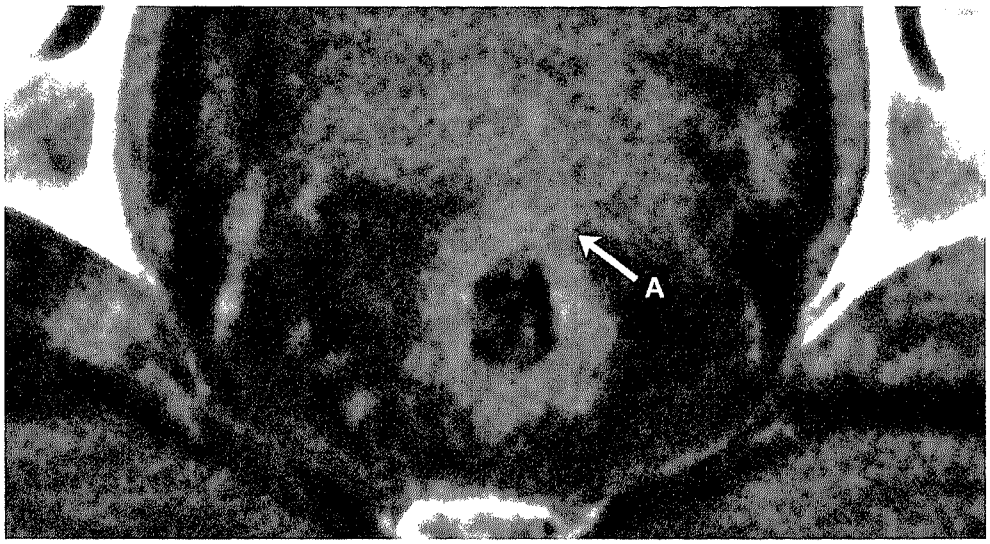

Figure 4.7A. Axial contrast enhanced CT shows a locally advanced rectal cancer invading the mesorectal fascia and the seminal vesicles (A).

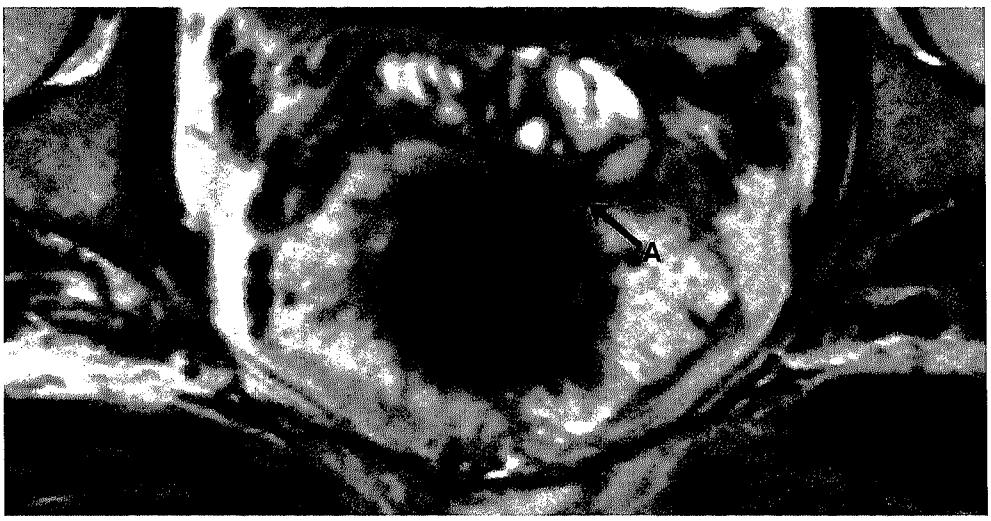

Figure 4.7B. Corresponding axial T2W FSE (TR/TE 3427/150 ms) MR image shows that the tumor is invading the mesorectal fascia but not the seminal vesicles (A). So the tumor had been over staged by CT again due to lack of contrast resolution.

Other imaging techniques, such as EUS guided fine needle aspiration and computed tomography/positron emission tomography (CT-PET), have not been included in the present meta-analysis because of the limited number of studies. EUS guided fine needle aspiration has been reported to be a very reliable method, with accuracies up to 100% [29, 30]. A major drawback of this method is the invasiveness of the procedure and the skill that is required. Wide acceptance of this procedure seems to be improbable. The few preliminary publications on CT-PET show disappointing results for N-staging in rectal cancer. Heriot et al. [31] demonstrated a sensitivity of only 29% for predicting lymph node involvement. This can be explained by the recognized limitation of CT-PET in detection of low-bulk disease.

The present imaging modalities are not able to accurately detect nodal metastases in rectal cancer. Evidently, further research must be done to investigate new methods to improve staging lymph node involvement in rectal cancer. In the pursuit of more accurate lymph node staging, the radiologist is pushed forward by new developments. New MRI contrast agents, such as ultrasmall super paramagnetic iron oxide (USPIO), will, hopefully, help improve sensitivity and specificity for nodal involvement. There are only a few studies on the use of USPIO in the detection of nodal metastases in rectal cancer; nevertheless, they show promising results [32,33].

Conclusions

When radiologists are able to accurately predict the risk factors for local recurrence, involved CRM, and nodal status, low risk groups can be distinguished from high-risk groups. Clinicians can then tailor the treatment to the individual patient, varying from surgery only to extensive neoadjuvant (chemo)radiotherapy. At present, MRI is the only modality that predicts the circumferential resection margin with good accuracy. Predicting the N-status remains a problem for the radiologist, although with the new developments in MR imaging, this may change in the near future.

Appendix

A method for fitting a summary ROC curve through pairs of sensitivity and specificity derived from individual studies has been described by Moses et al. [109]. Sensitivity is equal to the true positive rate (TPR) and 1-specificity is equal to the false positive rate (FPR). The method is based on the principle that there is a linear relationship between logit (TPR) and logit (FPR), where using natural logs,

logit (TPR) = log (TPR / (1 - TPR)) and

logit (FPR) = log (FPR / (1 - FPR))

For each study the following variables were calculated:

D = logit (TPR) - logit (FPR)

S = logit (TPR) - logit (FPR)

where D represents the natural logarithm of the diagnostic odds ratio (log DOR) and S is a function of the threshold for a positive test result. Next, the relationship between D and S can be estimated by the linear regression model.

$D = a + b0 \times S$

The intercept of the model (a) is the estimated log DOR when S+0; the regression coefficient provides an estimate of the extent to which the log DOR depends on the threshold (for a positive test result) used. The regression coefficient b0 for S determines the asymmetry of the summary ROC curve. If the coefficient equals zero, the curve is symmetrical. The model can be transformed back to the conventional axes of TPR against FPR according to a formula given by Moses et al. [109]. For this review, we extended the model by adding two dummy variables representing CT and MRI, respectively. US was used as the reference test, because the largest number of studies was available for US.

$D = a + b0 \times S + b1 \times CT + b2 \times MRI$

After fitting this model to the data, the intercept and regression coefficients were estimated. The intercept (a) defines the log DOR of the reference test US (for S = 0). Adding the regression coefficient for CT defines the log DOR for CT (for S = 0) and adding the regression coefficient for MRI defines the log DOR for MRI (for S = 0). If b0 is small, this term can be omitted from the model. In this case, the log DOR for the compared diagnostic modalities is no longer dependent on S and the diagnostic performance of each modality can be summarized by one diagnostic odds ratio. The diagnostic odds ratios of the modalities are calculated by exponentiation of the log DOR.

References

1. *Hermanek P, Wiebelt H, Staimmer D, Riedl S. Prognostic factors of rectum carcinoma--experience of the German Multicentre Study SGCRC. German Study Group Colo-Rectal Carcinoma. Tumori 1995; 81:60-64.*
2. *Heald RJ, Ryall RD. Recurrence and survival after total mesorectal excision for rectal cancer. Lancet 1986; 1:1479-1482.*
3. *Herrera L, Brown MT. Prognostic profile in rectal cancer. Dis Colon Rectum 1994; 37:S1-5.*
4. *Adam IJ, Mohamdee MO, Martin IG, et al. Role of circumferential margin involvement in the local recurrence of rectal cancer. Lancet 1994; 344:707-711.*
5. *Wibe A, Rendedal PR, Svensson E, et al. Prognostic significance of the circumferential resection margin following total mesorectal excision for rectal cancer. Br J Surg 2002; 89:327-334.*
6. *Nagtegaal ID, Marijnen CA, Kranenbarg EK, van de Velde CJ, van Krieken JH. Circumferential margin involvement is still an important predictor of local recurrence in rectal carcinoma: not one millimeter but two millimeters is the limit. Am J Surg Pathol 2002; 26:350-357.*
7. *Blomqvist L, Rubio C, Holm T, Machado M, Hindmarsh T. Rectal adenocarcinoma: assessment of tumour involvement of the lateral resection margin by MRI of resected specimen. Br J Radiol 1999; 72:18-23.*
8. *Bipat S, Glas AS, Slors FJ, Zwinderman AH, Bossuyt PM, Stoker J. Rectal cancer: local staging and assessment of lymph node involvement with endoluminal US, CT, and MR imaging--a meta-analysis. Radiology 2004; 232:773-783.*
9. *Moses LE, Shapiro D, Littenberg B. Combining independent studies of a diagnostic test into a summary ROC curve: data-analytic approaches and some additional considerations. Stat Med 1993; 12:1293-1316.*
10. *Glas AS, Lijmer JG, Prins MH, Bonsel GJ, Bossuyt PM. The diagnostic odds ratio: a single indicator of test performance. J Clin Epidemiol 2003; 56:1129-1135.*
11. *Irwig L, Tosteson AN, Gatsonis C, et al. Guidelines for meta-analyses evaluating diagnostic tests. Ann Intern Med 1994; 120:667-676.*
12. *Vliegen RF, Beets GL, von Meyenfeldt MF, et al. Rectal cancer: MR imaging in local staging--is gadolinium-based contrast material helpful? Radiology 2005; 234:179-188.*
13. *Martling A, Holm T, Bremmer S, Lindholm J, Cedermark B, Blomqvist L. Prognostic value of preoperative magnetic resonance imaging of the pelvis in rectal cancer. Br J Surg 2003; 90:1422-1428.*
14. *Mathur P, Smith JJ, Ramsey C, et al. Comparison of CT and MRI in the pre-operative staging of rectal adenocarcinoma and prediction of circumferential resection margin*

involvement by MRI. Colorectal Dis 2003; 5:396-401.

15. *Brown G, Radcliffe AG, Newcombe RG, Dallimore NS, Bourne MW, Williams GT. Preoperative assessment of prognostic factors in rectal cancer using high-resolution magnetic resonance imaging. Br J Surg 2003; 90:355-364.*
16. *Botterill ID, Blunt DM, Quirke P, et al. Evaluation of the role of pre-operative magnetic resonance imaging in the management of rectal cancer. Colorectal Dis 2001; 3:295-303.*
17. *Bissett IP, Fernando CC, Hough DM, et al. Identification of the fascia propria by magnetic resonance imaging and its relevance to preoperative assessment of rectal cancer. Dis Colon Rectum 2001; 44:259-265.*
18. *Quirke P, Durdey P, Dixon MF, Williams NS. Local recurrence of rectal adenocarcinoma due to inadequate surgical resection. Histopathological study of lateral tumour spread and surgical excision. Lancet 1986; 2:996-999.*
19. *Birbeck KF, Macklin CP, Tiffin NJ, et al. Rates of circumferential resection margin involvement vary between surgeons and predict outcomes in rectal cancer surgery. Ann Surg 2002; 235:449-457.*
20. *Beets-Tan RG, Beets GL, Vliegen RF, et al. Accuracy of magnetic resonance imaging in prediction of tumour-free resection margin in rectal cancer surgery. Lancet 2001; 357:497-504.*
21. *Strassburg J. Magnetic resonance imaging in rectal cancer: the MERCURY experience. Tech Coloproctol 2004; 8 Suppl 1:s16-18.*
22. *Kapiteijn E, Marijnen CA, Nagtegaal ID, et al. Preoperative radiotherapy combined with total mesorectal excision for resectable rectal cancer. N Engl J Med 2001; 345:638-646.*
23. *Moran MR, James EC, Rothenberger DA, Goldberg SM. Prognostic value of positive lymph nodes in rectal cancer. Dis Colon Rectum 1992; 35:579-581.*
24. *Park YJ, Park KJ, Park JG, Lee KU, Choe KJ, Kim JP. Prognostic factors in 2230 Korean colorectal cancer patients: analysis of consecutively operated cases. World J Surg 1999; 23:721-726.*
25. *Heriot AG, Grundy A, Kumar D. Preoperative staging of rectal carcinoma. Br J Surg 1999; 86:17-28.*
26. *Kotanagi H, Fukuoka T, Shibata Y, et al. The size of regional lymph nodes does not correlate with the presence or absence of metastasis in lymph nodes in rectal cancer. J Surg Oncol 1993; 54:252-254.*
27. *Brown G, Richards CJ, Bourne MW, et al. Morphologic Predictors of Lymph Node Status in Rectal Cancer with Use of High-Spatial-Resolution MR Imaging with Histopathologic Comparison. Radiology 2003; 227:371-377.*
28. *Kim JH, Beets GL, Kim MJ, Kessels AG, Beets-Tan RG. High-resolution MR imaging for nodal staging in rectal cancer: are there any criteria in addition to the size? Eur J Radiol 2004; 52:78-83.*

29. *Saha S, Wiese D, Badin J, et al. Technical details of sentinel lymph node mapping in colorectal cancer and its impact on staging. Ann Surg Oncol 2000; 7:120-124.*
30. *Shami VM, Parmar KS, Waxman I. Clinical impact of endoscopic ultrasound and endoscopic ultrasound-guided fine-needle aspiration in the management of rectal carcinoma. Dis Colon Rectum 2004; 47:59-65.*
31. *Heriot AG, Hicks RJ, Drummond EG, et al. Does positron emission tomography change management in primary rectal cancer? A prospective assessment. Dis Colon Rectum 2004; 47:451-458.*
32. *Bellin MF, Roy C, Kinkel K, et al. Lymph node metastases: safety and effectiveness of MR imaging with ultrasmall superparamagnetic iron oxide particles--initial clinical experience. Radiology 1998; 207:799-808.*
33. *Koh D-M, Brown G, Temple L, et al. Rectal Cancer: Mesorectal Lymph Nodes at MR Imaging with USPIO versus Histopathologic Findings--Initial Observations. Radiology 2004; 231:91-99.*
34. *Rifkin MD, Wechsler RJ. A comparison of computed tomography and endorectal ultrasound in staging rectal cancer. Int J Colorectal Dis 1986; 1:219-223.*
35. *Cho E, Nakajima M, Yasuda K, Ashihara T, Kawai K. Endoscopic ultrasonography in the diagnosis of colorectal cancer invasion. Gastrointest Endosc 1993; 39:521-527.*
36. *Norton SA, Thomas MG. Staging of rectosigmoid neoplasia with colonoscopic endoluminal ultrasonography. Br J Surg 1999; 86:942-946.*
37. *Beynon J. An evaluation of the role of rectal endosonography in rectal cancer. Ann R Coll Surg Engl 1989; 71:131-139.*
38. *Boyce GA, Sivak MV, Jr., Lavery IC, et al. Endoscopic ultrasound in the pre-operative staging of rectal carcinoma. Gastrointest Endosc 1992; 38:468-471.*
39. *Steele SR, Martin MJ, Place RJ. Flexible endorectal ultrasound for predicting pathologic stage of rectal cancers. Am J Surg 2002; 184:126-130.*
40. *Fedyaev EB, Volkova EA, Kuznetsova EE. Transrectal and transvaginal ultrasonography in the preoperative staging of rectal carcinoma. Eur J Radiol 1995; 20:35-38.*
41. *Nielsen MB, Pedersen JF, Christiansen J. Rectal endosonography in the evaluation of stenotic rectal tumors. Dis Colon Rectum 1993; 36:275-279.*
42. *Harewood GC, Wiersema MJ, Nelson H, et al. A prospective, blinded assessment of the impact of preoperative staging on the management of rectal cancer. Gastroenterology 2002; 123:24-32.*
43. *Adams DR, Blatchford GJ, Lin KM, Ternent CA, Thorson AG, Christensen MA. Use of preoperative ultrasound staging for treatment of rectal cancer. Dis Colon Rectum 1999; 42:159-166.*
44. *Akahoshi K, Kondoh A, Nagaie T, et al. Preoperative staging of rectal cancer using a 7.5 MHz front-loading US probe. Gastrointest Endosc 2000; 52:529-534.*

45. *Starck M, Bohe M, Fork FT, Lindstrom C, Sjoberg S. Endoluminal ultrasound and low-field magnetic resonance imaging are superior to clinical examination in the preoperative staging of rectal cancer. Eur J Surg 1995; 161:841-845.*
46. *Lindmark G, Kraaz W, Elvin P, Glimelius B. Rectal cancer: evaluation of staging with endosonography. Radiology 1997; 204:533-538.*
47. *Kim NK, Kim MJ, Yun SH, Sohn SK, Min JS. Comparative study of transrectal ultrasonography, pelvic computerized tomography, and magnetic resonance imaging in preoperative staging of rectal cancer. Dis Colon Rectum 1999; 42:770-775.*
48. *Herzog U, von Flue M, Tondelli P, Schuppisser JP. How accurate is endorectal ultrasound in the preoperative staging of rectal cancer? Dis Colon Rectum 1993; 36:127-134.*
49. *Holdsworth PJ, Johnston D, Chalmers AG, et al. Endoluminal ultrasound and computed tomography in the staging of rectal cancer. Br J Surg 1988; 75:1019-1022.*
50. *Tada M, Endo M. Ultrasonographic examination for lateral lymphatic spread and local recurrence of rectal cancer. Preoperative detection and evaluation. Dis Colon Rectum 1995; 38:1047-1052.*
51. *Dershaw DD, Enker WE, Cohen AM, Sigurdson ER. Transrectal ultrasonography of rectal carcinoma. Cancer 1990; 66:2336-2340.*
52. *Hildebrandt U, Klein T, Feifel G, Schwarz HP, Koch B, Schmitt RM. Endosonography of pararectal lymph nodes. In vitro and in vivo evaluation. Dis Colon Rectum 1990; 33:863-868.*
53. *Thaler W, Watzka S, Martin F, et al. Preoperative staging of rectal cancer by endoluminal ultrasound vs. magnetic resonance imaging. Preliminary results of a prospective, comparative study. Dis Colon Rectum 1994; 37:1189-1193.*
54. *Barbaro B, Schulsinger A, Valentini V, Marano P, Rotman M. The accuracy of transrectal ultrasound in predicting the pathological stage of low-lying rectal cancer after preoperative chemoradiation therapy. International Journal of Radiation Oncology*Biology*Physics 1999; 43:1043-1047.*
55. *Saitoh N, Okui K, Sarashina H, Suzuki M, Arai T, Nunomura M. Evaluation of echographic diagnosis of rectal cancer using intrarectal ultrasonic examination. Dis Colon Rectum 1986; 29:234-242.*
56. *Bernini A, Deen KI, Madoff RD, Wong WD. Preoperative adjuvant radiation with chemotherapy for rectal cancer: its impact on stage of disease and the role of endorectal ultrasound. Ann Surg Oncol 1996; 3:131-135.*
57. *Nielsen MB, Qvitzau S, Pedersen JF, Christiansen J. Endosonography for preoperative staging of rectal tumours. Acta Radiol 1996; 37:799-803.*
58. *Szklaruk J, Tamm EP, Choi H, Varavithya V. MR Imaging of Common and Uncommon Large Pelvic Masses. RadioGraphics 2003; 23:403-424.*

59. *Rifkin MD, Ehrlich SM, Marks G. Staging of rectal carcinoma: prospective comparison of endorectal US and CT. Radiology 1989; 170:319-322.*
60. *Glaser F, Schlag P, Herfarth C. Endorectal ultrasonography for the assessment of invasion of rectal tumours and lymph node involvement. Br J Surg 1990; 77:883-887.*
61. *Detry RJ, Kartheuser AH, Lagneaux G, Rahier J. Preoperative lymph node staging in rectal cancer: a difficult challenge. Int J Colorectal Dis 1996; 11:217-221.*
62. *Sailer M, Leppert R, Kraemer M, Fuchs KH, Thiede A. The value of endorectal ultrasound in the assessment of adenomas, T1- and T2-carcinomas. Int J Colorectal Dis 1997; 12:214-219.*
63. *Napoleon B, Pujol B, Berger F, Valette PJ, Gerard JP, Souquet JC. Accuracy of endosonography in the staging of rectal cancer treated by radiotherapy. Br J Surg 1991; 78:785-788.*
64. *Rifkin MD, Marks GJ. Transrectal US as an adjunct in the diagnosis of rectal and extrarectal tumors. Radiology 1985; 157:499-502.*
65. *Hulsmans F, Bosma A, Mulder P, Reeders J, Tytgat G. Perirectal lymph nodes in rectal cancer: in vitro correlation of sonographic parameters and histopathologic findings. Radiology 1992; 184:553-560.*
66. *Lindmark G, Elvin A, Pahlman L, Glimelius B. The value of endosonography in preoperative staging of rectal cancer. Int J Colorectal Dis 1992; 7:162-166.*
67. *Jochem RJ, Reading CC, Dozois RR, Carpenter HA, Wolff BG, Charboneau JW. Endorectal ultrasonographic staging of rectal carcinoma. Mayo Clin Proc 1990; 65:1571-1577.*
68. *Milsom JW, Graffner H. Intrarectal ultrasonography in rectal cancer staging and in the evaluation of pelvic disease. Clinical uses of intrarectal ultrasound. Ann Surg 1990; 212:602-606.*
69. *Milsom JW, Lavery IC, Stolfi VM, et al. The expanding utility of endoluminal ultrasonography in the management of rectal cancer. Surgery 1992; 112:832-840; discussion 840-831.*
70. *Gualdi GF, Casciani E, Guadalaxara A, d'Orta C, Polettini E, Pappalardo G. Local staging of rectal cancer with transrectal ultrasound and endorectal magnetic resonance imaging: comparison with histologic findings. Dis Colon Rectum 2000; 43:338-345.*
71. *Garcia-Aguilar J, Pollack J, Lee SH, et al. Accuracy of endorectal ultrasonography in preoperative staging of rectal tumors. Dis Colon Rectum 2002; 45:10-15.*
72. *Scialpi M, Andreatta R, Agugiaro S, Zottele F, Niccolini M, Dalla Palma F. Rectal carcinoma: preoperative staging and detection of postoperative local recurrence with transrectal and transvaginal ultrasound. Abdom Imaging 1993; 18:381-389.*
73. *Glaser F, Layer G, Zuna I, van Kaick G, Schlag P, Herfarth C. [Preoperative assessment of perirectal lymph nodes by ultrasound]. Chirurg 1990; 61:587-591.*

74. *Di Candio G, Mosca F, Campatelli A, Cei A, Ferrari M, Basolo F. Endosonographic staging of rectal carcinoma. Gastrointest Radiol 1987; 12:289-295.*
75. *Scialpi M, Rotondo A, Angelelli G. Water enema transvaginal ultrasound for local staging of stenotic rectal carcinoma. Abdom Imaging 1999; 24:132-136.*
76. *Maldjian C, Smith R, Kilger A, Schnall M, Ginsberg G, Kochman M. Endorectal surface coil MR imaging as a staging technique for rectal carcinoma: a comparison study to rectal endosonography. Abdom Imaging 2000; 25:75-80.*
77. *Zainea GG, Lee F, McLeary RD, Siders DB, Thieme ET. Transrectal ultrasonography in the evaluation of rectal and extrarectal disease. Surg Gynecol Obstet 1989; 169:153-156.*
78. *Bedrosian I, Rodriguez-Bigas MA, Feig B, et al. Predicting the node-negative mesorectum after preoperative chemoradiation for locally advanced rectal carcinoma. Journal of Gastrointestinal Surgery 2004; 8:56-63.*
79. *Akasu T, Kondo H, Moriya Y, et al. Endorectal ultrasonography and treatment of early stage rectal cancer. World J Surg 2000; 24:1061-1068.*
80. *Kim JC, Cho YK, Kim SY, Park SK, Lee MG. Comparative study of three-dimensional and conventional endorectal ultrasonography used in rectal cancer staging. Surg Endosc 2002; 16:1280-1285.*
81. *Mehta VK, Poen J, Ford J, et al. Radiotherapy, concomitant protracted-venous-infusion 5-fluorouracil, and surgery for ultrasound-staged T3 or T4 rectal cancer. Dis Colon Rectum 2001; 44:52-58.*
82. *Spinelli P, Schiavo M, Meroni E, et al. Results of EUS in detecting perirectal lymph node metastases of rectal cancer: the pathologist makes the difference. Gastrointest Endosc 1999; 49:754-758.*
83. *Okizuka H, Sugimura K, Ishida T. Preoperative local staging of rectal carcinoma with MR imaging and a rectal balloon. J Magn Reson Imaging 1993; 3:329-335.*
84. *Blomqvist L, Holm T, Rubio C, Hindmarsh T. Rectal tumours--MR imaging with endorectal and/or phased-array coils, and histopathological staging on giant sections. A comparative study. Acta Radiol 1997; 38:437-444.*
85. *Vogl TJ, Pegios W, Mack MG, et al. Accuracy of staging rectal tumors with contrast-enhanced transrectal MR imaging. AJR Am J Roentgenol 1997; 168:1427-1434.*
86. *de Lange E, Fechner R, Edge S, Spaulding C. Preoperative staging of rectal carcinoma with MR imaging: surgical and histopathologic correlation. Radiology 1990; 176:623-628.*
87. *Said B, McCart JA, Libutti SK, Choyke PL. Ferumoxide-enhanced MRI in patients with colorectal cancer and rising CEA: surgical correlation in early recurrence. Magnetic Resonance Imaging 2000; 18:305-309.*
88. *Urban M, Rosen HR, Holbling N, et al. MR Imaging for the Preoperative Planning of*

Sphincter-saving Surgery for Tumors of the Lower Third of the Rectum: Use of Intravenous and Endorectal Contrast Materials. Radiology 2000; 214:503-508.

89. *Hadfield MB, Nicholson AA, MacDonald AW, et al. Preoperative staging of rectal carcinoma by magnetic resonance imaging with a pelvic phased-array coil. Br J Surg 1997; 84:529-531.*
90. *Wallengren NO, Holtas S, Andren-Sandberg A. Preoperative staging of rectal carcinoma using double-contrast MR imaging. Technical aspects and early clinical experiences. Acta Radiol 1996; 37:791-798.*
91. *McNicholas MM, Joyce WP, Dolan J, Gibney RG, MacErlaine DP, Hyland J. Magnetic resonance imaging of rectal carcinoma: a prospective study. Br J Surg 1994; 81:911-914.*
92. *Hodgman CG, MacCarty RL, Wolff BG, et al. Preoperative staging of rectal carcinoma by computed tomography and 0.15T magnetic resonance imaging. Preliminary report. Dis Colon Rectum 1986; 29:446-450.*
93. *Matsuoka H, Nakamura A, Masaki T, et al. A prospective comparison between multidetector-row computed tomography and magnetic resonance imaging in the preoperative evaluation of rectal carcinoma. The American Journal of Surgery 2003; 185:556-559.*
94. *Drew PJ, Farouk R, Turnbull LW, Ward SC, Hartley JE, Monson JR. Preoperative magnetic resonance staging of rectal cancer with an endorectal coil and dynamic gadolinium enhancement. Br J Surg 1999; 86:250-254.*
95. *Kim NK, Kim MJ, Park JK, Park SI, Min JS. Preoperative staging of rectal cancer with MRI: accuracy and clinical usefulness. Ann Surg Oncol 2000; 7:732-737.*
96. *Indinnimeo M, Grasso RF, Cicchini C, et al. Endorectal magnetic resonance imaging in the preoperative staging of rectal tumors. Int Surg 1996; 81:419-422.*
97. *Schnall M, Furth E, Rosato E, Kressel H. Rectal tumor stage: correlation of endorectal MR imaging and pathologic findings. Radiology 1994; 190:709-714.*
98. *Gagliardi G, Bayar S, Smith R, Salem RR. Preoperative staging of rectal cancer using magnetic resonance imaging with external phase-arrayed coils. Arch Surg 2002; 137:447-451.*
99. *Maier AG, Kersting-Sommerhoff B, Reeders JW, et al. Staging of rectal cancer by double-contrast MR imaging using the rectally administered superparamagnetic iron oxide contrast agent ferristene and IV gadodiamide injection: results of a multicenter phase II trial. J Magn Reson Imaging 2000; 12:651-660.*
100. *Akin O, Nessar G, Agildere AM, Aydog G. Preoperative local staging of rectal cancer with endorectal MR imaging: comparison with histopathologic findings. Clin Imaging 2004; 28:432-438.*
101. *Okizuka H, Sugimura K, Yoshizako T, Kaji Y, Wada A. Rectal carcinoma: prospective*

comparison of conventional and gadopentetate dimeglumine enhanced fat-suppressed MR imaging. J Magn Reson Imaging 1996; 6:465-471.

102. *Chiesura-Corona, Muzzio, Giust, Zuliani, Pucciarelli, Toppan. Rectal cancer: CT local staging with histopathologic correlation. Abdominal Imaging 2001.*

103. *Filippone A, Ambrosini R, Fuschi M, Marinelli T, Genovesi D, Bonomo L. Preoperative T and N Staging of Colorectal Cancer: Accuracy of Contrast-enhanced Multi-Detector Row CT Colonography--Initial Experience. Radiology 2004; 231:83-90.*

104. *Netri G, Coco C, Valentini V, et al. Clinical staging of rectal cancer. Results of a prospective continuing study. Ital J Surg Sci 1985; 15:169-174.*

105. *Matsuoka H, Nakamura A, Masaki T, et al. Preoperative staging by multidetector-row computed tomography in patients with rectal carcinoma. The American Journal of Surgery 2002; 184:131-135.*

106. *Angelelli G, Macarini L, Lupo L, Caputi-Jambrenghi O, Pannarale O, Memeo V. Rectal carcinoma: CT staging with water as contrast medium. Radiology 1990; 177:511-514.*

107. *Thompson WM, Halvorsen RA, Foster WL, Jr., Roberts L, Gibbons R. Preoperative and postoperative CT staging of rectosigmoid carcinoma. AJR Am J Roentgenol 1986; 146:703-710.*

108. *Beynon J, Mortensen NJ, Foy DM, Channer JL, Rigby H, Virjee J. Preoperative assessment of mesorectal lymph node involvement in rectal cancer. Br J Surg 1989; 76:276-279.*

109. *Moses LE, Shapiro D, Littenberg B. Combining independent studies of a diagnostic test into a summary ROC curve: data-analytic approaches and some additional considerations. Stat Med 1993; 12:1293-1316,*

MR PREDICTION OF THE RISK FACTORS -CIRCUMFERENTIAL RESECTION MARGIN, T-STAGE AND NODAL STATUS- IN PRIMARY RECTAL CANCER: A MULTICENTER STUDY

IN PREPARATION FOR PUBLICATION

M.J. LAHAYE
S.M.E. ENGELEN
G.L. BEETS
A.G.F. KESSELS
P.J.M. DOHMEN
G.R.J. OPDENAKKER
P.J.M. POST
C.J.H. VAN DE VELDE
J.M.A. VAN ENGELSHOVEN
AND R.G.H. BEETS-TAN

5

Purpose

To evaluate the accuracy of USPIO MRI to predict the distance to the mesorectal fascia, T- and N-stage in primary staging of rectal cancer in patients not receiving chemoradiation in the setting of a general hospital and the setting of an expert center.

Materials and methods

Between February 2003 and January 2008 a multicenter prospective rectal cancer project included 296 patients with biopsy proven primary rectal cancer. Patients underwent MRI 24hrs. after i.v. administration of USPIO. Sequences used were axial 2D T2W FSE, 3D T1W GRE & 3DT2*. The general radiologists (general setting) and an experienced MR radiologist (university setting) prospectively predicted the circumferential resection margin (CRM), T-stage and the nodal status first on T2 TSE images (USPIO-), then on the combined T2 FSE and 3DT2* weighted images (USPIO+), blinded for each other's results. The expert prospectively double read each MR of the regional study patients. Mainly on the basis of these risk factors for local recurrence the treatment strategy was decided: surgery only, surgery after 5 x 5 Gy RT, or surgery after a long course of chemoradiation. In 59 patients surgery was performed without any neoadjuvant treatment and in 91 patients after 5 x 5 Gy RT. These 150 were included in the present study, as only in these patients the histology can serve as the reference standard.

Results

The prediction of CRM had an NPV of 100%. The expert radiologist had a PPV for prediction of pT0-2 of 95%, for the general radiologists (as a group) 87% resp. The AUC and NPV for prediction of malignant nodes on T2 FSE images for the expert radiologist was 0.84 and 92%, for the general radiologists (as a group) 0.81 and 83% resp. The AUC and NPV for prediction of malignant nodes on USPIO enhanced images for the expert radiologist was 0.92 and 97%, for the general radiologists (as a group) 0.87 and 95% resp. If the latter two risk factors (T- and N-stage) were combined expert and general radiologists could also accurately predict Stage I disease with a PPV of 0.94 and 0.92 respectively.

Conclusion

Expert and general radiologists can accurately predict a noninvolved CRM with MR imaging. USPIO MRI can accurately predict tumors limited to the bowel wall with a high PPV and select NC patients with a high NPV for the prediction of nodal disease. Stage I disease can reliably be predicted in both referral and general setting.

Introduction

Colorectal cancer is one of the leading causes of death in the Western world. In rectal cancer patients the specific problem is the high rate of local recurrences [1-3]. Nowadays clinicians can choose between a range of therapeutic options: from a local excision for the early tumors to a more invasive treatment, such as extensive resections combined with neoadjuvant chemo- and/or radiotherapy for the more locally advanced tumors. Reliable preoperative imaging of the risk factors for local recurrence is essential to choose the most optimal treatment. EUS, CT and MRI are currently used for this purpose. At least in many European centers the distance of the tumor to the mesorectal fascia, and the corresponding prediction of a close or involved resection margin is considered one of the most important factors that guides the choice between the different neoadjuvant treatment options. In many single center studies MRI has been shown to be very accurate in the assessment of the extent of the primary tumor, and the relation to the mesorectal fascia. A multicenter study by the Mercury Study Group confirmed this [4].

In other settings, such as in many US centers, the clinical T- and N-staging is more used for decisions on neoadjuvant therapy than the anticipated CRM. Patients with Stage I disease (T1-2N0M0) have repeatedly been shown to have a very low risk for local recurrence and do not benefit from neoadjuvant therapy [5-7]. Conventional nodal staging with EUS, CT and MRI, however, is only moderately accurate, with a recent meta-analysis reporting an overall sensitivity of 55 to 67% and specificity of 74 to 78% [8]. An improved method of nodal imaging would not only be of benefit for the selection of Stage I disease, but could also be of help in selecting patients for a local excision, and in the follow up of patients after a local excision of a small rectal cancer. Lymph node specific MR contrast agent could provide a higher accuracy. Will et al. reported encouraging results in a meta-analysis on the MR contrast agent ultrasmall superparamagnetic iron oxide (USPIO) for predicting tumoral nodes in a wide variety of cancers [9].

The purpose of the present study to evaluate the accuracy of MRI with USPIO to predict the most commonly used risk factors for local recurrence in rectal cancer: distance to mesorectal fascia, T- and N-stage in primary staging of rectal cancer. A second purpose was to evaluate the MR performance in the setting of a general hospital as compared to the setting of an expert center.

Materials and methods

Patients

Between February 2003 and January 2008 a multicenter prospective rectal cancer project included 296 patients with biopsy proven primary rectal cancer. The tumor was considered rectal when the inferior margin was not further than 15 cm from the anal verge on endoscopy. The institutional review boards from all participating centers approved the project. All patients gave written informed consent. The Dutch Cancer Society funded the project. The MRI contrast agent USPIO, not commercially available during the study period, was provided free of charge by Guerbet Laboratories (Roissy, France) as vials of Sinerem®. Guerbet Laboratories had no control of inclusion or data.

The main aim of the project was to study the local control after a differentiated treatment with three treatment options: surgery only, surgery after short course 5 x 5 Gy radiotherapy, and surgery after a long course of chemoradiation. The treatment choices were based on a risk assessment for local recurrence that relied mainly on MR imaging. Tumors were classified as low, intermediate, and high risk based on the distance of the tumor to the mesorectal fascia, the nodal status, T-stage and distance of the tumor from the anal margin.

For the present study that addresses the accuracy of MRI in assessing the risk factors all patients were included in whom the standard of reference of histological examination after surgery was available. Histology was not available in 45 patients who were not operated because of widespread metastatic disease and/or comorbidity (37) or patient refusal (8). Five patients were excluded because of MRI-related problems like artifacts and refusal. Ninety-five patients who were treated with neoadjuvant chemoradiation were excluded because the histology is no longer representative of the status at initial presentation due to the downsizing and downstaging effect of the neoadjuvant treatment. One patient was excluded for the same reason because chemotherapy was administered between the MRI and the rectal resection because of a coexisting malignancy (see Figure 5.1).

This results for the present study in a group of 150 patients (83 men, 67 women, mean age 69.8 years, range 38-92 years). In 59 patients surgery was performed without any neoadjuvant treatment and in 91 patients after 5 x 5 Gy radiotherapy. A

short radiotherapy scheme with immediate surgery is known not to downstage the T-stage or nodal status, and histology can be used as the standard of reference [10].

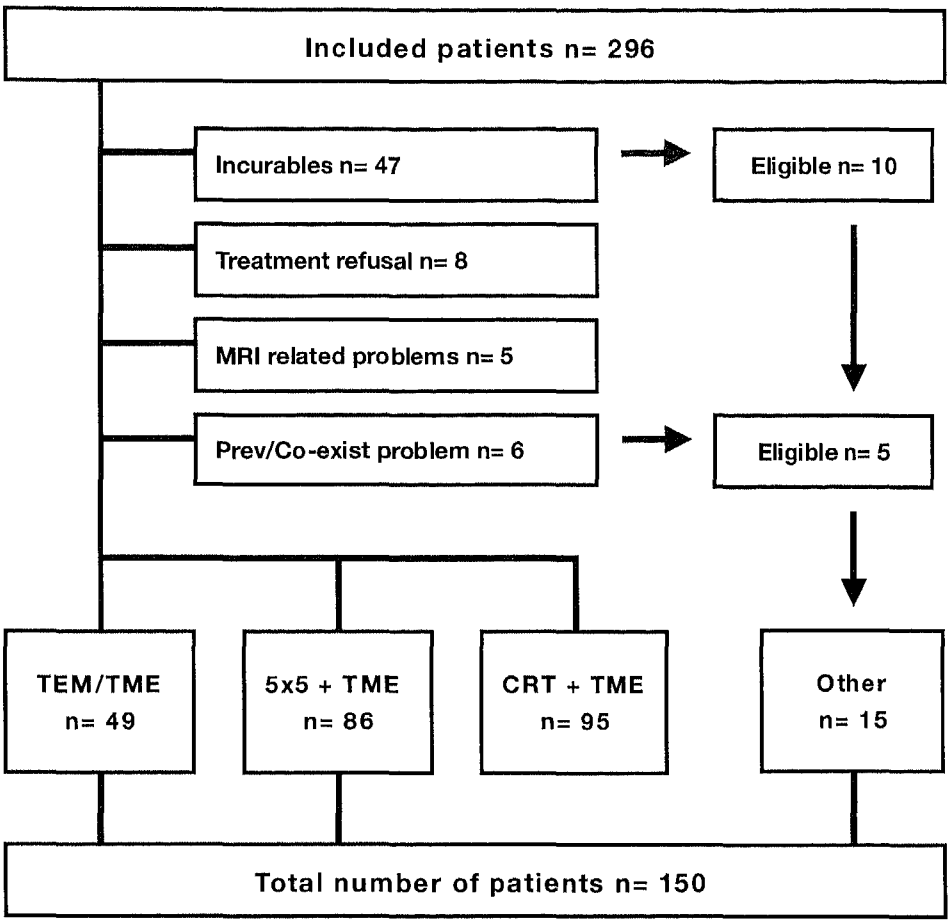

Figure 5.1. Flowchart of patient inclusion.

Ultrasmall superparamagnetic iron oxides

The USPIO MR contrast agent, Sinerem®, consists of nanoparticles iron oxide coated with dextran. Sinerem® is supplied as a powder in a glass vial containing 315 mg and must be reconstituted by using 15 mL of normal saline. A dose of 0.13 mL

per kilogram of body weight (2.6 mg Fe/kg) of the reconstituted solution was diluted in 100 mL of normal saline. This was administered intravenously through a microfilter within a period of approximately 45 minutes. Administration was performed at the preparation room of the MRI unit or at the day care unit in other centers. Administration was completed 24-36 hours before MR imaging was planned. The nanoparticles iron oxide accumulate in macrophages within the lymph node [11, 12] and cause a decrease in signal intensity within the node due to susceptibility artifacts on T2*-weighted images. The metastatic part of the lymph node will show no signal decrease and will be depicted as a white region within the lymph node due to the replacement of macrophages by tumor cells. An estimated area of white region within the node larger than 30% is highly predictive for a malignant node with a sensitivity of 93% and a specificity of 96% on a nodal basis [13].

MR IMAGING

Patients did not receive bowel or any other preparation. All axial images were angled perpendicular to the rectal tumor. The total scan time was 32-45 minutes. Sequences used are sagittal and axial 2D T2 weighted TSE for predicting the T-stage and the nodal status. T2*-weighted images were obtained in all patients and were used to interpreter the USPIO uptake patterns within the nodes. 3D T1-weighted images were obtained to locate lymph nodes and to differentiate them from other anatomic structures like small blood vessels. Two regional hospitals had a Siemens Magnetom Impact Expert 1.0T (Siemens AG, Erlangen, Germany), while the university and one regional hospital had a 1.5T MRI (Intera (Philips Medical Systems, Best, Netherlands) and Siemens Symphony 1.5T (Siemens AG, Erlangen, Germany), respectively. Overall 130 of 150 patients were scanned at 1.5T MRI and 20 at 1.0T MRI. See Table 5.1 for MR sequences and parameters.

Table 5.1. MR sequences and parameters.

Sequences & Parameters	1.0T MRI		1.5T MRI	
	A	B	C	D
2D T2W FSE				
Repetition time/Echo time (msec)	5289/120	5289/120	3427/150	3427/150
Slice Thickness (mm)	5	5	5	5
Flip angle (degrees)	90	90	90	90
Matrix	256 x 256	256 x 256	256 x 256	256 x 256
FOV (mm)	250	250	200	200
No. of slices	22	22	22	22
Axial 3D T1W Gradient Echo				
Repetition time/Echo time (msec)	15/7	14.30/7	10/4.60	9.8/4.76
Slice Thickness (mm)	2	2	1	1
Flip angle (degrees)	15	15	15	15
Matrix	256 x 256	256 x 256	384 x 512	384 x 512
FOV (mm)	300	300	440	440
No. of slices	102	102	200	208
Axial 3D T2*W				
Repetition time/Echo time (msec)	17/7	17/7	23/18.41	38/ 18
Slice Thickness (mm)	2	2	1.25	2
Flip angle (degrees)	20	20	20	8
Matrix	256 x 256	256 x 256	512 x 512	512 x 512
FOV (mm)	300	300	440	440
No. of slices	106	106	200	208

Image evaluation

All MR images of the general hospitals were first read and interpreted prospectively by the general radiologist of that center (experience: 20-40 rectal cancer MR readings a year (around 5 years experience)). MR images were also sent to the university center, where the images were prospectively double read by an expert radiologist (R.B.T. with 150 rectal cancer MR readings a year (10 years experience)), blinded for the general radiologist's results. The MR images of patients of the university center were only interpreted by the expert radiologist.

To assess the quality of the MRI images all MR evaluations were rated by all readers and scored as 'poor' or 'good'.

The anticipated CRM was measured on axial T2 weighted images as the shortest distance between the tumor and the mesorectal fascia. If this distance was less than 2 mm it was recorded as an involved margin. In all other cases the anticipated CRM was considered as noninvolved.
The assessment of T-stage was performed on standard axial images (T2 FSE-weighted images). Radiologists were asked to predict the tumor stage from T1 to T4. As however the distinction between T1 and T2 is notoriously difficult on MRI, and only the distinction between T1-2 tumors and T3-4 tumors was considered relevant in the decision process, the data were dichotomized along this distinction. A tumor was considered as T1-2 (limited to the bowel wall) when the bowel wall was depicted as an intact line of low signal intensity.
The nodal status on a patient basis was prospectively scored using a confidence level score (definitely node negative = 0 to definitely node positive = 4). This was first based on the conventional T2-weighted FSE images and thereafter on the combination of T2-weighted FSE plus USPIO-enhanced images T2*-weighted images. On T2 FSE images the short and long axis of the node, border irregularity and homogenous signal intensity were used as criteria for nodal prediction, as previously defined in literature [14, 15]. On USPIO-enhanced T2*-weighted images the radiologists used the estimated percentage of the white region within the node [13]. When the white region within the node was estimated larger than 30%, the node was staged as N+.

Surgical procedure and histological evaluation

129 patients underwent a standard total mesorectal excision and 21 with very small tumors underwent a local excision with the transanal endoscopic microsurgical (TEM) technique. The histological examination of the TME specimen was standardized: it was fixed in formalin for 24-48h after the circumferential resection plane was inked. The specimen was then sectioned transversely every 5 mm perpendicular to the mesorectum. Careful examination was performed of the circumferential margin for involvement, measuring the shortest distance to the tumor, both macroscopically and microscopically on haematoxylin-eosin (HE) stained sections. The depth of invasion into the bowel wall and the assessment of the lymph

nodes were performed according to a standard protocol on HE sections. The pathologist reported his findings concerning T-stage, CRM and nodal status blinded for the radiological predictions. All rectal specimens resected by TEM were examined for cancer invasion depth within the different layers of the bowel wall, and the specimens were evaluated whether the margins were free. Because with a TEM procedure the mesorectum is not removed and histological information on lymph nodes is lacking, patients underwent a second USPIO MRI 3-6 months and a third USPIO MRI 12 months after their TEM procedure to provide a surrogate standard reference for the lymph node status instead of postoperative histology.

Statistical analysis

The majority of patients with an involved or close resection margin on MRI received neoadjuvant chemoradiation and were excluded from the present study. For the MR assessment of the CRM only the NPV can therefore be meaningfully evaluated. For the detection of tumors limited to the bowel wall and the detection of the nodal status the accuracy, sensitivity, specificity, and positive predictive values (PPV) and negative predictive values (NPV) of were calculated. For the prediction of the nodal status ROC curves were constructed and areas under the curve (AUCs) were calculated. For the MR prediction of Stage I disease, a combination of T and N prediction, the accuracy, sensitivity, specificity, and positive and negative predictive values were calculated.

Comparisons between conventional and USPIO enhanced MRI, between the expert reader and the general radiologists, and between 1.0T and 1.5T were made using diagnostic odds ratio analyses and the Delong, Delong and Clarke-Pearson method where appropriate [16]. To determine the interobserver agreement, square weighted kappa's [17, 18] were calculated with a 95%-Confidence Interval.

The kappa and odds ratio analyses were performed by using STATA software (Stata Statistical Software: Release 9. College Station, TX: StataCorp LP). All other analyses were performed using a statistical software program (SPSS, version 12.0.1, 2003; SPSS, Chicago, Ill.).

Results

During this study all patients tolerated the USPIO contrast agent well and no serious adverse events were reported. The quality of the 1.0T MR images was assessed "poor" by the non-experts in 50% of the patients, while 1.5T MRI had "poor" MR image quality in only 12% of the patients.
87 of the eligible 150 patients were staged as pT1-2 tumors at the histopathological examination, 61 had T3 tumors and 2 patients had a T4 tumor. In 49 patients the histological examination revealed malignant nodes. This resulted in 71 patients with Stage I disease, 30 patients with Stage II disease and 49 patients with at least Stage III disease at histopathological examination. Six patients had an involved/close CRM at the histological examination. At the histological examination an average of 10.7 nodes were found per patient.

Accuracy of MRI for predicting CRM

Almost all patients with an anticipated positive CRM on MR imaging receive neoadjuvant chemoradiation, therefore only the NPV can be calculated. In 148/150 patients the MR had predicted a CRM of more than 2 mm. In the two patients with a predicted involved margin a palliative resection was performed without a long course of chemoradiation, and this resulted in an involved margin in both patients. Of the 148 patients with a predicted free CRM 4 patients had an involved margin at histology. This was the result of errors in surgical technique in all 4 patients, as the histological examination showed a ruptured specimen at the level of the tumor (3) or a defect in the mesorectum (1).
These four patients should therefore not be considered as false negative MR findings. This results in a NPV of 100% (148/148), without any difference between 1.0T and 1.5T MR machines and for expert and general radiologists.

Accuracy of MRI for predicting tumors limited to the bowel wall (T1-2)

Table 5.2 shows the accuracy, sensitivity, specificity, positive predictive value (PPV) and negative predicting value (NPV). The high PPV of 0.95 for detection of a tumor limited to the bowel wall (T1-2) for experts, and 0.87 for general radiologists using 1.5T MRI are clinically useful. Using 1.0T MRI the expert and general radiologists predicted a tumor limited to the bowel wall with a disappointing PPV of 0.75 and 0.73, respectively.

Table 5.2. This table shows the accuracy, sensitivity (sens), specificity (spec), positive predictive value (PPV) and negative predicting value (NPV) for tumors limited to the bowel wall for 1.5T and 1.0T MRI.

	1.0T MRI		1.5T MRI	
Detection of pT1-2 tumors	**General setting**	**Referral setting**	**General setting**	**Referral setting**
Accuracy	0.70 ((11+3)/20)	0.65 ((9+4)/20)	0.74 ((13+18)/42)	0.82 ((53+53)/130)
Sens	0.85 (11/(11+2))	0.69 (9/(9+4))	0.59 (13/(13+9))	0.72 (53/(53+21))
Spec	0.43 (3/(3+4))	0.57 (4/(4+3))	0.90 (18/(18+2))	0.95 (53/(53+3))
PPV	0.73 (11/(11+4))	0.75 (9/(9+3))	0.87 (13/(13+2))	0.95 (53/(53+3))
NPV	0.60 (3/(3+2))	0.50 (4/(4+4))	0.67 (18/(18+9))	0.72 (53/(53+21))

At 1.5T MRI the AUCs for the prediction of the nodal status on USPIO enhanced images and T2W FSE images for the expert were 0.84 and 0.92, and for the general radiologists 0.81 and 0.87 respectively. The AUCs for nodal status using USPIO enhanced images and T2 FSE images at 1.0T MRI for the expert were 0.68 and 0.58, and for general radiologists 0.72 and 0.51, respectively (see Figure 5.2A & B). Table 5.3A & B show the corresponding sensitivity, specificity, PPV and NPV using T2 FSE images and USPIO-enhanced prediction. The expert and general radiologist both improved their prediction using USPIO-enhanced MR images. For the general radiologists this improvement was statistically significantly for 1.0T ($P<0.024$) and not 1.5T MRI ($P<0.331$), as opposed to the expert radiologist where the improvement was significant for 1.5T MRI ($P<0.010$) and not 1.0T MRI ($P<0.430$). Overall 1.5T MRI showed a positive trend for improved results for nodal staging with USPIO than 1.0T ($P<0.060$).

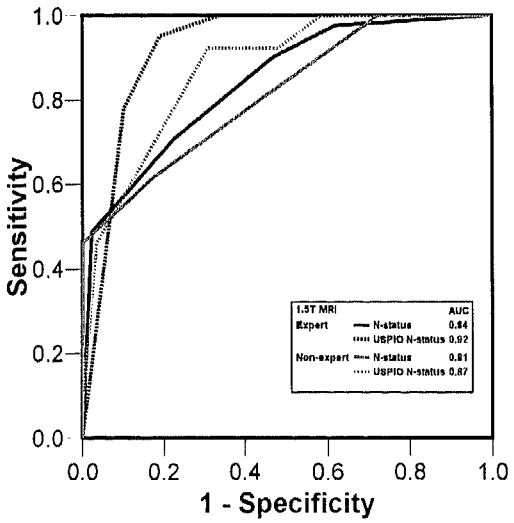

Figure 5.2A.
Receiver operating characteristic (ROC) curves and areas under the curve (AUC) for expert and general radiologists, for the detection of malignant lymph nodes using T2W FSE images and USPIO-enhanced images for 1.5T MRI.

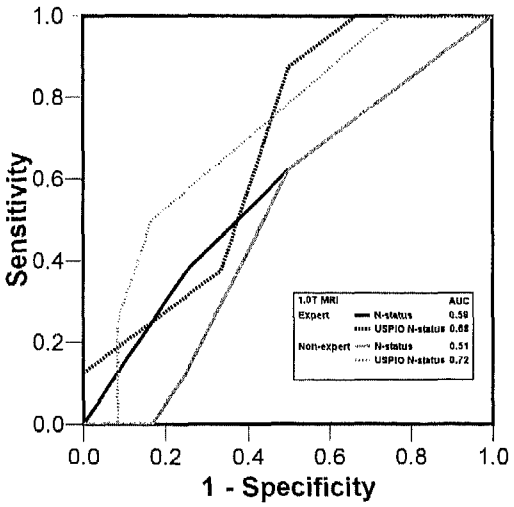

Figure 5.2B.
Receiver operating characteristic (ROC) curves and areas under the curve (AUC) for expert and general radiologists, for the detection of malignant lymph nodes using T2W FSE images and USPIO-enhanced images for 1.0T MRI.

Table 5.3A. This table shows the area under the ROC curve (AUC) and the corresponding sensitivity (sens), specificity (spec), positive predictive value (PPV) and negative predicting value (NPV) for the T2W FSE images and USPIO enhanced prediction of the nodal status for 1.5T MRI.

Detection of N+ 1.5T MRI	T2W FSE MRI		USPIO MRI	
	General setting	Referral setting	General setting	Referral setting
AUC (95% CI)	0.81 (0.67-0.96)	0.84 (0.77-0.91)	0.87 (0.76-0.98)	0.92 (0.88-0.97)
Sens	0.62 (8/(8+5))	0.90 (37/(37+4))	0.92 (12/(12+1))	0.95 (39/(39+2))
Spec	0.83 (24/(24+5))	0.53 (47/(47+42))	0.69 (20/(20+9))	0.81 (72/(72+17))
PPV	0.62 (8/(8+5))	0.47 (37/(37+42))	0.57 (12/(12+9))	0.70 (39/(39+17))
NPV	0.83 (24/(24+5))	0.92 (47/(47+4))	0.95 (20/(20+1))	0.97 (72/(72+2))

Table 5.3B. This table shows the area under the ROC curve (AUC) and the corresponding sensitivity (sens), specificity (spec), positive predictive value (PPV) and negative predicting value (NPV) for the T2W FSE images and USPIO enhanced prediction of the nodal status for 1.0T MRI.

Detection of N+ 1.0T MRI	T2W FSE MRI		USPIO MRI	
	General setting	*Referral setting*	*General setting*	*Referral setting*
AUC (95% CI)	0.51 (0.25-0.76)	0.58 (0.32-0.84)	0.72 (0.49-0.95)	0.68 (0.44-0.91)
Sens	0.63 (5/(5+3))	0.63 (5/(5+3))	0.50 (4/(4+4))	0.88 (7/(7+1))
Spec	0.50 (6/(6+6))	0.50 (6/(6+6))	0.83 (10/(10+2))	0.50 (6/(6+6))
PPV	0.45 (5/(5+6))	0.45 (5/(5+6))	0.67 (4/(4+2))	0.62 (7/(7+6))
NPV	0.67 (6/(6+3))	0.67 (6/(6+3))	0.71 (10/(10+4))	0.77 (6/(6+1))

Accuracy of MRI for predicting stage I disease

Table 5.4 shows the accuracy, sensitivity, specificity, PPV and NPV for the prediction of Stage I disease. The clinically relevant PPV for experts and general radiologists using 1.5T USPIO MRI was 0.94 and 0.92 respectively. Using 1.0T USPIO MRI the expert and general radiologists predicted Stage I disease with a lower PPV of 0.64 and 0.80, respectively.

Interobserver agreement

The interobserver agreement between the general and expert MR radiologist for predicting tumors limited to the bowel wall was good (K=0.70) using 1.5T MRI and moderate (K=0.44) using 1.0T MRI (see Table 5.5).

Table 5.4. This table shows the accuracy, sensitivity (sens), specificity (spec), positive predictive value (PPV) and negative predicting value (NPV) for Stage I disease for 1.5T and 1.0T MRI.

Detection of Stage I disease	1.0T MRI		1.5T MRI	
	General setting	Referral setting	General setting	Referral setting
Accuracy	0.70 ((7+7)/20)	0.70 ((4+10)/20)	0.79 ((12+21)/42)	0.85 ((45+65)/130)
Sens	0.78 (7/(7+2))	0.44 (4/(4+5))	0.60 (12/(12+8))	0.73 (45/(45+17))
Spec	0.64 (7/(7+4))	0.91 (10/(10+1))	0.95 (21/(21+1))	0.96 (65/(65+3))
PPV	0.64 (7/(7+4))	0.80 (4/(4+1))	0.92 (12/(12+1))	0.94 (45/(45+3))
NPV	0.78 (7/(7+2))	0.67 (10/(10+5))	0.72 (21/(21+8))	0.79 (65/(65+17))

Table 5.5. Interobserver agreements for the prediction of the tumors, nodal status and Stage 1 disease by expert and non-expert radiologist using 1.0T and 1.5T USPIO MRI.

Interobserver agreement (Kappa)	1.0T MRI	1.5T MRI
T1-2	0.44	0.70
USPIO N-status	0.02	0.71
Stage I disease	0.05	0.74

Using 1.5T MRI the interobserver agreement between the expert and the general radiologist MRI for the USPIO-enhanced prediction of the nodal status was substantial (K=0.71), whereas a slight (K=0.02) agreement was found using 1.0T MRI. The interobserver agreement between the general and expert MR radiologist for

predicting Stage I disease was substantial (K=0.74) using 1.5T MRI and only slight agreement (K=0.05) was found using 1.0T MRI. There was no disagreement between expert and general radiologists concerning the CRM prediction.

Discussion

This multicenter study shows that expert and general radiologists could accurately detect a noninvolved CRM as demonstrated by the high NPV. A tumor that is limited to the bowel wall could also be accurately predicted with a high PPV using 1.5T MRI by all radiologists. This study also proved that both expert and general radiologists showed a high NPV for predicting malignant nodes on USPIO enhanced 1.5T MR images. Furthermore, experts and general radiologists could accurately detect Stage I disease with a high PPV using 1.5T USPIO MRI.

Accuracy of MRI for predicting CRM

This multicenter study demonstrated a high negative predictive value for the prediction of an involved or close (<2mm) anticipated CRM at the mesorectal fascia. Many studies have shown that a close resection margin is a very important prognostic indicator for local recurrence [19-21]. Quirke et al. [20] have demonstrated that microscopically positive resection margins resulted in a local recurrence rate of 83%. Even with a short course of preoperative radiotherapy is insufficient to prevent local recurrences, and these patients should be treated with a long course of chemoradiation [22]. So far MRI is the only modality that has been shown to be accurate for the prediction of the relation of the tumor to the mesorectal fascia. This was demonstrated in many single center studies [23], confirmed by the multicenter Mercury trial [24], and again confirmed in this study. In the design of the present study a confirmation of the ability to image an involved mesorectal fascia was not possible, as these patients went on to receive a long course of chemoradiation, and thereby loosing histology as the reference standard.

Accuracy of MRI for predicting tumors limited to the bowel wall (T1-2)

Expert and general radiologists accurately predicted a tumor limited to the bowel wall with a high PPV of 0.95 and 0.87, respectively. Although a clear distinction between pT1 and pT2 cannot be made on T2W TSE images, the distinction between a T2 and T3 tumor appears easier to be made on MR images. The criterion of an intact rectal wall seems to be a highly predictive sign for pT1-2 tumors (see Figure 5.3). The low NPV was due to considerable overstaging in borderline pT2 tumors with strandlike desmoplastic reactions in the perirectal fat (see Figure 3B). A significant proportion of the overstaging errors occurred, especially with less experienced radiologists. Overstaging problems have been well documented, with reports of overstaging of 38-62% of pT2 tumors as T3 tumors by several studies [23, 25]. Although EUS is better in distinguishing the individual layers of the bowel wall, it is also known to have the same limitation in distinguishing between pT2 and pT3 with overstaging errors of up to 36% in pT2 patients [26].

Accuracy of MRI for predicting lymph node involvement

This multicenter study demonstrated good results for prediction of the nodal status with USPIO enhanced 1.5T MRI both in a university and in general setting (see Figure 5.4). Especially the high NPV (0.95) is promising, because it implicates that USPIO MRI could accurately select patients with a N0 status. We, however, encountered a considerable number of false positive results. There are several explanations. First, the project was designed to avoid undertreatment, since false positive findings were considered less problematic than false negatives, thereby encouraging radiologists to overstage rather than understage in doubtful cases. Secondly, several benign conditions like focal granulamatous reactions or a fatty hilum can also cause a white region in the center of the node, thus mimicking a malignant node (see Figure 5.5). The few false negatives that were seen were small clusters of micrometastases of less than 0.2 mm.

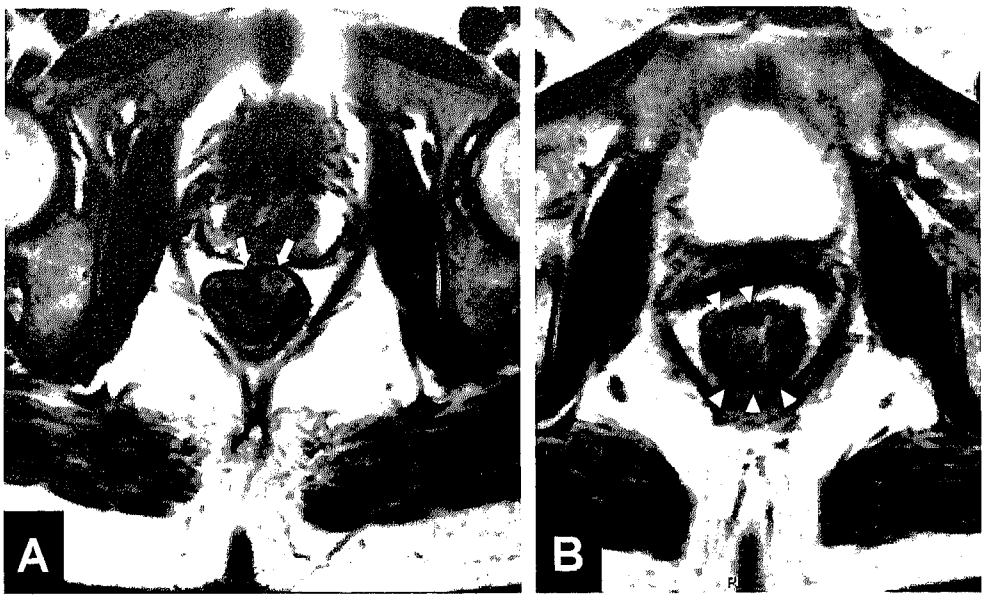

Figure 5.3A/B. (A) Axial T2W TSE MR image shows a distal tumor in which the rectal wall (arrows) is intact, therefore this was correctly staged as a T2 tumor. (B) Axial T2W TSE MR image shows another distal tumor; in this case the bowel wall is not intact with fibrotic stranding in the perirectal fat (arrowheads). Therefore the expert and general radiologist staged this as a T3 tumor, however at histology this tumor was staged as a T2 tumor. Due to this overstaging error the CRM was preoperatively believed to be involved and thus this patients was wrongly stratified for chemoradiation (locally advanced tumor) instead of 5 x 5 Gy radiotherapy (non-locally advanced tumor).

The use of a lymph node specific MR contrast agent (USPIO) resulted in an improvement of AUC for all radiologists, although not all improvements were statistically significant. Overall it seems, however, that USPIO improves the accuracy in the order of 10%. The use of morphological criteria in standard MR without contrast such as border and heterogeneous signal intensity results in a reasonable accuracy that is better than when only size criteria are used. This confirms earlier reports on the usefulness of these morphological criteria [14, 15].

A drawback of USPIO is that in Europe USPIO's application for a marketing authorization at the Committee for Medical Products for Human Use (CHMP) has recently been withdrawn by the manufacturer while in the United States the approval

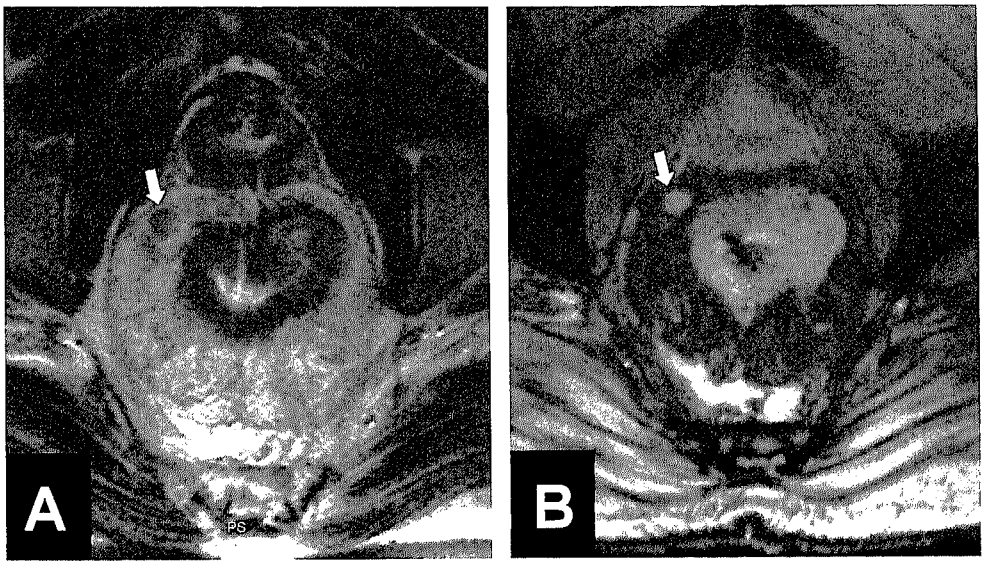

Figure 5.4A/B. A 5 mm malignant mesorectal node, detected with USPIO MRI: (A) on T2-weighted FSE image it is difficult to differentiate between malignant and benign, (B) on USPIO-enhanced T2* image the node has a high signal intensity, indicating that this is a malignant node. At histology this patient confirmed to have a N1 status.

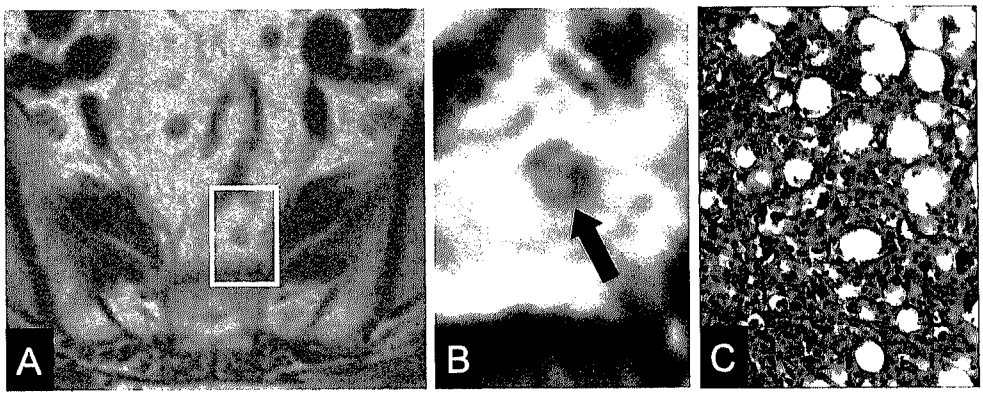

Figure 5.5A/B/C. (A) T2-weighted TSE image in the axial plane of the pelvis with a 5 mm mesorectal lymph node (rectangle) in a rectal cancer patient. (B) On the corresponding UPSIO-enhanced T2*-weighted image the same lymph node (arrow) showed central high signal intensity, indicating no USPIO uptake. (C) However, this correlated at histological examination (HE staining) with the centrally located granulamatous reactions in a benign node and not with tumor. This is an example of a false positive result.

by the Food and Drugs Administration (FDA) is still pending. When eventually USPIO would not be marketed our studies would still have shown that lymph node staging can be improved with a lymph node specific contrast agent, stimulating the search for other reliable contrast agents or new MR techniques.

Accuracy of MRI for predicting stage I disease

Expert and general radiologists accurately predicted Stage I disease with a high PPV of 0.94 and 0.92, respectively. This means that radiologists can play an important role in the multidisciplinary approach of rectal cancer selecting those low risk patients who do not benefit from neoadjuvant treatment. It remains to be established whether MRI is accurate enough to allow a selection of patients who could be treated with a local excision. The lymph node metastases that have been detected in T1 tumors are generally smaller than in T2 or T3 tumors, with a higher risk of false negative MR findings [27]. Further clinical studies in this setting are required.

Interobserver agreement

The high interobserver agreement between expert and general radiologists for identifying pT1-2 tumors, nodal involvement at 1.5T MRI and Stage I disease illustrates that MR results were consistent and reproducible, indicating that MRI staging can be done not only in the setting of an expert center, but also in the setting of a general hospital.

Field strength

The results of this study show that overall there was some difference in performance for T- and N-stage prediction at 1.0 Tesla compared to 1.5 Tesla, with 1.0 Tesla MRI performing less good. This difference was statistically significant for the T-staging, but only showed a tendency towards significance for the N-staging. Although the total number of patients enrolled at both 1.0 Tesla centers were disproportionately

lower (20/150) as compared to that enrolled at both 1.5 Tesla centers (130/150) and definite conclusions cannot be drawn, the results suggest that T- and N-stage assessment in rectal cancer staging at 1.0 Tesla MR should not be relied on heavily. Because of the low field strength 1.0 Tesla MR there is an inherent inferior signal to noise ratio when trying to obtain small pixel volumes, as compared to 1.5 Tesla MR. In the balance between the best contrast and the best spatial resolution, we cannot but compromise on the spatial resolution for the 1.0 Tesla protocol. As a consequence the pixel volumes with 1.0 Tesla MRIs for the 2D T2W, 3D T1W and 3D T2*W sequences are 7, 3 and 3.7 times larger as with the 1.5 Tesla MRI. This could well explain the difference in subjective interpretation of 'good' and 'poor' image quality, and the lower performance of T- and N-staging with 1.0 Tesla. The assessment of the anticipated circumferential margin did not appear to suffer from this limitation.

Conclusion

This multicenter study shows that radiologists can accurately predict a noninvolved CRM with MR imaging. Furthermore, USPIO MRI at 1.5T can accurately predict tumors limited to the bowel wall with a high PPV. USPIO MRI at 1.5T can also accurately select pN0 patients with a high NPV for the prediction of malignant nodes. The performances of an experienced and less experienced radiologist were equal; indicating that preoperative selection with MRI can also be reliable in the setting of a general hospital.

References

1. *Parkin DM, Bray F, Ferlay J, Pisani P. Estimating the world cancer burden: Globocan 2000. Int J Cancer 2001; 94:153-156.*
2. *Jemal A, Tiwari RC, Murray T, et al. Cancer statistics, 2004. CA Cancer J Clin 2004; 54:8-29.*
3. *Boyle P, Ferlay J. Cancer incidence and mortality in Europe, 2004. Ann Oncol 2005; 16:481-488.*
4. *Brown G, Daniels IR. Preoperative staging of rectal cancer: the MERCURY research project. Recent Results Cancer Res 2005; 165:58-74.*
5. *Pahlman L, Glimelius B. Pre- or postoperative radiotherapy in rectal and rectosigmoid carcinoma. Report from a randomized multicenter trial. Ann Surg 1990; 211:187-195.*
6. *Improved survival with preoperative radiotherapy in resectable rectal cancer. Swedish Rectal Cancer Trial. N Engl J Med 1997; 336:980-987.*
7. *Kapiteijn E, Marijnen CA, Nagtegaal ID, et al. Preoperative radiotherapy combined with total mesorectal excision for resectable rectal cancer. N Engl J Med 2001; 345:638-646.*
8. *Bipat S, Glas AS, Slors FJ, Zwinderman AH, Bossuyt PM, Stoker J. Rectal cancer: local staging and assessment of lymph node involvement with endoluminal US, CT, and MR imaging--a meta-analysis. Radiology 2004; 232:773-783.*
9. *Will O, Purkayastha S, Chan C, et al. Diagnostic precision of nanoparticle-enhanced MRI for lymph-node metastases: a meta-analysis. Lancet Oncol 2006; 7:52-60.*
10. *Marijnen CA, Nagtegaal ID, Klein Kranenbarg E, et al. No downstaging after short-term preoperative radiotherapy in rectal cancer patients. J Clin Oncol 2001; 19:1976-1984.*
11. *Weissleder R, Elizondo G, Wittenberg J, Rabito CA, Bengele HH, Josephson L. Ultrasmall superparamagnetic iron oxide: characterization of a new class of contrast agents for MR imaging. Radiology 1990; 175:489-493.*
12. *Frija G, Clement O, Le Guen O, Cuenod CA, Siauve N, Benderbous S. Experimental investigation of the delivery pathway of ultrasmall superparamagnetic iron oxide to lymph nodes. Acad Radiol 1996; 3 Suppl 2:S299-300.*
13. *Lahaye MJ, Engelen SM, Kessels AG, et al. USPIO-enhanced MR Imaging for Nodal Staging in Patients with Primary Rectal Cancer: Predictive Criteria. Radiology 2008.*
14. *Brown G, Richards CJ, Bourne MW, et al. Morphologic Predictors of Lymph Node Status in Rectal Cancer with Use of High-Spatial-Resolution MR Imaging with Histopathologic Comparison. Radiology 2003; 227:371-377.*
15. *Kim JH, Beets GL, Kim MJ, Kessels AG, Beets-Tan RG. High-resolution MR imaging for nodal staging in rectal cancer: are there any criteria in addition to the size? Eur J Radiol 2004; 52:78-83.*
16. *DeLong ER, D. M. DeLong, and D. L. Clarke-Pearson. . Comparing the areas under two*

or more correlated receiver operating curves: A nonparametric approach. . Biometrics 1988; 44:837-845.

17. *Cohen J. A coefficient of agreement for nominal scales. Educational and Psychological Measurement 1960; 20:37-46.*
18. *Cohen J. Weighted Kappa: nominal scale agreement with provision for scaled disagreement or partial credit. Psychol Bull 1968; 70:213-230.*
19. *Adam IJ, Mohamdee MO, Martin IG, et al. Role of circumferential margin involvement in the local recurrence of rectal cancer. Lancet 1994; 344:707-711.*
20. *Quirke P, Durdey P, Dixon MF, Williams NS. Local recurrence of rectal adenocarcinoma due to inadequate surgical resection. Histopathological study of lateral tumour spread and surgical excision. Lancet 1986; 2:996-999.*
21. *Birbeck KF, Macklin CP, Tiffin NJ, et al. Rates of circumferential resection margin involvement vary between surgeons and predict outcomes in rectal cancer surgery. Ann Surg 2002; 235:449-457.*
22. *Marijnen CA, Nagtegaal ID, Kapiteijn E, et al. Radiotherapy does not compensate for positive resection margins in rectal cancer patients: report of a multicenter randomized trial. Int J Radiat Oncol Biol Phys 2003; 55:1311-1320.*
23. *Beets-Tan RG, Beets GL, Vliegen RF, et al. Accuracy of magnetic resonance imaging in prediction of tumour-free resection margin in rectal cancer surgery. Lancet 2001; 357:497-504.*
24. *Strassburg J. Magnetic resonance imaging in rectal cancer: the MERCURY experience. Tech Coloproctol 2004; 8 Suppl 1:s16-18.*
25. *Poon FW, McDonald A, Anderson JH, et al. Accuracy of thin section magnetic resonance using phased-array pelvic coil in predicting the T-staging of rectal cancer. Eur J Radiol 2005; 53:256-262.*
26. *Marusch F, Koch A, Schmidt U, et al. Routine use of transrectal ultrasound in rectal carcinoma: results of a prospective multicenter study. Endoscopy 2002; 34:385-390.*
27. *Landmann RG, Wong WD, Hoepfl J, et al. Limitations of early rectal cancer nodal staging may explain failure after local excision. Dis Colon Rectum 2007; 50:1520-1525.*

USPIO MRI FOR NODAL STAGING OF PATIENTS WITH PRIMARY RECTAL CANCER: PREDICTIVE CRITERIA

PUBLISHED IN *RADIOLOGY 2008; VOLUME 246, ISSUE 3, PAGES 801-11*

M.J. LAHAYE

S.M.E. ENGELEN

A.G.F. KESSELS

A.P. DE BRUÏNE

M.F. VON MEYENFELDT

J.M.A. VAN ENGELSHOVEN

C.J.H. VAN DE VELDE

G.L. BEETS

AND R.G.H. BEETS-TAN

6

Purpose

To prospectively determine the diagnostic performance of various predictive criteria for USPIO MRI nodal staging in primary rectal cancer patients, using histology as the reference standard.

Materials and methods

Institutional review board approval and informed consent were obtained. 28 Rectal cancer patients (18 males and 10 females, mean age 68, range 54-89 years) underwent USPIO MRI with 2DT2WFSE, 3DT1WGRE and 3DT2*-weighted sequences. Two observers with different reading experience evaluated each node on 3DT2*-weighted images for: border irregularity, short and long axis and estimated percentage of white region within the node, categorized as: <30%, 30-50% or >50%. A ratio for the white region was also calculated ($Ratio_A$). Signal intensity (SI) measurements within muscle (SI_{muscle}), total node (SI_{TN}), white (SI_{white}) and dark (SI_{dark}) region within the node were used to calculate ratios: SI_{TN}/SI_{muscle} and SI_{white}/SI_{dark}. Lesion-by-lesion analysis was performed with histology as the reference standard. Receiver operating characteristic (ROC) curves and interobserver agreement analysis were performed. The most accurate and practical criterion was then evaluated by observer 3.

Results

236 lymph nodes in 28 patients were studied. The area under the ROC-curve (AUC) of estimated percentage of white region and $Ratio_A$ for observer 1 and 2 were: 0.96 & 0.99 and 0.95 & 0.97, respectively. The AUC of the estimated percentage criterion for observer 3 was 0.96. The AUC of border, short axis, long axis, SI_{TN}/SI_{muscle} and SI_{white}/SI_{dark} for observer 1 were: 0.65, 0.75, 0.79, 0.85, 0.75 and observer 2: 0.58, 0.75, 0.79, 0.89 and 0.79, respectively. The interobserver agreement (*K* value) for the estimated white region between observer 1 & 2, 1 & 3, 2 & 3 were 0.77, 0.79, 0.84, respectively. K value for observer 1 & 2 for the border was 0.28. The Intra Class Correlation for observer 1 & 2 for the short axis, long axis diameter, the $Ratio_A$, the SI_{TN}/SI_{muscle} and SI_{white}/SI_{dark} were 0.91, 0.96, 0.91, 0.72 and 0.92.

Conclusion

The estimated percentage of white region and measured $Ratio_A$ are the most accurate criteria for predicting malignant nodes with USPIO MRI, of which the first is the most practical.

Introduction

Rectal cancer is a common malignancy with a highly variable local recurrence rate of 3-32% [1]. In the recent past besides total mesorectal excision (TME), neoadjuvant rather than adjuvant radio(chemo)therapy is advocated to reduce the local recurrence rate [2, 3]. Furthermore, to avoid over and undertreatment a tailor-made neoadjuvant approach for every rectal cancer patient, based on preoperative prediction of the risk for local recurrence, seems to be favorable. Important risk factors are T-stage, circumferential resection margin (CRM), nodal status and height of the tumor. Preoperative imaging is essential to identify these risk factors.

The nodal status is a well-established important prognostic risk factor. The higher the number of positive nodes, the higher the risk for a local recurrence [4, 5]. However, prediction of the nodal status remains a problem for the radiologist. The results of a meta-analysis show that for identification of nodal disease endoluminal ultrasound (EUS), magnetic resonance imaging (MRI) and computed tomography (CT) lack sufficient accuracy for clinical decision making [6].

Ultrasmall superparamagnetic iron oxide (USPIO) MRI has been reported to be promising in differentiating benign from malignant nodes. A recent meta-analysis showed that USPIO MRI is superior to all other modalities in detection of lymph node metastases for various tumors [7]. Despite many promising results concerning USPIO MRI, there is still insufficient knowledge of which specific USPIO MRI criteria can be used for characterizing lymph nodes as benign or malignant. Thus, the purpose of our study was to prospectively determine the diagnostic performance of various predictive criteria for USPIO MRI nodal staging in primary rectal cancer patients, using histology as the reference standard.

Materials and methods

Guerbet Laboratories (Roissy, France) only provided free vials of Sinerem®, that still was not commercially available at time of this study, and Guerbet Laboratories had no control of inclusion, data or the information submitted for this publication. The study was financed by the Dutch Cancer Society.

Patients

Institutional review board approval and informed consent were obtained. During the study period of June 2004 to July 2006 a total of eighty-seven consecutive patients were diagnosed with biopsy proven primary rectal cancer at our centre. All rectal tumors were defined by an inferior tumor margin < 15 cm from the anal verge as described by endoscopy. Fourteen patients with non-resectable disease or contraindications for MRI were excluded from the study. Forty-five patients with locally advanced tumors (involved CRM or N2 status) underwent neoadjuvant chemoradiation, and were excluded because after chemoradiation histology cannot be considered representative of the primary nodal status. Twenty-eight patients were eligible for this prospective study (18 males and 10 females, mean age 68, range 54-89 years). These patients underwent USPIO MRI before their standard treatment. The standard treatment in our country for non-locally advanced rectal cancer is a short course of radiotherapy (5 x 5 Gy) immediately followed by total mesorectal excision surgery [8]. The short course of radiotherapy is known not to downstage the nodal status in rectal cancer patients [9].

Ultrasmall superparamagnetic iron oxide

The USPIO MR contrast agent, Sinerem (Guerbet Laboratories, Roissy, France), consists of low molecular weight iron oxide coated with dextran. Sinerem is supplied as a powder in a glass vial containing 210 mg and must be reconstituted by using 10 mL of normal saline. A dose of 0.13 mL per kilogram of body weight (2.6 mg Fe/kg) of the reconstituted solution was diluted in 100 mL of normal saline. This was administered in the preparation room of the MR unit. The contrast agent was given intravenously within a period of approximately 45 minutes by slow drip infusion with a microfilter. Administration was closely monitored for any adverse effects and completed 24-36 hours before post contrast MR imaging was planned. No precontrast MRI was performed. No adverse events relating to the USPIO infusion were observed in this study.

In the literature two main mechanisms are described for transportation of the nanoparticles to the lymph nodes. The major pathway is direct transcapillary

passage of the nanoparticles from blood vessels into the medullary sinuses of the lymph node. The other pathway is nonselective endothelial transcytosis across permeable capillaries into the interstitium, from where nanoparticles are transported through the lymphatic system and accumulate in macrophages within the lymph node [10, 11]. The nanoparticles cause a decrease in signal intensity within the node due to susceptibility artifacts on 3DT2*-weighted images. Variation of signal intensity within a node can be explained on the basis of the concentration of macrophages (nanoparticles) in a particular region in the node. A region with a normal concentration of macrophages (nanoparticles) will produce an area with signal decrease. This means that enlarged inflamed nodes will also show a significant fall in signal intensity. The involved part of the lymph node will show no signal decrease due to the replacement of macrophages by tumor cells creating a region of increased signal intensity within the node (white region).

MR IMAGING

MR imaging was performed on a 1.5T system Gyroscan, Powertrak 6000, NT release 6.2.1, 23.0 mT.m, rise time 0.2 ms, slew-rate 105 T 1/ms (Philips Medical Systems, Best, Netherlands) using a pelvic phased array coil with the patient in feet-first, supine position. Sequences used are sagittal and axial 2D T2 weighted TSE. 3DT2*-weighted axial images were obtained with 23/18.41 (TR/TE), 20 degree flip angle, a 512x512 matrix, and 1.25-mm slice thickness. 3D T1-weighted axial images were obtained with shortest 10/4.60 (TR/TE), 15 degree flip angle, a 384x512 matrix, and 1 mm slice thickness to locate lymph nodes and to differentiate them from blood vessels. All axial images were angled perpendicular to the rectal tumor. Patients did not receive bowel or other preparation. The total scan time was 32-40 minutes.

IMAGE EVALUATION

Two observers (1) R.G.H. and (2) M.J.L. (with approximately 3000 and 300 MR pelvic reading experience, respectively) prospectively and blinded to each other's results and histological results evaluated each node on axial 3DT2*-weighted images for the

following items: border (sharp, indistinct or disrupted), short and long axis diameter. Furthermore, the percentage of white region within the node was estimated and categorized as: <30%, 30-50% or >50% on 3DT2*-weighted images (Figure 6.1).
Beside this visual assessment of the percentage of white region within the node, the proportion of white region within the node was also quantitatively measured. The surface area of white region within the node and the surface area of total node were determined on an axial 3DT2*-weighted image, where the node was the largest, using the workstation's measurement tools. By dividing the surface area of white region by the surface area of the total node, a quantitatively measured ratio of white region was calculated for both observers. This is further referred to as $Ratio_A$. $Ratio_A$ was not categorized.
By placing regions of interests (ROIs) completely over the white and dark region within the node the signal intensity (SI) was measured. ROIs of the same size were used to measure the signal intensity of the total node and that of the gluteus muscle. These signal intensities were used to calculate the following two ratio's for both observers: SI_{white}/SI_{dark} and SI_{TN}/SI_{muscle}.

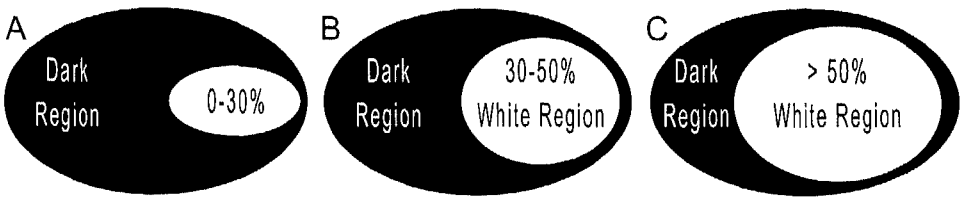

Figure 6.1. A schematic diagram of a lymph node on USPIO enhanced T2*-weighted images with (A) white region of <30%, (B) white region 30-50% and (C) white region >50%.

The observer with the highest level of experience, observer 1, also prospectively recorded the localization of each visible lymph node depicted by 3DT2*-weighted MR images on an anatomical map (Figure 6.2). This anatomical map was used as a template to compare with the nodes depicted by the other observers and the nodes found at histopathological evaluation.
A third observer was introduced to evaluate the most accurate and practical predictive criterion for nodal status of observer 1 & 2. Observer 3 (S.M.E.) had similar reading experience as observer 2 (approximately 300 pelvic MR readings).

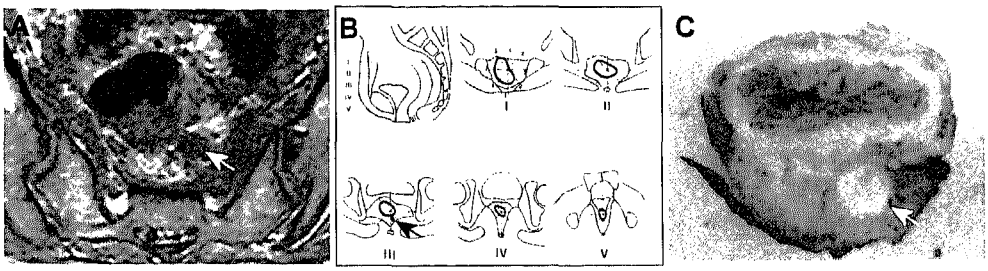

Figure 6.2. The MR radiologist predicted each visible lymph node on MR images (A). Each visible node was recorded on an anatomical 'roadmap'. (B). Each node was harvested from the histological specimen. The anatomical map was used as a template to match the nodes found at the histological evaluation (C) with the nodes depicted on MRI.

Histopathological evaluation

The standard surgical procedure was a TME, as described by Heald [12]. The rectum with the complete surrounding mesorectal fat and mesorectal lymph nodes was removed by sharp dissection along the mesorectal fascia. Histological examination was standardized: the specimen was fixed in formalin for 24-48h and the circumferential resection plane inked. The specimen was then sectioned every 5 mm transversely and thus also perpendicular to the mesorectum. A dedicated pathologist made a careful search for lymph nodes in each histological tissue slice. Each lymph node found was matched to the corresponding node visible on the MR images using the anatomical map as a template. This nodal harvesting procedure was performed by a pathologist (A.P.B., with 17 years of experience) together and side by side with observer 1 to ensure an accurate lesion-by-lesion analysis. Accurate nodal matching was only possible due to the detailed knowledge of the MR images using specific characteristics like the size of the lymph node and the position of the lymph node in relation to the rectal wall, small vessels, mesorectal fascia, tumor and other lymph nodes. In cases in which nodal matching was not possible it was recorded as such. Each harvested lymph node was placed in marked individual trays, and processed according to standard methods and stained with haematoxylin-eosin. Then the same pathologist, blinded to the USPIO MRI predictions, reported the status of each lymph node: benign or malignant. In this manner accurate lesion-by-lesion analysis for mesorectal lymph nodes could be performed.

Statistical analysis

Based on the results of a pilot study at our center we expect a sensitivity of 99%. 30 positive lymph nodes are needed to reject with a power of 75% that the lower limit of the 95% confidence interval of sensitivity of the USPIO MRI is 90% or lower. The number of patients needed to include 30 positive lymph nodes can be calculated as follows: 10% of the nodes found will be malignant and an average of 12 nodes in each patient will be found at histopathological examination; this means that we need 300 nodes at histopathological examination and thus 25 patients.

To determine the interobserver agreement, weighted kappas [13, 14] were calculated for the ordinal variables and Intra Class Correlations (ICC) for interval scaled variables [15], all with their 95%-confidence intervals. A kappa value (K value) of less than 0.00 indicates poor agreement; 0.00-0.20 slight agreement; 0.21-0.40 fair agreement; 0.41-0.60 moderate agreement; 0.61-0.80 substantial agreement and 0.81-1.00 almost perfect agreement [16]. The ICC ranges from 0 to 1, with a value of 0 indicating a completely unreliable measurement, and a value of 1 indicating a 100% reproducible measurement.

Diagnostic performance of the different evaluation methods were analyzed with logistic regression model and generalized estimating equations (GEE) were used to estimate marginal effects. With the results receiver operating characteristic (ROC) curves were constructed and area under the curves (AUCs) & 95%-confidence levels were calculated using STATA software (Stata Statistical Software: Release 9. College Station, TX: StataCorp LP).

Results

Histology

In 28 patients MR imaging found 362 lymph nodes in the mesorectum. After surgical resection 333 lymph nodes were found at histology; 27 malignant and 306 benign lymph nodes. Of the 333 (27 + 306) nodes there were 236 nodes at histology that could exactly be matched with nodes found on MRI, while 97 nodes found at histology could not be exactly matched with MRI. These 97 nodes, all benign, were excluded from the analysis. This leaves us with 236 lymph nodes for the lesion-by-lesion analysis (Figure 6.3). Only 176 nodes were eligible for SI measurements, because 60 nodes were too small to accurately measure the signal intensity of the node. The mean short- and long axis diameter of the total lymph node were 3.6 mm (range 2-9 mm) and 4.7 mm (range 2-13 mm), respectively.

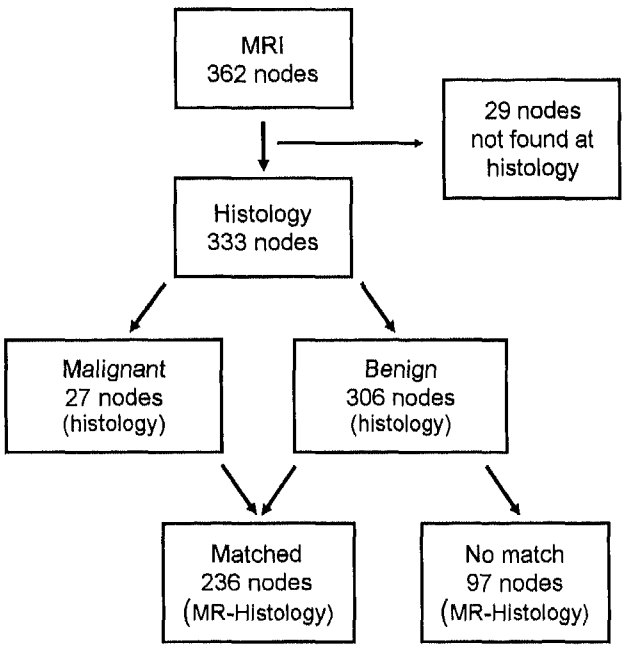

Figure 6.3. A flowchart of the lymph nodes found on MR imaging and at histology.

Diagnostic performance

The AUC of border, short axis, long axis, SI_{TN}/SI_{muscle} and SI_{white}/SI_{dark} for observer 1 were: 0.65, 0.75, 0.79, 0.85, 0.75 and for observer 2: 0.58, 0.75, 0.79, 0.89 and 0.79, respectively (see Table 6.1 and Figure 6.4).

Table 6.1. Area under the curve (AUC) and 95%-Confidence Intervals for observer 1 and 2 for all criteria used to distinguish between malignant and benign nodes.

	Observer 1		Observer 2		Number of Nodes
	AUC	95% CI	AUC	95% CI	
Short Ø LN	0.75	0.61-0.89	0.75	0.64-0.87	236
Long Ø LN	0.79	0.67-0.91	0.79	0.69-0.90	236
Border	0.65	0.60-0.79	0.58	0.48-0.68	236
Estimated % white region	0.96	0.90-1.0	0.95	0.90-1.0	236
$Ratio_A$	0.99	0.98-1.0	0.97	0.91-1.0	236
SI_{TN}/SI_{muscle}	0.85	0.75-0.94	0.89	0.80-0.97	176
SI_{white}/SI_{dark}	0.75	0.60-0.90	0.79	0.66-0.91	176

The highest AUC for the prediction of the nodal status were found for the estimated percentage and measured $Ratio_A$ of white region within the node (0.96 and 0.99, respectively, for observer 1 and 0.95 and 0.97, respectively, for observer 2). When the white region within the node is estimated as more than 30%, the sensitivity and specificity for detection of malignant nodes is 93% and 96%, respectively (Figure 6.5 and 6.6).

Of the two criteria that were the most accurate in predicting the nodal status with USPIO MRI, the estimated percentage of white region within the node was the most practical to use in the clinical practice. Therefore, this criterion was chosen to be

evaluated by observer 3. The AUC (95%-confidence level) of observer 3 for this criterion was 0.96 (0.91-1.0).

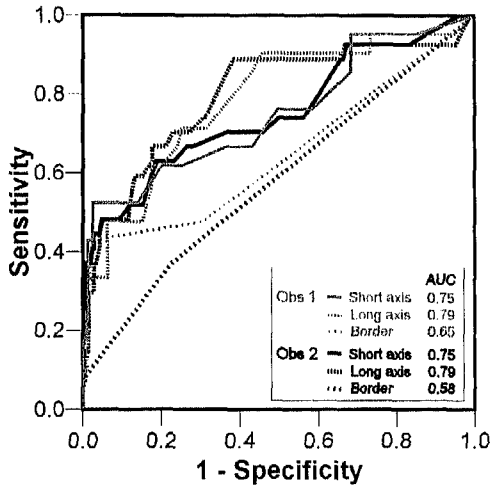

Figure 6.4.
Receiver operating characteristic (ROC) curves and areas under the curve (AUC) for observer 1 and 2, for the detection of malignant lymph nodes using the short & long axis diameter and border of the lymph node.

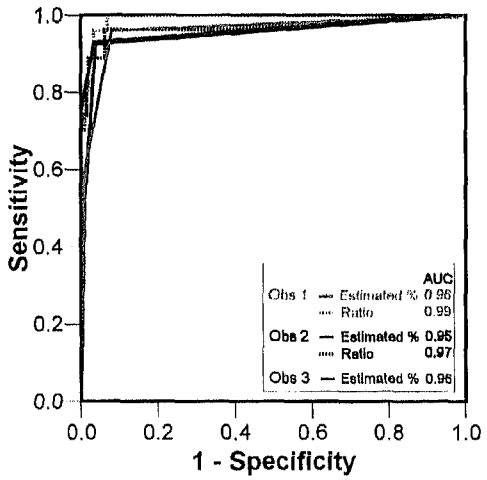

Figure 6.5.
Receiver operating characteristic (ROC) curves and areas under the curve (AUC) (observer 1, 2 & 3) for the detection of malignant lymph nodes using the estimated % of white region within the node and the measured $Ratio_A$ (observer 1 & 2).

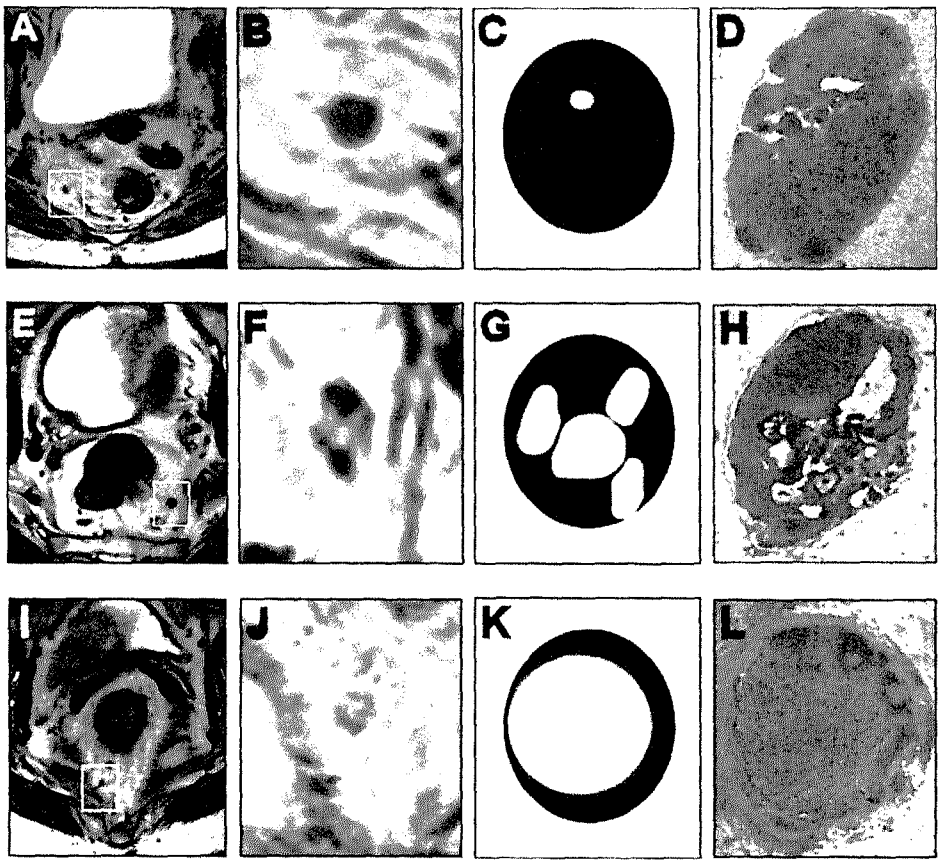

Figure 6.6. A, B, C, D. A benign mesorectal node, diagnosed on USPIO enhanced MRI: (A) on T2-weighted FSE image smaller than 5 mm and difficult to differentiate between malignant and benign, (B) on USPIO enhanced T2* image causing a black blooming artifact with (C) less than 30% white region within the node indicating a benign node, (D) at histology confirmed to be a benign node.

Figure 6.6. E, F, G, H. A small malignant mesorectal node, detected with USPIO MRI: (E) on T2-weighted FSE image smaller than 5 mm and difficult to differentiate between malignant and benign, (F) on USPIO enhanced T2* image showing incomplete blackening of the node, (G) with an estimated 30-50% white region within the node, suggesting a malignant node, (H) at histology confirmed to be a partially involved metastatic node.

Figure 6.6. I, J, K, L. An ultrasmall malignant mesorectal node, detected with USPIO MRI: (I) on T2-weighted FSE image smaller than 3 mm and difficult to differentiate between malignant and benign, (J) on USPIO enhanced T2* image remaining white indicating no iron uptake, (K) with more than 50% white area within the node, suggesting a malignant node, (L) at histology confirmed a massively involved tumoral node.

Intra class correlation

The Intra Class Correlation for observer 1 & 2 for the short axis, long axis diameter, the $Ratio_A$, the SI_{TN}/SI_{muscle} and SI_{white}/SI_{dark} were 0.91, 0.96, 0.91, 0.72 and 0.92 (see Table 6.2). Generally the interobserver agreement was good to excellent. There was more agreement for the $Ratio_A$, short and long axis diameter than for the SI_{TN}/SI_{muscle}.

Table 6.2. Intra Class Correlations (ICC) and 95%-confidence intervals (CI) for all for interval scaled criteria for observer 1 and 2.

	Intra Class Correlation	95% CI
Short Ø LN	0.91	0.87-0.94
Long Ø LN	0.96	0.97-0.99
$Ratio_A$	0.91	0.87-0.94
SI_{TN}/SI_{muscle}	0.72	0.57-0.82
SI_{white}/SI_{dark}	0.92	0.86-0.96

Interobserver agreement

The interobserver agreement (K value) for the estimated white region between observer 1 and 2 was good (K=0.77), while that for the border was only fair (K=0.28). The K value analysis of the estimated white region for observer 1 & 3 and observer 2 & 3 were good (K=0.79) and excellent (K=0.84), respectively.

Discussion

Our results show that for observer 1 and 2 both the estimated as well as the measured ratio of the white region within the node were very accurate predictors for malignant nodes in rectal cancer. The results of observer 3 confirmed that the estimated percentage of the white region within the node could serve as a reliable and practical criterion for the prediction of malignant nodes on USPIO MRI.

Size criteria, such as long and short axis of the node, and border morphology were only moderately accurate for the distinction between malignant and benign lymph nodes.

An estimated area of white region within the node larger than 30% was highly predictive for an involved node with a sensitivity of 93% and a specificity of 96%. The measured $Ratio_A$ was also an accurate predictor for malignant lymph nodes. The larger the area of white region, the more likely the node is malignant. The white region in the lymph node is caused by no or very little uptake of USPIO in that malignant part of the lymph node. Benign conditions like focal nodal fibrosis, granulamatous disease or a fatty hilum can also be depicted as a white region due to the lack of macrophages, thus mimicking malignant nodes. These white regions, however, are usually 30% or less of the total node area. Another way to differentiate between a white fatty hilum and a white tumoral region is to compare the 3DT2*-weighted images with the 3DT1-weighted images where a fatty hilum is depicted as a white region within the node, while tumor is not. In the same manner the dark region can hide small micrometastases. The clinical implication of micrometastases, however, is debatable. Although there is a small overlap in MR features of benign and malignant nodes, a general rule of thumb is that when the white region is less than 30% the nodes are most often benign.

To our knowledge no literature is published concerning the estimated or measured ratio of the white region within the node. A range of patterns of contrast enhancement have been described to discriminate between malignant and non-malignant lymph nodes using USPIO MRI [17]. The use of patterns to predict nodes has a major drawback. The radiologist's mind must choose from a variety patterns and assess which of the patterns would fit best to a malignant and which to a benign node. This involves a certain level of subjectivity and constitutes a potential source of erroneous interpretation. Our study shows that a simple estimation or

measurement of the white region within the node is reliable for the identification of malignant nodes. The interobserver agreement between an experienced reader and less experienced readers (observer 1 vs. observer 2 or 3) for the estimated white region were good, indicating a high consistency in interpreting the images independent of the experience of the readers. The K value of 0.84 for observer 2 vs. 3 even shows that two less experienced readers can have an excellent agreement among each other. These findings suggest that USPIO MRI could become a promising tool for nodal malignancy prediction not only for experienced but also for less experienced readers.

The SI_{TN}/SI_{muscle} measurements show that the higher the signal intensity of the total node is, the higher the risk of a malignant node. These findings confirm earlier reports of signal intensities in USPIO MRI. Harisinghani et al. [18] demonstrated that a distinction between malignant and benign nodes could be made on the basis of signal intensity of the total node. In our study the SI ratio measurements between the white and dark region within the node (SI_{white}/SI_{dark}) were disappointing. The moderate AUC can be explained by the difficulties of measuring a white and a dark region within a very tiny node. The white and dark regions within the node are often too small or too irregular to accurately position a ROI. In this study 26% of all nodes could not be measured, obviously making this criterion less valuable in clinical practice.

Size criteria were insufficient to consistently distinguish between malignant and benign lymph nodes in patients with rectal cancer. The disappointing results concerning the size criteria are due to the high rate of relatively small involved lymph nodes in rectal cancer. Brown et al. [19] showed that even mesorectal lymph smaller than 5 mm still had a prevalence of positive lymph nodes of 15%. As early as 1989 Roadwork et al. [20] showed that 32% of the patients with involved nodes had only small (5 mm or less) involved nodes. This partly explains why EUS, CT and nonenhanced MR studies on nodal prediction in rectal cancer patients using size criteria have shown disappointing results [6]. Additional MR criteria have therefore been studied, such as border and signal intensity. Kim et al. [21] and Brown et al. [19] found that the border and signal intensity characteristics of lymph nodes on T2W FSE images were useful for identification of malignant nodes in rectal cancer. The aspect of the border and the homogeneity of the signal, however, are generally easier to evaluate in the "larger" nodes (>5 mm). In our study, however, we mainly included

patients with non-locally advanced tumors with predominantly smaller nodes. In our experience USPIO MRI and its characteristics are especially of additional benefit in the evaluation of these small nodes (<5 mm), where border and signal intensity criteria tend to be less helpful.

A limitation of our study is the relative limited number of positive nodes. This is due to the study's patient selection of "non-locally advanced" rectal cancer stratified for a short preoperative radiation course in order to be able to perform a lesion-by-lesion analysis. Another issue is that no preoperative radiation would probably have been more convincing for exact lesion-by-lesion correlation. However, nowadays that standard preoperative radiotherapy has definitely shown benefit for the reduction of the local recurrence rate in rectal cancer patients, treating patients with non-superficial rectal cancer without preoperative radiation would be unethical. Furthermore, literature shows that no downstaging occurs after short-term of preoperative radiation [9].

In conclusion the estimated percentage of white region within the node and the measured $Ratio_A$ are the most accurate predictive criteria for USPIO MRI. In the busy daily practice of a radiologist there is little room for time-consuming measurements of numerous nodes. Therefore, the estimated percentage of white region within the node would be most practical to use. Our study indicates that this was an accurate criterion not only among experienced readers, but also for two less experienced readers.

References

1. *Sagar PM, Pemberton JH: Surgical management of locally recurrent rectal cancer. Br J Surg 1996;83:293-304.*
2. *Pahlman L, Glimelius B: Pre- or postoperative radiotherapy in rectal and rectosigmoid carcinoma. Report from a randomized multicenter trial. Ann Surg 1990;211:187-195.*
3. *Sauer R, Becker H, Hohenberger W, et al.: Preoperative versus postoperative chemoradiotherapy for rectal cancer. N Engl J Med 2004;351:1731-1740.*
4. *Moran MR, James EC, Rothenberger DA, Goldberg SM: Prognostic value of positive lymph nodes in rectal cancer. Dis Colon Rectum 1992;35:579-581.*
5. *Park YJ, Park KJ, Park JG, et al.: Prognostic factors in 2230 Korean colorectal cancer patients: analysis of consecutively operated cases. World J Surg 1999;23:721-726.*
6. *Lahaye MJ, Engelen SM, Nelemans PJ, et al.: Imaging for predicting the risk factors--the circumferential resection margin and nodal disease--of local recurrence in rectal cancer: a meta-analysis. Semin Ultrasound CT MR 2005;26:259-268.*
7. *Will O, Purkayastha S, Chan C, et al.: Diagnostic precision of nanoparticle-enhanced MRI for lymph-node metastases: a meta-analysis. Lancet Oncol 2006;7:52-60.*
8. *Kapiteijn E, Marijnen CA, Nagtegaal ID, et al.: Preoperative radiotherapy combined with total mesorectal excision for resectable rectal cancer. N Engl J Med 2001;345:638-646.*
9. *Marijnen CA, Nagtegaal ID, Klein Kranenbarg E, et al.: No downstaging after short-term preoperative radiotherapy in rectal cancer patients. J Clin Oncol 2001;19:1976-1984.*
10. *Weissleder R, Elizondo G, Wittenberg J, et al.: Ultrasmall superparamagnetic iron oxide: characterization of a new class of contrast agents for MR imaging. Radiology 1990;175:489-493.*
11. *Frija G, Clement O, Le Guen O, et al.: Experimental investigation of the delivery pathway of ultrasmall superparamagnetic iron oxide to lymph nodes. Acad Radiol 1996;3 Suppl 2:S299-300.*
12. *Heald RJ: A new approach to rectal cancer. Br J Hosp Med 1979;22:277-281.*
13. *Cohen J: A coefficient of agreement for nominal scales. Educational and Psychological Measurement 1960;20:37-46.*
14. *Cohen J: Weighted Kappa: nominal scale agreement with provision for scaled disagreement or partial credit. Psychol Bull 1968;70:213-230.*
15. *Shrout PE, Fleiss J.L.: Intraclass Correlations: Uses in Assessing Rater Reliability. 1974;86:420-428.*
16. *Landis JR, Koch GG: The measurement of observer agreement for categorical data. Biometrics 1977;33:159-174.*
17. *Koh D-M, Brown G, Temple L, et al.: Rectal Cancer: Mesorectal Lymph Nodes at MR Imaging with USPIO versus Histopathologic Findings--Initial Observations. Radiology*

2004;231:91-99.

18. *Harisinghani MG, Saini S, Slater GJ, et al.: MR imaging of pelvic lymph nodes in primary pelvic carcinoma with ultrasmall superparamagnetic iron oxide (Combidex): preliminary observations. J Magn Reson Imaging 1997;7:161-163.*
19. *Brown G, Richards CJ, Bourne MW, et al.: Morphologic Predictors of Lymph Node Status in Rectal Cancer with Use of High-Spatial-Resolution MR Imaging with Histopathologic Comparison. Radiology 2003;227:371-377.*
20. *Dworak O: Number and size of lymph nodes and node metastases in rectal carcinomas. Surg Endosc 1989;3:96-99.*
21. *Kim JH, Beets GL, Kim MJ, et al.: High-resolution MR imaging for nodal staging in rectal cancer: are there any criteria in addition to the size? Eur J Radiol 2004;52:78-83.*

USPIO MRI IMAGING AFTER NEOADJUVANT CHEMORADIATION: CRITERIA FOR PREDICTING INVOLVED NODES IN RECTAL CANCER PATIENTS

MODIFIED VERSION IN PRESS *RADIOLOGY 2009*

M.J. LAHAYE

G.L. BEETS

S.M.E. ENGELEN

A.G.F. KESSELS

A.P. DE BRUÏNE

H.W.S. KWEE

J.M.A. VAN ENGELSHOVEN

C.J.H. VAN DE VELDE

AND R.G.H. BEETS-TAN

7

Purpose

To prospectively determine the diagnostic performance of predictive criteria for USPIO MRI in nodal restaging after chemoradiation in patients with rectal cancer.

Materials and methods

IRB approval and informed consent were obtained. 39 Included patients (24 males and 15 females, mean age 64, range 35-87 years) with locally advanced rectal cancer underwent a restaging USPIO MRI 6-8 weeks after chemoradiation with 2DT2WFSE, 3DT1WGRE and 3DT2*-weighted sequences. Two observers evaluated each node on T2-weighted images: border irregularity, short and long axis diameter and on T2*-weighted images: estimated percentage of white region (area with no USPIO uptake) within the node, categorized as: <30%, 30-50% or >50%. This percentage was also measured ($Ratio_A$). Signal intensity (SI) measurements within muscle (SI_{GM}) and total node (SI_{TN}) were used to calculate the SI_{TN}/SI_{GM} ratio. Histology was used as reference standard. Receiver operating characteristic (ROC) curves and interobserver agreement analysis were performed. The constructed ROC curves were compared.

Results

A lesion-by-lesion analysis was feasible in 201 lymph nodes. The area under the ROC-curve (AUC) of border, short and long axis size criteria for observer 1 were: 0.85, 0.87 and 0.88, for observer 2: 0.70, 0.89 and 0.87, respectively. The AUC for estimated percentage of white region within the node, $Ratio_A$ and SI_{TN}/SI_{GM} for observer 1 were: 0.98, 0.99 and 0.62, and for observer 2: 0.97, 0.98 and 0.65, respectively. The AUC for USPIO MR criteria were significantly better than for conventional MR criteria ($P<0.01$). Except for border irregularity and SI_{TN}/SI_{GM} all criteria showed high interobserver agreement ($K > 0.80$).

Conclusion

The most reliable predictors for identifying benign nodes after chemoradiation of rectal cancer on a restaging USPIO enhanced MRI are the estimated and measured ration of white region within the node. In contrast to the results with primary staging, size measurements on standard T2W FSE sequences offers a reasonably good accuracy to identify benign lymph nodes after chemoradiation.

Introduction

The standard treatment for locally advanced rectal cancer is preoperative chemoradiation followed by a standard resection of the rectum, with surrounding organs when required. Neoadjuvant chemoradiation has shown result in 15-30% complete tumor response rates and almost 50% partial response rates, leading to improved respectability and local control. Sterilization of involved lymph nodes also occurs, with a reported decline in the rate of node positive tumors found at histopathology from 40% before chemoradiation to 25% after chemoradiation [1-4]. The clinical question that arises is what to do with a good response after chemoradiation? Patients with a good response could be selected for a local excision when imaging would allow identification of a tumor remnant that is confined to the bowel wall and identification of node negative disease. This chapter focuses on the assessment of the response in the lymph nodes. Although a good response in the primary tumor generally is accepted to correspond with a good response in the lymph nodes, there are some conflicting reports with rates of involved nodes ranging from 1.7% to 17% in patients with a complete response in the primary tumor [5, 6]. This further indicates the need for a reliable imaging tool to assess the lymph node status after chemoradiation.

Nodal staging in rectal cancer remains a problem for the radiologist. Two meta-analyses have shown that for the identification of nodal disease on a patient basis in primarily rectal cancer all currently used imaging modalities lack sufficient accuracy for clinical decision making. The estimated sensitivity for endoluminal ultrasound (EUS), magnetic resonance imaging (MRI) and computed tomography (CT) was 67%, 55%, and 66%, with corresponding specificity estimates of 78%, 74% and 76% [7, 8]. All modalities heavily rely on size criteria, and size on its own is insufficient to reliably distinguish between malignant and benign lymph nodes in rectal cancer. Brown et al. showed that 3 or 5 mm large lymph nodes still had a prevalence of positive lymph nodes of 10% and 28%, respectively [9]. MRI using Ultrasmall Superparamagnetic Iron Oxides (USPIO MRI) has shown promising results for detecting malignant nodes in the head and neck area, in the axilla and in the pelvis [10]. In a previous study we have confirmed the good performance of USPIO in the primary staging of rectal cancer patients, with a very high sensitivity and specificity for detection of malignant lymph nodes of around 95% [11].

Secondary staging after chemoradiation should be considered separately, as the behavior of a treated previously involved node may differ from a primary benign lymph node. There have been only a few reports on the accuracy of MR imaging methods to detect lymph node disease on a patient basis after chemoradiation, showing accuracy rates of 65-88% with sensitivities and specificities varying from 33-82% and 68-95%, respectively [12-15]. To date, there have been no lesion-by-lesion studies on rectal cancer lymph nodes after chemoradiation that could provide criteria, and no studies on USPIO MRI. It is not known whether our previously established criteria for the prediction of involved nodes in primarily untreated rectal cancer also apply after chemoradiation: the estimated percentage and the measured $Ratio_A$ of white region (the region with no USPIO uptake) within the black node on T2*-weighted images.
The purpose of this study is therefore to prospectively determine the diagnostic performance of predictive criteria for USPIO MRI in nodal restaging after chemoradiation in patients with rectal cancer.

Materials and methods

This study was partly financed by the Dutch Cancer Society. Guerbet Laboratories (Roissy, France) only provided the USPIO contrast agent and had no control of the data. The authors had full control of the data and information submitted for publication.

Patients

Between February 2003 and January 2008 a multicenter prospective rectal cancer project included 296 patients with rectal cancer. The main aim was to study the local control after a MRI based differentiated treatment. The institutional review board approved the study. Written informed consent was obtained from all patients. Exclusion criteria were pregnancy, age below 18, mental disability precluding informed consent, and contraindications for MRI (pacemaker, neurostimulator, insulin pump, certain vascular clips (e.g. used in brain surgery), cochlear implants, metallic

splinters in the eye or any other metal implant not securely fixed or electronic device).

In this large prospective project all patients underwent an USPIO MRI for primary staging and were stratified into low, intermediate and high-risk groups for a local recurrence based on the MR findings. The high-risk tumors were defined as tumors with a threatened or involved circumferential resection margin (CRM), tumors with >3 involved lymph nodes (N2 status), and any T3 or N1 distal tumor. The recommended treatment for these tumors was chemoradiation (5FU based chemotherapy with 28 x 1.8 Gy radiotherapy) followed by a resection 6-8 weeks after completion of chemoradiation. Most of these patients also underwent a second 'restaging' USPIO MRI 4 to 6 weeks after completion of the chemoradiation, and 1-2 weeks (mean 4 days, range 1-14 days) before the resection.

For the present study that addresses the diagnostic performance of predictive criteria for USPIO MRI in nodal restaging after chemoradiation patients were eligible for inclusion when 1) they were treated with chemoradiation, 2) a restaging USPIO MRI was performed, and 3) they underwent a resection, providing the standard of reference of histological examination. The sample size required for the present study, calculated as shown in the statistics section below, was set at the harvest of at least 40 malignant nodes. At the start of the project it was therefore decided to include patients for the lesion-by-lesion analysis until this number was achieved. At the end of the project overall 95 patients had received chemoradiation. The required number of malignant nodes was obtained after including the first 39 consecutive eligible patients. These 24 men and 15 women with a mean age of 64 years (range 35 – 87) form the basis of the present study.

Ultrasmall superparamagnetic iron oxides

The USPIO MR contrast agent, Sinerem (Guerbet Laboratories, Roissy, France), consists of low molecular weight iron oxide coated with dextran. Sinerem is supplied as a powder in a glass vial containing 210 mg and must be reconstituted by using 10 mL of normal saline. A dose of 0.13 mL per kilogram of body weight (2.6 mg Fe/kg) of the reconstituted solution was diluted in 100 mL of normal saline. This was administered intravenously by a slow drip infusion through a microfilter within a

period of approximately 45 minutes at the preparation room of the MRI unit. During infusion all patients were closely monitored for any adverse effects. The most common adverse events described in literature for this contrast agent are headache (2.9%), back pain (3.3%) and urticaria (2.4%). Administration was completed 24-36 hours before MR imaging.

The variation of signal intensity on MRI within a node can be explained on the basis of the concentration of nanoparticles in a particular region in the node. The nanoparticles cause a decrease in signal intensity within the node due to susceptibility artifacts on T2*-weighted images. Nanoparticles are taken up by macrophages located in the node [16]. The part of the lymph node involved with tumor will show no signal decrease due to the replacement of macrophages by tumor cells and thus will be depicted as a white region.

MR IMAGING

Post chemoradiation MR imaging was performed 24-36 hours after administration of the contrast agent USPIO. No precontrast MRI was performed, because no benefit was shown from a precontrast MRI in published series with USPIO [17]. MR imaging was performed on a 1.5-T Philips Gyroscan, Powertrak 6000 (Philips Medical Systems, Best, Netherlands) and 1.0T Siemens Magnetom Impact Expert (Siemens AG, Erlangen, Germany). Patients were placed in the magnet in the feet first supine position. The entire pelvis was scanned with standard 2D T2-weighted fast spin echo sequences in three planes: sagittal, axial and coronal. The MRI in sagittal plane was used as a reference to plan the axial and coronal T2W planes exactly perpendicular and parallel to the primary tumor axis.

To evaluate the morphologic uptake pattern of the iron oxide particles within the nodes 3D T2*-weighted images were used. 3D T1W GRE sequence was performed in exactly the same obliquity to serve as an anatomical template for better depiction of small lymph nodes. The detailed pulse sequence parameters are provided in Table 7.1. Patients did not receive bowel or other preparation. Total imaging time was 42-50 minutes.

Table 7.1. MR sequences and parameters.

Sequences & Parameters	1.0T MRI	1.5T MRI
2D T2W FSE		
Repetition time/Echo time (msec)	5289/120	3427/150
Slice Thickness (mm)	5	5
Flip angle (degrees)	90	90
Matrix	256 x 256	256 x 256
FOV (mm)	250	200
No. of slices	22	22
Axial 3D T1W Gradient Echo		
Repetition time/Echo time (msec)	15/7	10/4.60
Slice Thickness (mm)	2	1
Flip angle (degrees)	15	15
Matrix	256 x 256	384 x 512
FOV (mm)	300	440
No. of slices	102	200
Axial 3D T2*W		
Repetition time/Echo time (msec)	17/7	23/18.41
Slice Thickness (mm)	2	1.25
Flip angle (degrees)	20	20
Matrix	256 x 256	512 x 512
FOV (mm)	300	440
No. of slices	106	200

Image analysis

Post chemoradiation MR images were analyzed in this study independently by two observers (1) R.B.T. and (2) M.J.L. (with approximately 3000 and approximately 300 MR pelvic reading experience, respectively). The prechemoradiation MRI were available for review reflecting the daily practice. Both observers were blinded to each other's results and the results of the histopathological examination. Both observers prospectively evaluated each node on standard T2-weighted images first for the following items: border (sharp, indistinct or spiculated), short and long axis diameter.
Then the 3D T2* sequences were evaluated for each node for the following criteria: the percentage of the area with no uptake (white region) within the node after chemoradiation estimated and categorized as: <30%, 30-50% or >50% (see Figure 6.1). In addition to this visual assessment, the proportion of white region within the node was also quantitatively measured. The surface area of white region within the node and the surface area of total node were determined on axial T2*-weighted images using regions of interest (ROIs) at the section with greatest visualized diameter. By dividing the surface area of white region by the surface area of the total node, a quantitatively measured ratio of white region was calculated for both observers. This ratio is further referred to as $Ratio_A$, which was not categorized.
Additionally, the signal intensity (SI) of the total node and that of the gluteus muscle were measured after chemoradiation by placing regions of interests. These signal intensities were used to calculate the ratio: SI_{TN}/SI_{GM} for both observers.
The observer with the highest level of experience, observer 1, also prospectively recorded the localization of each visible lymph node depicted by T2*-weighted MR images after chemoradiation on an anatomical map. This anatomical map was used as a template for matching of each node depicted by observer 1 with the nodes found at by the pathologist as well as for matching with the nodes depicted by observer 2. All images were evaluated using a PACS workstation (KODAK Carestream PACS, version 10, Rochester, NY, USA).

Surgical procedure and histological evaluation

The standard surgical procedure was a total mesorectal excision (TME), as described by Heald [18]. In some patients a more extensive en bloc resection of adjacent structures or organs was required based on the findings of the primary staging MRI. The histological examination was standardized: the specimen was inked and fixed in formalin for 24-48h. The specimen was then sectioned every 5 mm transversely and thus perpendicular to the mesorectum. A careful search for lymph nodes was made in each histological tissue slice by dedicated pathologists (A.P.B. and H.W.S.K., with both more than 10 years of experience). Each harvested lymph node was processed according to standard methods and stained with haematoxylin-eosin. The pathologists, blinded to the radiological findings, reported the status of each lymph node. Each lymph node was matched to the corresponding node visible on the MR images using the anatomical map as a template (M.J.L., S.M.E. and R.B.T.). This was possible due to specific characteristics like the size of the lymph node and the position of the lymph node in relation to the rectal wall, small vessels, mesorectal fascia, tumor and other lymph nodes. In this manner accurate lesion-by-lesion analysis for mesorectal lymph nodes could be performed (see Figure 7.1). In cases in which nodal matching was not possible with high accuracy it was recorded as such, and these nodes were excluded from the analyses. When available, the histological details of these non-matching nodes were recorded.

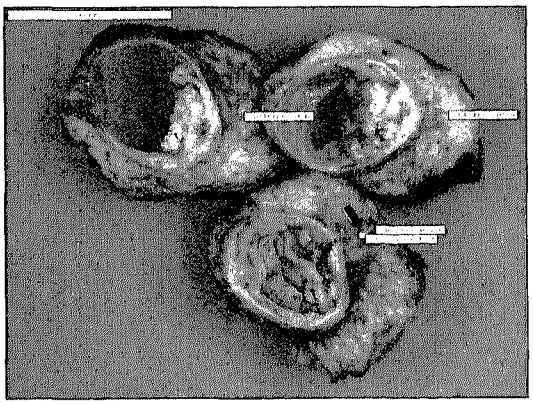

Figure 7.1.
Three histological slices of a rectum specimen with a 3 mm lymph node (black arrow) and several measurements, i.e. distance from the node to the tumor and the circumferential resection margin, needed for an accurate lesion-by-lesion analysis.

Statistical analysis

The diagnostic accuracy was assessed on a per node, lesion-by-lesion analysis. Based on the results of a pilot study at our center we expect a sensitivity of 99%. Forty positive lymph nodes are needed to reject with a power of 94% that the lower limit of the 95% confidence interval of sensitivity of the USPIO MRI is 89% or lower. Patients were therefore included until a total of forty malignant lymph nodes were harvested at histology. To determine the diagnostic performance of each criteria ROC curves were constructed and area under the curves (AUCs) and 95% confidence levels (CI) were calculated. The constructed ROC curves were compared and P-values were constructed using the Delong, Delong and Clarke-Pearson method [19]. For the calculation of corresponding sensitivity, specificity, positive predictive value (PPV) and negative predictive value (NPV) the variables were dichotomized at the most optimal cut off point determined at the highest NPV with still a reasonable PPV. To determine the interobserver agreement, weighted kappa's [20, 21] were calculated for the ordinal variables and Intra Class Correlations (ICC) for interval scaled variables [22], all with their 95%-CI. A kappa value (K value) of less than 0.00 indicates poor agreement; 0.00-0.20 slight agreement; 0.21-0.40 fair agreement; 0.41-0.60 moderate agreement; 0.61-0.80 substantial agreement and 0.81-1.00 almost perfect agreement [23]. All analyses, with the exception of the kappa analyses and P-values analysis, were performed using a statistical software program (SPSS, version 12.0.1, 2003; SPSS, Chicago, Ill.). The kappa analyses and P-values analysis were performed using STATA software (Stata Statistical Software: Release 9. College Station, TX: StataCorp LP). The statistical analysis was performed by a statistician (A.H.F.K.).

Results

There were no adverse events related to the USPIO infusion. Observer 1 identified and evaluated 320 mesorectal nodes in 39 patients on USPIO MR after chemoradiation. After surgical resection 325 nodes were found at histology; 40 malignant and 285 benign lymph nodes. The average number of nodes found at histology per patient was 8.3 (range: 1-16 nodes). At histology, 28 patients had no

malignant mesorectal nodes (ypN0), 6 patients had 0 - 3 malignant nodes (ypN1) and 5 patients had four or more malignant lymph nodes (ypN2).
Of the 325 nodes harvested at histology 201 could be accurately matched with MR imaging. All of the 40 malignant lymph nodes found at histology could be matched. The remaining 124 nodes harvested at histology could not be matched with MRI with great certainty and therefore were excluded from the analysis (see Figure 7.2).

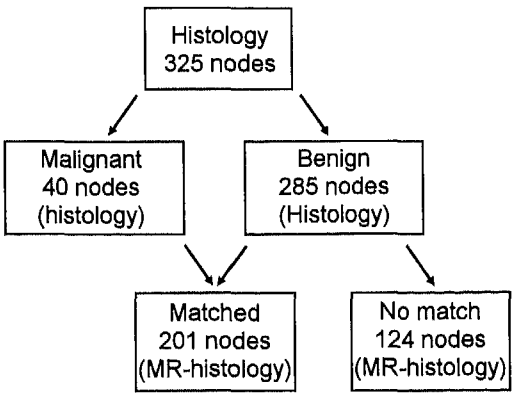

Figure 7.2.
A flowchart of the lymph nodes found at histology in rectal cancer patients after chemoradiation.

These 124 non-matched lymph nodes were all benign at histology, and almost all them were very small (< 2 mm). There were 110 'nodes' that were detected on MRI that could not be matched with histology with certainty. On MRI these 'nodes' were all staged as benign nodes. There are three reasons for a 'node' seen on MRI that could not be matched with histology. Firstly, small blood vessel or small areas of fibrosis can be interpreted as lymph nodes on MR images. Secondly, the 'nodes' seen on MRI are real lymph nodes, but cannot be found at histopathological examination. Thirdly, the 'nodes' were also found during histopathological examination, but cannot be matched with certainty.
The mean short- and long axis diameter at histology of the 201 matched lymph nodes were 3.2 mm (range 1-13 mm) and 4.6 mm (range 1.5-19 mm), respectively (see Figure 7.3). Quantitative measurement on 3D T2* weighted MR images was feasible in all matched nodes even in the very small nodes because the blooming artefact of the iron oxide on the T2*-weighted images is large enough for

quantification of signal intensity. Each node evaluated by observer 1 and matched with histology was also identified and evaluated by observer 2.

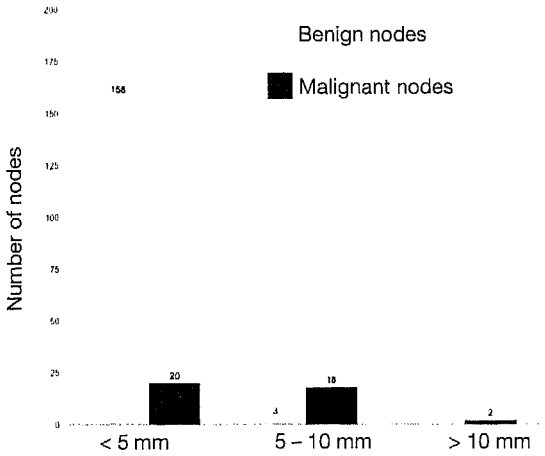

Figure 7.3.
A graph showing the number of lymph nodes according to short axis (<5 mm; 5-10; >10 mm).

Diagnostic performance

The area under the receiver operating characteristic curve (AUC) for the short and long axis diameter of the nodes on 2D T2W sequences was 0.87 and 0.88, respectively, for observer 1 and 0.89 and 0.87, respectively, for observer 2 on T2-weighted images. The optimal cut-off value was at a short axis of 3.3 mm, with a corresponding sensitivity and specificity for the detection of malignant nodes of 85% and 78%, respectively. The optimal cut-off value of the long axis diameter was 4.8 mm with a sensitivity and specificity for the detection of malignant nodes of 83% and 82%, respectively (see Table 7.2 and Figure 7.4). The area under the receiver operating characteristic curve (AUC) for a sharp; distinct or speculated border on T2 weighted images had an AUC of 0.85 and 0.70 for observer 1 and 2, respectively.
The AUC of the estimated percentage of white region within the node for the prediction of the nodal status on T2*-weighted images was 0.98 for observer 1 and 0.97 for observer 2. When the white region within the node was estimated as more than 30%, the sensitivity and specificity for detection of malignant nodes on post chemoradiation MR images was 100% and 95%, respectively (see Table 7.3 and Figure 7.5).

Table 7.2. This table gives the Area under the curve (AUC) and 95%-Confidence Intervals, sensitivity, specificity, PPV and NPV for observer 1 and 2 for all criteria used to distinguish between malignant and benign nodes using T2W FSE images.

Detection of N+ T2W FSE	Observer 1			Observer 2		
	Short diameter LN	Long diameter LN	Border	Short diameter LN	Long diameter LN	Border
AUC (95% CI)	0.87 (0.82-0.94)	0.88 (0.81-0.93)	0.85 (0.76-0.94)	0.89 (0.84-0.95)	0.87 (0.81-0.94)	0.70 (0.60-0.80)
Accuracy	0.81 ((32+130)/201)	0.82 ((33+132)/201)	0.90 ((29+151)/201)	0.80 ((34+126)/201)	0.78 ((33+124)/201)	0.67 ((26+109)/201)
Sens	0.80 (32/(32+8))	0.83 (33/(33+7))	0.74 (29/(29+10))	0.85 (34/(34+6))	0.83 (33/(33+7))	0.65 (26/(26+14))
Spec	0.81 (130/(130+31))	0.82 (132/(132+29))	0.93 (151/(151+11))	0.78 (126/(126+35))	0.77 (124/(124+37))	0.68 (109/(109+52))
PPV	0.51 (32/(32+31))	0.53 (33/(33+29))	0.72 (29/(29+11))	0.49 (34/(34+35))	0.47 (33/(33+37))	0.33 (26/(26+52))
NPV	0.94 (130/(130+8))	0.95 (132/(132+7))	0.94 (151/(151+10))	0.95 (126/(126+6))	0.95 (124/(124+7))	0.89 (109/(109+14))

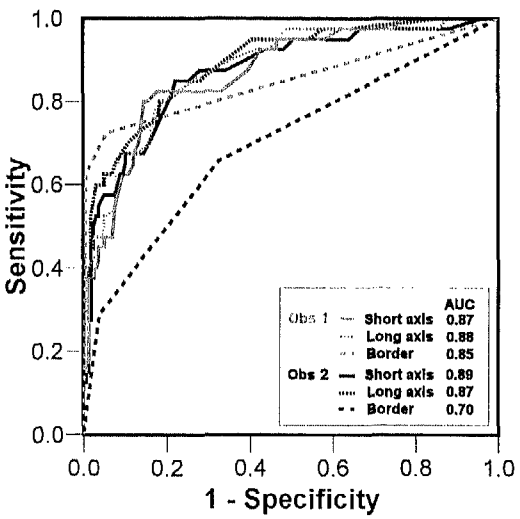

Figure 7.4.
Receiver operating characteristic (ROC) curves and areas under the curve (AUC) for observer 1 and 2, for the detection of malignant lymph nodes using the short & long axis diameter and border of the lymph node.

Table 7.3. This table gives the Area under the curve (AUC) and 95%-Confidence Intervals, sensitivity, specificity, PPV and NPV for observer 1 and 2 for all criteria used to distinguish between malignant and benign nodes using USPIO MRI.

Detection of N+ USPIO MRI	Observer 1			Observer 2		
	Estimated % white region	$Ratio_A$	SI_{TN}/SI_{GM}	Estimated % white region	$Ratio_A$	SI_{TN}/SI_{GM}
AUC (95% CI)	0.98 (0.96-1.00)	0.99 (0.99-1.00)	0.62 (0.51-0.73)	0.97 (0.95-0.99)	0.98 (0.96-1.00)	0.65 (0.55-0.76)
Accuracy	0.96 ((39+153)/201)	0.97 ((40+155)/201)	0.54 ((22+87)/201)	0.96 ((40+153)/201)	0.95 ((40+151)/201)	0.56 ((21+92)/201)
Sens	0.98 (39/(39+1))	1.00 (40/(40+0))	0.55 (22/(22+18))	1.00 (40/(40+0))	1.00 (40/(40+0))	0.53 (21/(21+19))
Spec	0.94 (153/(153+8))	0.96 (155/(155+6))	0.54 (87/(87+74))	0.95 (153/(153+8))	0.94 (151/(151+10))	0.57 (92/(92+69))
PPV	0.83 (39/(39+8))	0.87 (40/(40+6))	0.26 (22/(22+74))	0.83 (40/(40+8))	0.80 (40/(40+10))	0.23 (21/(21+69))
NPV	0.99 (153/(153+1))	1.00 (155/(155+0))	0.83 (87/(87+18))	1.00 (153/(153+0))	1.00 (151/(151+0))	0.83 (92/(92+19))

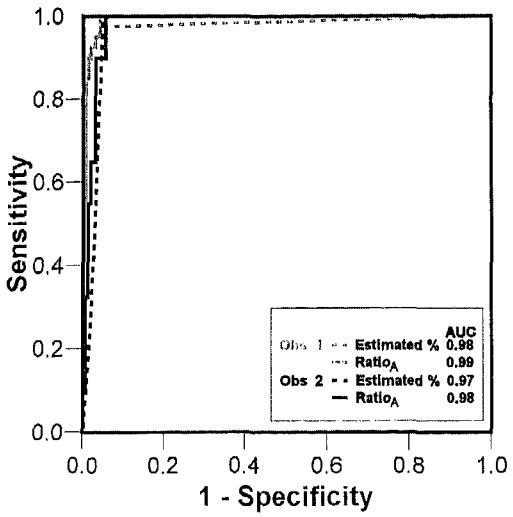

Figure 7.5.
Receiver operating characteristic (ROC) curves and areas under the curve (AUC) for observer 1 & 2, for the detection of malignant lymph nodes using the estimated percentage of white region within the node and measured $Ratio_A$.

The AUC of the measured $Ratio_A$ within the node for the prediction of the nodal status was 0.99 for observer 1 and 0.98 for observer 2 on T2*-weighted images. The most clinically relevant cut-off value of $Ratio_A$ was 0.34. When the $Ratio_A$ was 0.34, the sensitivity and specificity for the prediction of malignant nodes was 100% and 96%, respectively. The AUCs of SI_{TN}/SI_{GM} were 0.62 for observer 1 and 0.65 for observer 2. The AUC of the USPIO MR criteria estimated and calculated ($Ratio_A$) percentage of white region in the node was significantly better than the AUC of the conventional size measurements for both observers ($p<0.01$ for all comparisons).

Intra class correlation and interobserver agreement

The Intra Class Correlation (ICC) for observer 1 and 2 for the short axis, long axis diameter, the $Ratio_A$ and the SI_{TN}/SI_{GM} on post chemoradiation MRI were 0.94, 0.97, 0.83 and 0.73, respectively, after chemoradiation. Generally, the interobserver agreement was good to excellent. There was more agreement for the $Ratio_A$, short and long axis diameter than for the SI_{TN}/SI_{GM}. The interobserver agreement (K value) for the estimated white region between observer 1 and 2 was almost excellent (K=0.79), while that for the border was only fair (K=0.36).

Discussion

Our study shows that in patients with rectal cancer treated with neoadjuvant chemoradiation the most accurate predictors for malignant nodes on a restaging MRI using a lymph node specific USPIO contrast were both the estimated as well as the measured ($Ratio_A$) area of the white region within the node with an AUC of 0.98 and 0.99, respectively, for the experienced reader and an AUC of 0.97 and 0.98, respectively, for the less experienced reader. With a low prevalence of malignant nodes after chemoradiation of about 20%, the high sensitivity leads to a NPV of almost 100%, irrespective of the experience of the radiologist. Measurements of short and long axis diameter of the node on standard T2W FSE sequences were significantly less reliable predictors for malignant nodes, but with still a good AUC of 0.87 and 0.88, respectively, for observer 1 and 0.89 and 0.87, respectively, for

observer 2. Border irregularity and signal intensity measurements were unreliable criteria for detection of malignant nodes.

In contrast to the results of a previous study in primary staging with MRI [11], where size criteria were not reliable enough with an AUC of 0.75, size criteria after chemoradiation provide a higher AUC of 0.85-0.89. The sensitivity en specificity are around 80%, and with a low prevalence of nodal disease after chemoradiation of 20%, this results in a high NPV both for the experienced and less experienced reader. The specificity of 80% in this group of patients results in a PPV of only 50%, resulting in overstaging, a problem that is well known [15, 24]. There are several observations that could explain the better performance of size criteria after chemoradiation than in primary staging. Small nodes often cause interpretation difficulties on standard T2W sequences, and after chemoradiation the number of lymph nodes harvested during histopathological examination is reduced by 30% [13, 25]. In our experience the lymph nodes smaller than 5 mm often disappear or become very small (<2 mm), while the larger nodes become smaller but remain visible on MR images (see Figure 7.6). This could lead to less interpretation errors in small nodes, improving the accuracy. Additionally, the radiologist can compare the images after chemoradiation with the images before chemoradiation. The knowledge that the lymph nodes that are still malignant after chemoradiation are initially the larger nodes and that the initially small malignant nodes often are often sterilized by chemoradiation can increase the confidence of the radiologist in judging the smaller lymph nodes as benign.

There have been two studies addressing USPIO MRI in primary nodal staging (without chemoradiation). The study by Koh et al. describes the initial observations on a range of patterns of contrast enhancement to discriminate between malignant and non-malignant lymph nodes [26]. A study from our research group demonstrated that a simple estimation or measurement of the white region within the node is a reliable tool in primary nodal staging [11]. Our present study shows that these criteria are also valid in a postchemoradiation setting. Apparently tumoral nodes that before chemoradiation show no uptake of nanoparticles, regain their ability to uptake the USPIO contrast when the nodes are sterilized by the chemoradiation. This suggests that after sterilization by chemoradiation, tumor cells are replaced by normal lymphoid tissue with macrophages, responsible for the uptake of nanoparticles of iron oxide (see Figure 7.7).

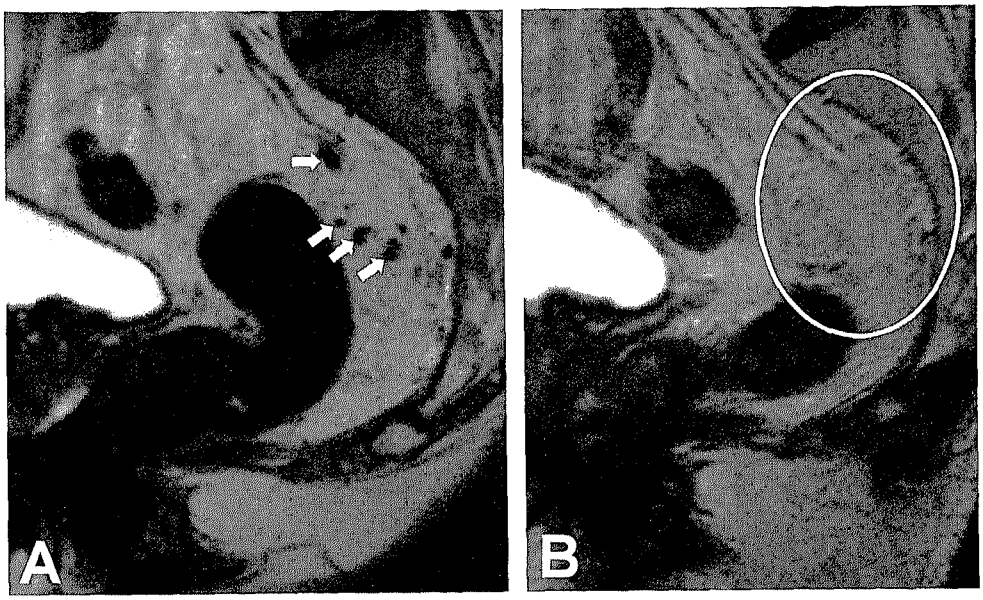

Figure 7.6. A) T2 weighted sagittal image of a rectal cancer patient with a multiple small and borderline sized nodes (≤ 5 mm, white arrows). After chemoradiation (B) the exact same sagittal view in the same patient shows that the small mesorectal lymph nodes disappeared (white circle).

Whereas studies on individual lymph nodes with a lesion-by-lesion analysis are very valuable to establish radiological criteria, the assessment of the nodal status on a patient basis is clinically more relevant for decision-making. The clinical data analyses of our larger multicenter cohort study shows that on a patient basis the sensitivity of USPIO MRI to detect malignant lymph nodes after chemoradiation is close to 90% with a specificity of 80% [27]. In a group of patients with a prevalence of nodal disease of 29% this leads to a clinical useful NPV of 95% with a lower PPV of 65% [27]. Most other imaging studies on prediction of nodal staging after chemoradiation report analyses on patient basis, with MRI without contrast agents showing sensitivities and specificities of 33-82% and 68-95%, with NPVs of 81-93% [12-14]. Reports on nodal restaging after chemoradiation with EUS and CT show only moderate accuracies of 0.61 and 0.62, comparable to primary nodal staging [14]. Studies on the use of 18Fluorodeoxyglucose (FDG) PET in restaging after chemoradiation mostly focus on the accuracy to detect complete responders or to evaluate the response and data on the prediction of nodal status are scarce. The

sensitivity to detect a complete response (in both the primary tumor and the lymph nodes) is 45% with a specificity of 79% [28, 29]. In prediction the nodal status in primary rectal FDG-PET performs poorly with a sensitivity of 21-29%, and it is not expected to perform much better after chemoradiation [30, 31], After chemoradiation the foci of tumor in malignant nodes are expected to be even smaller than in untreated rectal cancer, and detecting small volumes of tumor is a well known limitation of FDG-PET.

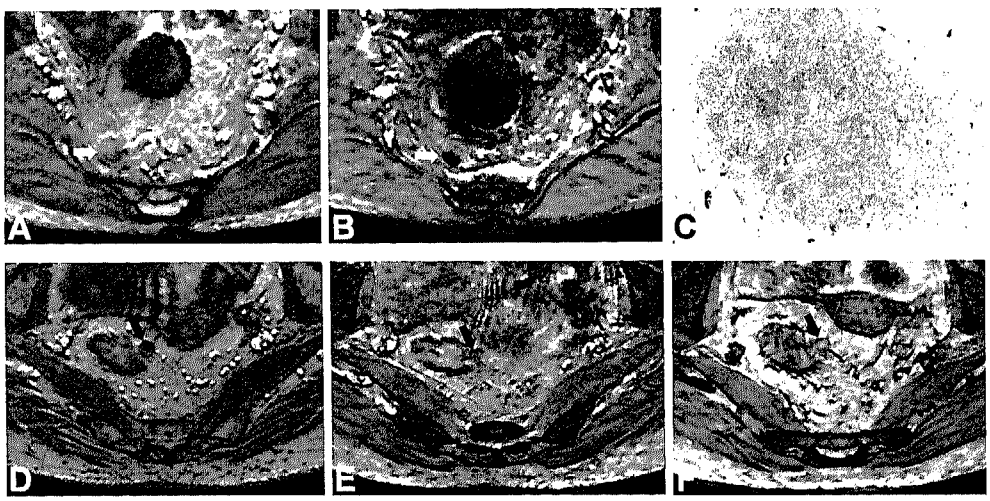

Figure 7.7. (A) USPIO enhanced T2* image of a rectal cancer patient with a node witch remains white indicating no iron uptake (white arrow). This means that this node is malignant. After chemoradiation (B) the exact same node shows a low signal intensity indicating iron uptake, suggesting sterilization of the malignant node. (C) At histopathological examination this nodes was indeed benign. This suggests that nodes, which are sterilized after chemoradiation, reacquire their ability to take up iron oxide.
(D) 3D T1-weighted image of a large lymph node close to the rectal wall (black arrow). (E) USPIO enhanced T2* image of a rectal cancer of the same node witch remains white indicating no iron uptake. (F) The exact same node after chemoradiation remains white, this means that the node is still malignant. At histopathological examination this nodes was indeed malignant.

A limitation of our study is the relatively high number of nodes at histology that could not be matched with certainty with MRI. In order not to pollute the analysis with faulty matched nodes, lymph nodes were only included when both the radiologist and the pathologist were confident about the matching. After chemoradiation most benign lymph nodes become smaller, and as lymph nodes smaller than 2 mm are difficult to depict with MRI and can easily be misinterpreted as small blood vessels or small areas of fibrosis, many of these small nodes could not be matched. Reassuring is the fact that the nodes seen on MRI that could not be matched with histology were all judged to be benign on MRI, and most importantly that all the nodes detected at histology that could not be matched with MRI were all proven to be benign on histology. Another drawback is that in Europe USPIO's application for a marketing authorization at the Committee for Medical Products for Human Use (CHMP) has recently been withdrawn by the manufacturer while in the United States the approval by the Food and Drugs Administration (FDA) is still pending. Should USPIO not be marketed our study will have shown that for lymph node staging after chemoradiation the accuracy of the size criteria can be improved with a lymph node specific contrast agent. This could stimulate the search for other reliable contrast agents.

Clinical relevance

Preoperative chemoradiation is now widely recognized as the treatment of choice for locally advanced rectal cancer. The majority of tumors become smaller, with complete remission rates of the primary tumor in 15-30%, and sterilization of lymph nodes in almost half of patients with involved nodes. These good responses challenge the classical concept that the complete area of the initial tumor and mesorectum should be entirely removed irrespective of the response to chemoradiation. In patients with a small tumor remnant in the bowel wall and with sterilized lymph nodes a transanal local excision could result in a good oncological control with less morbidity and mortality, as demonstrated in a recent of patients treated as such [32]. Even more controversial is a wait-and-see policy in complete responses in both the primary tumor and the lymph nodes [33]. To select patients for a local excision after chemoradiation both a residual tumor limited to the bowel wall

(ypT0-2) and a negative lymph node status (ypN0) is essential. The study of Dresen et al. has shown that MRI can reliably detect a tumor remnant limited to the bowel wall, and in this article we have shown that MRI with a lymph node specific contrast agent (USPIO) is able to distinguish benign from malignant lymph nodes after chemoradiation [34]. What are needed now are clinical studies evaluating the outcome of MRI based selection of good responders after chemoradiation for a local excision.

Conclusion

The most reliable predictors for identifying sterilized nodes in patients with locally advanced rectal cancer on a restaging USPIO enhanced MRI after chemoradiation are the estimated and measured ratio of white region within the node. In contrast to the results with primary staging MRI, size measurements on standard T2W FSE sequences offer a reasonably good accuracy to identify benign nodes after chemoradiation. The high agreement in both criteria between an experienced and less experienced reader indicates reproducibility of the readings in general setting. Our study suggests that a restaging MRI could be a useful diagnostic tool for the selection of good responders after chemoradiation with ypN0 status, who could be treated with a less invasive transanal local excision of the residual tumor.

References

1. *Lehnert T, Methner M, Pollok A, et al. Multivisceral resection for locally advanced primary colon and rectal cancer: an analysis of prognostic factors in 201 patients. Ann Surg 2002; 235:217-225.*
2. *Sauer R, Becker H, Hohenberger W, et al. Preoperative versus postoperative chemoradiotherapy for rectal cancer. N Engl J Med 2004; 351:1731-1740.*
3. *Govindarajan A, Coburn NG, Kiss A, et al. Population-based assessment of the surgical management of locally advanced colorectal cancer. J Natl Cancer Inst 2006; 98:1474-1481.*
4. *Reerink O, Verschueren RC, Szabo BG, et al. A favourable pathological stage after neoadjuvant radiochemotherapy in patients with initially irresectable rectal cancer correlates with a favourable prognosis. Eur J Cancer 2003; 39:192-195.*
5. *Coco C, Manno A, Mattana C, et al. The role of local excision in rectal cancer after complete response to neoadjuvant treatment. Surg Oncol 2007; 16 Suppl 1:S101-104.*
6. *Hughes R, Glynne-Jones R, Grainger J, et al. Can pathological complete response in the primary tumour following pre-operative pelvic chemoradiotherapy for T3-T4 rectal cancer predict for sterilisation of pelvic lymph nodes, a low risk of local recurrence and the appropriateness of local excision? Int J Colorectal Dis 2006; 21:11-17.*
7. *Lahaye MJ, Engelen SM, Nelemans PJ, et al. Imaging for predicting the risk factors--the circumferential resection margin and nodal disease--of local recurrence in rectal cancer: a meta-analysis. Semin Ultrasound CT MR 2005; 26:259-268.*
8. *Bipat S, Glas AS, Slors FJ, et al. Rectal cancer: local staging and assessment of lymph node involvement with endoluminal US, CT, and MR imaging--a meta-analysis. Radiology 2004; 232:773-783.*
9. *Brown G, Richards CJ, Bourne MW, et al. Morphologic Predictors of Lymph Node Status in Rectal Cancer with Use of High-Spatial-Resolution MR Imaging with Histopathologic Comparison. Radiology 2003; 227:371-377.*
10. *Will O, Purkayastha S, Chan C, et al. Diagnostic precision of nanoparticle-enhanced MRI for lymph-node metastases: a meta-analysis. Lancet Oncol 2006; 7:52-60.*
11. *Lahaye MJ, Engelen SM, Kessels AG, et al. USPIO-enhanced MR imaging for nodal staging in patients with primary rectal cancer: predictive criteria. Radiology 2008; 246:804-811.*
12. *Suppiah A, Hunter IA, Cowley J, et al. Magnetic Resonance Imaging Accuracy in Assessing Tumour Down-staging Following Chemo-radiation in Rectal Cancer. Colorectal Dis 2008.*
13. *Koh DM, Chau I, Tait D, et al. Evaluating mesorectal lymph nodes in rectal cancer before and after neoadjuvant chemoradiation using thin-section T2-weighted magnetic*

resonance imaging. Int J Radiat Oncol Biol Phys 2008; 71:456-461.

14. Maretto I, Pomerri F, Pucciarelli S, et al. The potential of restaging in the prediction of pathologic response after preoperative chemoradiotherapy for rectal cancer. Ann Surg Oncol 2007; 14:455-461.
15. Chen CC, Lee RC, Lin JK, et al. How accurate is magnetic resonance imaging in restaging rectal cancer in patients receiving preoperative combined chemoradiotherapy? Dis Colon Rectum 2005; 48:722-728.
16. Harisinghani MG, Dixon WT, Saksena MA, et al. MR lymphangiography: imaging strategies to optimize the imaging of lymph nodes with ferumoxtran-10. Radiographics 2004; 24:867-878.
17. Harisinghani MG, Barentsz JO, Hahn PF, et al. MR lymphangiography for detection of minimal nodal disease in patients with prostate cancer. Acad Radiol 2002; 9 Suppl 2:S312-313.
18. Heald RJ. A new approach to rectal cancer. Br J Hosp Med 1979; 22:277-281.
19. DeLong ER, D. M. DeLong, and D. L. Clarke-Pearson. Comparing the areas under two or more correlated receiver operating curves: A nonparametric approach. Biometrics 1988; 44:837-845.
20. Cohen J. A coefficient of agreement for nominal scales. Educational and Psychological Measurement 1960; 20:37-46.
21. Cohen J. Weighted Kappa: nominal scale agreement with provision for scaled disagreement or partial credit. Psychol Bull 1968; 70:213-230.
22. Shrout PE, Fleiss J.L. Intraclass Correlations: Uses in Assessing Rater Reliability. 1974; 86:420-428.
23. Landis JR, Koch GG. The measurement of observer agreement for categorical data. Biometrics 1977; 33:159-174.
24. Kuo LJ, Chern MC, Tsou MH, et al. Interpretation of magnetic resonance imaging for locally advanced rectal carcinoma after preoperative chemoradiation therapy. Dis Colon Rectum 2005; 48:23-28.
25. Habr-Gama A, Perez RO, Proscurshim I, et al. Absence of lymph nodes in the resected specimen after radical surgery for distal rectal cancer and neoadjuvant chemoradiation therapy: what does it mean? Diseases of the Colon & Rectum 2008; 51:277-283.
26. Koh D-M, Brown G, Temple L, et al. Rectal Cancer: Mesorectal Lymph Nodes at MR Imaging with USPIO versus Histopathologic Findings--Initial Observations. Radiology 2004; 231:91-99.
27. Engelen SM, Beets-Tan RG, Lahaye MJ. MRI after chemoradiotherapy of rectal cancer: a useful tool to select patients for local excision. Submitted 2008.
28. Capirci C, Rubello D, Chierichetti F, et al. Restaging after neoadjuvant chemoradiotherapy for rectal adenocarcinoma: role of F18-FDG PET. Biomed

Pharmacother 2004; 58:451-457.

29. *Kristiansen C, Loft A, Berthelsen AK, et al. PET/CT and histopathologic response to preoperative chemoradiation therapy in locally advanced rectal cancer. Dis Colon Rectum 2008; 51:21-25.*
30. *Abdel-Nabi H, Doerr RJ, Lamonica DM, et al. Staging of primary colorectal carcinomas with fluorine-18 fluorodeoxyglucose whole-body PET: correlation with histopathologic and CT findings. Radiology 1998; 206:755-760.*
31. *Llamas-Elvira JM, Rodriguez-Fernandez A, Gutierrez-Sainz J, et al. Fluorine-18 fluorodeoxyglucose PET in the preoperative staging of colorectal cancer. Eur J Nucl Med Mol Imaging 2007; 34:859-867.*
32. *Borschitz T, Wachtlin D, Mohler M, et al. Neoadjuvant chemoradiation and local excision for T2-3 rectal cancer. Ann Surg Oncol 2008; 15:712-720.*
33. *O'Neill BD, Brown G, Heald RJ, et al. Non-operative treatment after neoadjuvant chemoradiotherapy for rectal cancer. Lancet Oncol 2007; 8:625-633.*
34. *Dresen R, Beets G, Rutten HJ, et al. MRI for restaging after neoadjuvant chemoradiation in locally advanced rectal cancer. Part I: Are we able to predict tumor confined to the rectal wall? Radiology 2009; In press.*

GENERAL DISCUSSION

8

General discussion

In the past decades the treatment of rectal cancer patients has changed. It has developed from a single modality treatment to a variety of multimodal treatment options, combining surgical techniques with pre- or postoperative chemo- and/or radiotherapy. This has improved the outcome with less local recurrences and a better survival [1]. The standard surgical approach is a total mesorectal excision (TME). New developments in surgical technique are wider cylindrical excisions [2] to obtain wider lateral margins in distal rectal cancer and on the other hand less invasive techniques for very small tumors. A transanal endoscopic microsurgery (TEM) only removes the tumor bed in the bowel wall while all potential malignant mesorectal lymph nodes remain in the patient. A local excision can be considered in more superficial tumors to avoid the complications of extensive surgery. It can be confusing for the clinicians in this wide variety of therapeutic options to decide on the best treatment for an individual patient. Choices should be made on the basis of scientific evidence, ideally combining the best possible oncological control with as low as possible treatment related morbidity. For rectal cancer this requires a preoperative stratification of different risk groups for local recurrence. Preoperative imaging and staging can provide important prognostic factors for a local recurrence. The work presented in this thesis underlines the potential of MRI and the lymph node specific contrast agent ultrasmall superparamagnetic iron oxides (USPIO) for predicting these important prognostic factors: circumferential resection margin (CRM), T-stage and the nodal status.

Circumferential resection margin

Incomplete removal of the lateral spread of the tumor has been widely accepted as the cause of the majority of local recurrences [3]. Many studies have shown that a close resection margin is an essential prognostic indicator for local recurrences, distant metastases and patient survival. This has been thoroughly reviewed in a very recent paper by Nagtegaal and Quirke [4]. The meta-analysis in chapter four confirmed that MRI is the only modality, which performs well in predicting the CRM. In addition, the European Mercury Trial showed that conventional MRI can predict

the CRM not only in a university setting, but also in regional hospitals [5]. In conclusion, the CRM can accurately be predicted on MR images by experts and non-experts, and MRI can therefore serve as a tool to stratify rectal cancer patients in high and low risk groups according to their CRM prediction.

T-stage

A drawback of the T-staging system is that it does not discriminate between T3 tumors (non-locally advanced tumors) that can easily be resected with a wide resection margin and T3 tumors with a close or involved CRM (locally advanced tumors). Nevertheless, the T-staging system is widely used and provides validated prognostic information. Stage I tumors are tumors limited to the bowel wall (T1-2) without lymph node metastases and have a very good prognosis. Some of these patients can even be considered for a local excision rather than a TME procedure. The large multicenter study described in this thesis (chapter 5) showed that both experts and non-experts can accurately detect tumors limited to the bowel wall with a high PPV using 1.5T MRI at the expense of false positives, while 1.0T MRI showed disappointing results. This means that a tumor limited to the bowel wall (T1-2) can accurately be predicted on MR images by experts and non-experts, which enables us to stratify rectal cancer patients in high and low risk groups according to their T1-2 or T3-4 prediction. To identify Stage I disease requires not only a good T-stage prediction, but also a good N-stage prediction.

Nodal status

Nodal involvement and the CRM status are the two most important factors associated with a high local recurrence rate [6]. The meta-analysis of chapter four unfortunately demonstrated that the assessment of lymph node involvement remains a problem for all three investigated diagnostic imaging modalities: EUS, CT and MRI. These findings corroborate earlier reports on disappointing results for nodal prediction for the three modalities [7, 8]. The size of the lymph node is the main criterion that has been used so far to discriminate between malignant and benign.

The problem with this is that size criteria are inherently inadequate due to the high frequency of small (<5 mm) malignant nodes in rectal cancer. Additional criteria in EUS and MR imaging were developed to improve the accuracy in nodal staging, with some improvement in accuracy [9, 10]. EUS guided fine needle aspiration has been reported to be a very reliable method, but a major drawback of this rather cumbersome invasive method is the high operator dependency. The few preliminary publications on CT-PET showed disappointing results for detecting nodal involvement in rectal cancer caused by the well-known limitation of CT-PET in detection of low-bulk disease (<1 cm^3).

There have been more promising results in lymph node imaging with new lymph node specific MR contrast agents, like ultrasmall superparamagnetic iron oxides (USPIO) [11]. The iron oxide nanoparticles accumulate in macrophages in a benign region within lymph nodes causing a decrease in signal intensity in benign nodes due to susceptibility artifacts on 3D T2*-weighted images. Our study, described in chapter six, demonstrates that criteria like the estimated and measured white region within the nodes were highly predictive for a benign lymph node on USPIO enhanced MR images. These results were confirmed in our multicenter study, which demonstrated that also in a general hospital USPIO MRI was a good tool to detect malignant lymph nodes provided that proper USPIO training was given to the general radiologists. A striking finding was the good results of the expert for the nodal prediction using nonenhanced MR images, without the use of USPIO contrast agent. Additional MR criteria like border and heterogenous signal intensity apparently are useful, but need an extensive experience in predicting lymph nodes. For non-experts the lymph node specific USPIO contrast agent is of help in the nodal prediction to reach an accuracy that is good enough for clinical decision-making. Especially the high NPV of USPIO MRI indicated that N0 patients could be selected by experts and non-experts.

The Dutch TME Trial showed that preoperative radiotherapy (5 x 5 Gy) reduced the local recurrence rate especially in patients with a N+ status [6]. Accurate nodal staging can help selecting those patients who could benefit from preoperative radiotherapy. Small tumors without malignant lymph nodes can safely be removed with a TME without preoperative radiotherapy [12, 13].

The nodal status is also essential in patients in which TEM surgery is being considered. During TEM surgery all potential malignant lymph nodes remain in situ

and only the tumor in the bowel wall is removed. Accurate nodal staging and especially an accurate N0 prediction is therefore needed to safely perform TEM.
Nowadays chemoradiation is increasingly effective with large tumors being downsized and nodes sterilized. The debate is whether these good responders can be treated with a local excision instead of a more standard TME procedure. To select those patients who could benefit from a more local excision, nodal staging after chemoradiation is essential. As shown in chapter seven the same USPIO criteria used in primary staging of rectal cancer can be applied in restaging patients treated with chemoradiation by expert and non-expert readers. More surprisingly, conventional size criteria performed much better after chemoradiation than in non-irradiated patients for the detection of malignant nodes. In literature some reports with small patient populations confirm these results [14, 15]. This observation requires confirmation, as it would enable radiologists to predict the lymph node status in these patients without the use of contrast agents. With the ability to predict the nodal status after chemoradiation, MRI can help to select a small group of patients in whom less invasive therapeutic options can be considered.

Limitations

Despite the promising results for nodal prediction described in this thesis and other publications on USPIO MRI, the contrast agent (Sinerem®) is not yet commercially available. We hope it will become available in the near future, because it could have a real impact on patient management. Additionally, there are some other limitations of the contrast agent: the administration is quite time-consuming (50 minutes) and it must be administered 24-36 hours before the MRI scan, requiring a double visit for one MR scan. In our experience most cancer patients are very cooperative and do not mind the extra hospital visit.

Future prospects

There are other options than USPIO to detect malignant lymph nodes in rectal cancer with MR imaging. There are new Gadolinium-based MR contrast agents such

as Gd-DTPA, Gadofluorine and MS325 (Vasovist®). These contrast agents seem promising for the detection of malignant lymph nodes. Preclinical as well as clinical studies have shown encouraging results for staging oncological disease [16-18]. At present however, USPIO is the only agent with the largest evidence that it is effective in nodal staging of cancer patients.

Apart from contrast agents, new MR techniques like diffusion-weighted imaging (DWI) may become useful for the detection of malignant nodes. Functional diffusion mapping and apparent diffusion values are investigated to see whether they can differentiate between benign nodes and malignant nodes and whether they are able to predict patient outcome and tumor response to therapy.

Also accurate nodal prediction post chemoradiation is necessary in order to develop new therapeutic strategies after chemoradiation like a local excision or even a wait-and-see policy.

Recommendations for clinicians

The work presented in and the clinical knowledge acquired during this thesis lead to the following recommendations concerning the multidisciplinary work up of rectal cancer patients. First of all, rectal cancer patients must receive an 1.5T MRI for local staging, because it is the only modality that can accurately predict the most important risk factor, the CRM. An involved CRM is an indication for a long course of preoperative chemoradiation. Secondly a X-thorax and a CT abdomen must be performed preoperatively to detect any distant metastases.

The national guidelines state that TEM surgery for rectal cancer is only appropriate in pT1N0 tumors. In experienced hands EUS can identify pT1 tumors, while (USPIO) MRI can accurately identify pN0 patients. Together these two imaging modalities can accurately detect pT1N0 tumors eligible for TEM surgery. Although not a subject in this thesis, MRI is advised for follow-up after TEM surgery for early detection of "nodal recurrences".

New therapeutic strategies after chemoradiation like a local excision or even a wait-and-see policy are being investigated in rectal cancer patients. (USPIO) MRI should be incorporated in these studies for primary staging, staging after chemoradiation and follow up.

Conclusion

The work presented in this thesis show that USPIO MRI is a sensitive, reproducible and adequate tool in predicting the tumors limited to the bowel wall, CRM and N-status in primary rectal cancer in hands of experts and non-experts. Experts can accurately predict the nodal staging on conventional MR images. Non-experts, however, need a lymph node specific MR contrast agent to accurately predict the nodal status. (USPIO) MRI can help stratifying rectal cancer patients into different treatment groups according to their risk of a local recurrence. This works equally well in a university setting as in the setting of a general hospital, provided that there is a proper training provided for the radiologists. New MR sequences (diffusion imaging) and other lymph node specific MR contrast agents (Vasovist®) show promising results and will be evaluated in the near future.

References

1. *Folkesson J, Birgisson H, Pahlman L, et al.: Swedish Rectal Cancer Trial: long lasting benefits from radiotherapy on survival and local recurrence rate. J Clin Oncol 2005;23:5644-5650.*
2. *Marr R, Birbeck K, Garvican J, et al.: The modern abdominoperineal excision: the next challenge after total mesorectal excision. Ann Surg 2005;242:74-82.*
3. *Adam IJ, Mohamdee MO, Martin IG, et al.: Role of circumferential margin involvement in the local recurrence of rectal cancer. Lancet 1994;344:707-711.*
4. *Nagtegaal ID, Quirke P: What is the role for the circumferential margin in the modern treatment of rectal cancer? J Clin Oncol 2008;26:303-312.*
5. *Diagnostic accuracy of preoperative magnetic resonance imaging in predicting curative resection of rectal cancer: prospective observational study. Bmj 2006;333:779.*
6. *Kapiteijn E, Marijnen CA, Nagtegaal ID, et al.: Preoperative radiotherapy combined with total mesorectal excision for resectable rectal cancer. N Engl J Med 2001;345:638-646.*
7. *Heriot AG, Grundy A, Kumar D: Preoperative staging of rectal carcinoma. Br J Surg 1999;86:17-28.*
8. *Bipat S, Glas AS, Slors FJ, et al.: Rectal cancer: local staging and assessment of lymph node involvement with endoluminal US, CT, and MR imaging--a meta-analysis. Radiology 2004;232:773-783.*
9. *Kim JH, Beets GL, Kim MJ, et al.: High-resolution MR imaging for nodal staging in rectal cancer: are there any criteria in addition to the size? Eur J Radiol 2004;52:78-83.*
10. *Brown G, Richards CJ, Bourne MW, et al.: Morphologic Predictors of Lymph Node Status in Rectal Cancer with Use of High-Spatial-Resolution MR Imaging with Histopathologic Comparison. Radiology 2003;227:371-377.*
11. *Will O, Purkayastha S, Chan C, et al.: Diagnostic precision of nanoparticle-enhanced MRI for lymph-node metastases: a meta-analysis. Lancet Oncol 2006;7:52-60.*
12. *Pahlman L, Glimelius B: Pre- or postoperative radiotherapy in rectal and rectosigmoid carcinoma. Report from a randomized multicenter trial. Ann Surg 1990;211:187-195.*
13. *Sauer R, Becker H, Hohenberger W, et al.: Preoperative versus postoperative chemoradiotherapy for rectal cancer. N Engl J Med 2004;351:1731-1740.*
14. *Koh DM, Chau I, Tait D, et al.: Evaluating Mesorectal Lymph Nodes in Rectal Cancer Before and After Neoadjuvant Chemoradiation using Thin-Section T2-Weighted Magnetic Resonance Imaging. Int J Radiat Oncol Biol Phys 2007.*
15. *Maretto I, Pomerri F, Pucciarelli S, et al.: The potential of restaging in the prediction of pathologic response after preoperative chemoradiotherapy for rectal cancer. Ann Surg Oncol 2007;14:455-461.*
16. *Herborn CU, Lauenstein TC, Vogt FM, et al.: Interstitial MR lymphography with MS-325:*

characterization of normal and tumor-invaded lymph nodes in a rabbit model. AJR Am J Roentgenol 2002;179:1567-1572.

17. *Misselwitz B, Platzek J, Weinmann HJ: Early MR lymphography with gadofluorine M in rabbits. Radiology 2004;231:682-688.*

18. *Weissleder R, Elizondo G, Wittenberg J, et al.: Ultrasmall superparamagnetic iron oxide: an intravenous contrast agent for assessing lymph nodes with MR imaging. Radiology 1990;175:494-498.*

Summary

The treatment of rectal cancer patients has developed into a wide spectrum of therapeutic options: from single into multimodality treatment options, combining surgical techniques with pre- or postoperative chemo- and/or radiotherapy to a less invasive transanal endoscopic microsurgery for more superficial tumors. An individual tailored treatment based on stratification of high-risk versus low-risk patients is now being adopted in rectal cancer. Preoperative selection of these patients for an individual tailored treatment can only be made when preoperative imaging is able to determine the most important prognostic factors for a local recurrence: circumferential resection margin (CRM), T-stage and the nodal status (N-status) in rectal cancer patients.

In chapter two relevant MR anatomy is described. Predicting the most important risk factors for a local recurrence in rectal cancer patients starts with a detailed knowledge of the anatomy of the mesorectum and surrounding organs. A preoperative pelvic MRI can accurately visualize the bowel wall, the mesorectum and the surrounding mesorectal fascia. By understanding the MR pelvic anatomy, the distance of the tumor to the mesorectal fascia can be accurately identified and an involved or close circumferential resection margin of a standard total mesorectal excision (TME) specimen can be anticipated. Rather than proceeding with a standard resection and putting the patient at risk for a local recurrence, the clinician can choose for neoadjuvant (chemo)radiotherapy and/or a more extensive resection.

Chapter three gives a review of all available modern imaging techniques for identifying nodal disease in rectal cancer. Presently available imaging methods for prediction of N0 and N+ cancer patients seem not reliable for preoperative clinical decision-making. In rectal cancer patients, evidence exists that studies are needed to further improve the accuracy of nodal staging by improving the resolution of modern imaging techniques such as PET and MRI or the use of new contrast agents.

Chapter four analyzed whether preoperative imaging can accurately predict the two most important risk factors for local recurrence in rectal cancer, the circumferential resection margin (CRM) and the nodal status. This meta-analysis showed that MRI is the only modality that predicts the circumferential resection margin with good accuracy, making it a good tool to identify high and low risk patients. Predicting the nodal status, however, remained a problem for the radiologist; all modalities lack

clinical accuracy.

The study presented in chapter five evaluates the diagnostic performance of USPIO MRI for the T-stage and nodal status in both referral and general setting. This multicenter study shows that expert and non-experts can accurately detect a tumor limited to the bowel wall using 1.5T MRI. Another striking finding was that USPIO enhanced MRI, in comparison to nonenhanced MRI, improves the prediction of the nodal status for the expert and especially for non-expert radiologists using 1.5T MRI. 1.0T MRI showed poor results for the prediction of T-stage and nodal status for both the expert and non-experts.

In chapter six we investigated several criteria for the prediction of malignant nodes in rectal cancer patients using USPIO MRI. The estimated percentage of white region (the region with no USPIO contrast uptake) within the node was a practical and accurate criterion; an estimated area of white region within the node larger than 30% had a sensitivity of 93% and a specificity of 96% to predict a malignant node. Furthermore, even less experienced readers were able to produce similar results using this criterion. When this ratio of white region within the node was measured (RatioA), it was also a very strong predictor for malignant nodes in the hands of expert and non-expert readers. Simple size criteria on nonenhanced MR images were not accurate enough in their prediction of the nodal status.

In chapter seven we demonstrated that restaging MRI using USPIO is accurate for identifying sterilized nodes (ypN0). Although the use of USPIO contrast agent in restaging demonstrated superior results, size measurements are accurate enough for clinical decision making: nodes smaller than 5 mm on post chemoradiation MRI are likely to be sterilized. Reader's performance was equal both for expert and less experienced radiologist.

The present thesis shows that USPIO MRI is a sensitive, reproducible and adequate tool in predicting the tumors limited to the bowel wall, CRM and nodal status in primary rectal cancer in hands of experts and non-experts. (USPIO) MRI can help stratifying rectal cancer patients into different treatment groups according to their risk of a local recurrence. This works equally well in a university setting as in the setting of a general hospital. However, considering the unavailability of this USPIO MR contrast on the market at the time of this writing new MR techniques (e.g. diffusion weighted MR imaging) and other potential new MR contrast agents should be further investigated for its use in nodal staging of rectal cancer patients.

Samenvatting

De behandeling van patiënten met rectumkanker heeft tot zich ontwikkeld in een breed scala van therapeutische mogelijkheden; van eenvoudige tot multidisciplinaire behandelingsopties; van minimaal invasieve transanale endoscopische microchirurgie voor oppervlakkige tumoren tot invasieve chirurgische technieken al dan niet gecombineerd met pre- en/of postoperatieve (radio)chemotherapie. Een individuele, op maat gemaakte, therapie op basis van een individueel risicoprofiel wordt nu meer en meer toegepast. Preoperatieve selectie van de patiënten met rectumkanker voor een op maat gemaakte behandeling is enkel mogelijk als preoperatieve beeldvormende technieken in staat zijn de belangrijkste prognostische factoren te voorspellen; circumferentiële resectie marge, T-stage and de lymfklierstatus.

Het voorspellen van de belangrijkste risicofactoren voor een lokaal recidief bij patiënten met rectumkanker begint met een gedetailleerde kennis van de anatomie van het mesorectum en omliggende structuren. Hoofdstuk twee beschrijft de relevante MR anatomie. Een preoperatief MRI onderzoek van de onderbuik kan accuraat de rectumwand, het mesorectum en de omliggende mesorectale fascie afbeelden. Door voldoende kennis te hebben van de MR anatomie kan men de afstand tussen de mesorectale fascie en de tumor meten, en kan een bedreigde of geïnvadeerde circumferentiële resectie marge van een totale mesorectale excisie (TME) specimen worden voorspeld. Hierdoor kan de behandelend arts afwijken van de standaard TME en kiezen voor neoadjuvant (chemo)radiotherapy en/of een meer uitgebreide resectie om de kans op een lokaal recidief te verkleinen.

Hoofdstuk 3 geeft een overzicht van alle moderne beeldvormende technieken voor het identificeren van maligne lymfklieren in patiënten met rectumkanker. De huidige beschikbare beeldvormende technieken voor het identificeren van patiënten met een positieve lymfklierstatus blijken niet accuraat genoeg voor preoperatieve klinische besluitvorming. Meer onderzoek is nodig om de accuratesse te verbeteren van lymfklierstagering door de resolutie te verbeteren van moderne beeldvormende technieken als PET en MRI en door het gebruik van nieuwe contrast middelen.

Hoofdstuk vier analyseert of preoperatieve beeldvorming accuraat de twee belangrijkste risicofactoren voor een lokaal recidief in patiënten met rectumkanker, de circumferentiële resectie marge (CRM) en de lymfklierstatus, kan voorspellen.

Deze meta-analyse laat zien dat MRI de enige modaliteit is dat accuraat de CRM kan voorspellen, hierdoor kan MRI hoog van laag risico patiënten onderscheiden. Het voorspellen van de lymfklierstatus bleef echter nog een probleem voor de radioloog; alle non-invasieve beeldvormende modaliteiten missen de klinische benodigde accuratesse.

De studie beschreven in hoofdstuk vijf evalueert de diagnostische prestaties van USPIO MRI voor de T-stage en de lymfklierstatus in een academisch medisch centrum (expert) en in perifere ziekenhuizen (non-experts). Deze multicenter studie demonstreert dat experts en non-experts accuraat een tumor die zich beperkt tot de rectumwand kunnen voorspellen gebruikmakend van 1.5T MRI. Een andere opvallende bevinding was dat USPIO MRI in vergelijking met MRI zonder het USPIO contrastmiddel, de voorspelling van de lymfklierstatus verbeterde voor experts en vooral non-experts gebruikmakend van 1.5T MRI. 1.0T MRI liet minder goede resultaten zien voor het voorspellen van T-stage en de lymfklierstatus voor zowel experts als non-experts.

Hoofdstuk zes bestudeert verscheidene criteria voor het voorspellen van maligne lymfklieren in patiënten met rectumkanker gebruikmakend van USPIO MRI. Het geschatte percentage van de witte regio (de regio zonder USPIO opname) binnen een lymfklier was een praktisch en accuraat criterium; een geschatte witte regio van meer dan 30% had een sensitiviteit van 93% en een specificiteit van 96% voor het voorspellen van een maligne lymfklier. Zelfs minder ervaren beoordelaars konden deze goede resultaten reproduceren. Als deze ratio van het oppervlak van de witte regio binnen de lymfklier werd gemeten ($Ratio_A$), was dit een sterke voorspeller voor het detecteren van maligne lymfklieren voor experts en non-experts. Zonder het gebruik van USPIO bleken eenvoudige metingen van de maximale diameters van een lymfklier niet accuraat genoeg voor het voorspellen van de lymfklierstatus.

In hoofdstuk zeven wordt beschreven dat USPIO MRI voor het restadiëren van patiënten na chemoradiatie accuraat is voor het identificeren van gesteriliseerde lymfklieren (ypN0). Hoewel het gebruik van het USPIO contrastmiddel bij het restadiëren superieure resultaten liet zien, bleken ook metingen van de maximale diameters van een lymfklier accuraat genoeg te zijn voor klinische besluitvorming; lymfklieren kleiner dan 5 mm zijn meestal gesteriliseerd na chemoradiatie. De prestaties van expert en non-experts waren wederom bij dit onderzoek gelijk.

Deze thesis laat zien dat USPIO MRI een sensitieve, reproduceerbare en adequate

techniek is voor het voorspellen van tumoren beperkt tot de rectumwand, CRM en de lymfklierstatus in patiënten met rectumkanker, zowel door experts als non-experts. Hierdoor kan (USPIO) MRI helpen patiënten met rectumkanker te stratificeren in verschillende behandelingstrajecten volgens hun risico voor een lokaal recidief. Deze stratificatie is zowel mogelijk in een "expert" academisch medisch centrum als in perifere ziekenhuizen. Echter, gezien het feit dat tijdens het schrijven van deze thesis het USPIO contrastmiddel niet op de commerciële markt verkrijgbaar is, zullen nieuwe MR technieken (zoals bijvoorbeeld diffusie gewogen MR sequenties) en andere nieuwe contrastmiddelen verder moeten onderzocht worden voor het gebruik voor stagering van de lymfklierstatus in patiënten met rectumkanker.

Curriculum vitae

The author of this thesis, Max Jef Lahaye, was born April 12th, 1979 in Ede, The Netherlands. From 1991 he attended "Mgr. Frencken College" in Oosterhout, The Netherlands, where he graduated in 1997. Subsequently, he started his medical training at the Faculty of Medicine at the Catholic University of Leuven, Belgium. After one year he continued his medical training at the Faculty of Medicine at the University of Maastricht, The Netherlands. After following the extracurricular course; "Diseases in the Tropics" in 2001 he worked in Kathmandu, Nepal, for two months at the Paediatrics and Emergency Department in two local hospitals. During his academic career he joined the Sponsor Committee of Maastricht Medical Student Research Conference (MMSRC) and was an active member of O.M.S.G. Plutarchus. In the course of his first year of internships in 2002 he made his first encounter with the Radiology department. Fascinated by Radiology he started as a research assistant at the department of Radiology of the Maastricht University Medical Center (MUMC) under supervision of Prof. dr. R.G.H. Beets-Tan alongside his ongoing internships.

He obtained his medical doctor degree in September 2004. From 2004 to 2008 he worked as PhD student, with a grant of the Dutch Cancer Society, initiating a Dutch multicenter study performed at the University Hospital Maastricht, Laurentius Hospital Roermond, St. Jans Hospital Weert, VieCuri Medical Center Venlo/Venray, which resulted in this thesis. During his PhD project he was an organizing member of the Dr. Adrien Pélerin Foundation. In February 2008 the author obtained a position in the board of the residence association of the MUMC and started his radiological residency for a training period of five years at the MUMC.

List of publications

Book chapters

1. M.J. Lahaye, W.H. Lamers, G.L. Beets and R.G.H. Beets-Tan. Benign Anorectal Diseases: Anatomy of the Rectum and Mesorectum. Edited by G.A. Santoro and G. Di Falco. Springer Medizin Verlag 2006.
2. S.M.E. Engelen, G.L. Beets, M.J. Lahaye and R.G.H. Beets-Tan. Rectal Carcinoma. Encyclopedia of Diagnostic Imaging. Edited by A.L. Baert. Springer Medizin Verlag 2007.
3. M.J. Lahaye, R.B.J. de Bondt, S.M.E. Engelen, G.L. Beets and R.G.H. Beets-Tan. Clinical Blood Pool MR Imaging. Edited by T. Leiner. Springer Medizin Verlag 2008.

Articles

1. M.J. Lahaye, S.M.E. Engelen, P.J. Nelemans, G.L. Beets, C.J.H. van de Velde, J.M.A. van Engelshoven and R.G.H. Beets-Tan. Imaging for Predicting the Risk Factors, the Circumferential Resection Margin and Nodal Disease, of Local Recurrence in Rectal Cancer: a Meta-Analysis. Semin. US, CT & MRI 2005 Aug;26(4):259-68.
2. M.J. Lahaye, S.M.E. Engelen, A.G.H. Kessels, A.P. de Bruïne, M.F. von Meyenfeldt, J.M.A. van Engelshoven, C.J.H. van de Velde, G.L. Beets and R.G.H. Beets-Tan. USPIO MRI in Nodal Staging of Patients with Primary Rectal Cancer: Predictive Criteria. Radiology 2008 Mar;246(3):804-11.
3. S.M.E. Engelen, R.G.H. Beets-Tan, M.J. Lahaye, A.G.H. Kessels and G.L. Beets. Location of involved mesorectal and extramesorectal lymph nodes in patients with primary rectal cancer: Preoperative assessment with MR imaging. Eur J Surg Oncol. 2008 Jul;34(7):776-81.
4. M.J. Lahaye, G.L. Beets, S.M.E. Engelen, A.G.H. Kessels, A.P. de Bruïne, H.W.S. Kwee, J.M.A. van Engelshoven, C.J.H. van de Velde and R.G.H. Beets-Tan. USPIO MR Imaging after Neoadjuvant Chemoradiation: Criteria for Predicting Involved Nodes in Rectal Cancer Patients. Radiology in press.

Acknowledgements / Dankbetuigingen

Vanzelfsprekend heb ik met veel genoegen dit proefschrift geschreven. Ik ben bevoorrecht geweest met de ondersteuning en medewerking van velen. Het is helaas onmogelijk om iedereen bij naam te noemen; een enorm aantal mensen hebben rechtstreeks of zijdelings bijgedragen aan dit proefschrift. Hoewel ik ook vele personen al persoonlijk heb bedankt, wil ik een poging wagen om zo compleet mogelijk te zijn.

Allereerst gaat mijn dank uit naar de honderden patiënten verspreid over heel Nederland, die terwijl ze in één van de donkere perioden van hun leven zaten, tijd noch moeite bespaarden om te participeren in ons onderzoek. Het contact met deze patiënten heb ik als zeer waardevol ervaren en als een sterke stimulans voor ons werk gezien.

Promotor Prof. dr. Regina Beets-Tan, was de inspirerende motor achter dit proefschrift. Onze samenwerking begon in 2003 toen ik, als co-assistent, je vroeg of ik, als zelfbenoemde radioloog-in-spé, bij jou onderzoek kon doen. Je introduceerde mij in de wondere wereld van de radiologie. Talloze uurtjes heb je, ook als iedereen allang naar huis was, de taak op je genomen om mij wetenschappelijk schrijven, MRI's beoordelen en nog veel meer bewust aan te leren. Die grote investeringen in mij beschouw ik als zeer waardevol. Ik heb nog nooit iemand ontmoet die met zoveel enthousiasme en niet aflatende inzet, zoveel bergen werk verzet als jij. Je bent een grote inspiratiebron voor mij omdat je altijd het onderste uit kan wilt hebben voor je research, patiënten en je collega's.

Promotor Prof. dr. Jos van Engelshoven, onze paden kruisten pas in uw nadagen als hoofd van de afdeling Radiologie. De oprechte interesse van u en uw vrouw hebben ervoor gezorgd dat ik mij thuis voelde op de afdeling. Uw doortastend commentaar heeft onze artikelen naar een hoger niveau getild.

Co-promotor Dr. Geerard Beets, vormde de onmisbare brug tussen kliniek en wetenschap. Ondanks uw ontzettend drukke schema, heeft u altijd tijd gemaakt om ons met uw mening te verblijden. Niet alleen uw klinische inzicht maakt u tot een zeer waardevolle co-promotor, maar ook uw tact, mensenkennis en wetenschappelijke visie waren essentieel voor onze multicenter studie.

Prof. dr. Cornelis van de Velde, uw imposant werk, de Dutch TME trial, was de

wetenschappelijke fundering van ons onderzoek. U heeft ons onderzoek altijd gesteund. Helaas hebben we door de afstand elkaar niet veel gezien, maar gelukkig hebben we dit per email goed kunnen oplossen.
Prof dr. Jan Wilmink, bedankt voor het aanvaarden van de rol van voorzitter van de beoordelingscommissie van mijn proefschrift. Het is voor mij een eer dat u op deze manier toch bij ons onderzoek bent betrokken.
De laatste jaren heb ik nauw samengewerkt met Sanne Engelen, mijn paranimf. Samen hebben we deze studie opgezet, lopende gehouden, opgeschreven en tot een goed einde gebracht. De lange, maar vooral gezellige werkweken van de afgelopen jaren waar wij bijna nooit meer dan 3 meter uit elkaar zijn geweest zijn voorbij gevlogen. Ik heb echt van onze samenwerking genoten. Je werkt hard en bent punctueel. Kortom een ideale collega. We hebben altijd eerlijk en open met elkaar gecommuniceerd; in mijn ogen de sleutel van ons samenwerkingssucces. Ik wens je dan ook veel succes bij je opleiding tot chirurg. Gezien jouw kwaliteiten en de hoge eisen die je aan jezelf stelt zal je ongetwijfeld een zeer goede chirurg worden.
Een multicenter studie staat en valt bij de lokale medewerking. Het liefst zou ik iedereen in een lange lofrede bij naam noemen. Het enthousiasme en inzet van velen was van cruciaal belang voor het verloop van deze studie. Het feit dat de studie zo voorspoedig is verlopen, geeft direct aan welk gigantisch werk ook jullie hebben verzet. Enorm bedankt! Wij hebben nauw samengewerkt met de afdelingen Radiologie, Chirurgie en Pathologie van het Viecuri Medisch Centrum voor Noord-Limburg, het Laurentius ziekenhuis in Roermond en het St. Jans Gasthuis in Weert. Dank aan de radiologen Dr. Post, Bilderbeek, Opdenakker en Dohmen. Jullie hebben enorm veel (scan)tijd in dit onderzoek gestoken. Het feit dat jullie de radiologie zo goed in de vingers hebben zorgden voor mooie resultaten. Natuurlijk gaat mijn dank ook uit naar de chirurgen Dr. Konsten, van Berlo, Nijhuis, Estourgie, Rongen, Leijtens, Jansen en Verkooijen. Ook wil ik even stilstaan bij de inmiddels overleden chirurg Dr. Joop Debets, die ons enorm geholpen heeft de multicenter studie in Roermond op te zetten. Ik ben hem erg dankbaar voor zijn enthousiaste medewerking. Ik wens zijn naasten veel sterkte bij het verwerken van dit enorme verlies.
Dr. Willig en Dr. Kwee, beide pathologen, hebben ons meerdere keren geholpen als we op zoek waren naar die "ene klier". Eigenlijk waren alle radiologen, chirurgen,

pathologen, arts-assistenten, laboranten en verpleegkundigen die zich hebben ingezet voor onze studie in de participerende ziekenhuizen simpelweg onmisbaar.
Maar laten we onze thuisbasis, het MUMC, niet vergeten. We konden op veel steun rekenen binnen de afdelingen radiologie, chirurgie, MDL, pathologie en het onderzoeksinstituut GROW. Een speciaal woord van dank voor de arts-assistenten van de pathologie waar wij letterlijk uren en uren samen rectum preparaten hebben uitgesneden. De samenwerking met jullie had een ideale mix; goed precisiewerk met een lach. Ook binnen de radiologie hebben een verscheidenheid aan mensen met ons mee gedacht. Roy Vliegen en Allette Daniels-Gooszen waren in het begin van de studie een grote steun. Later hebben Frans Bakers en Vincent Cappendijk dat stokje feilloos overgenomen. Ik mag mij gelukkig prijzen met zulke capabele radiologen in de staf Radiologie. Ik weet dat ik nog heel veel van jullie ga leren. Ook wil ik Adriaan de Bruïne, Rob Jansen, Marc Bemelmans, Cees de Jong, Danielle de Haas-Kock, Ronald van Dam en Christiaan Hof bedanken voor hun steun en de leerzame maar ook zeer leuke momenten op congressen en multidisciplinaire besprekingen.
We hebben ons best gedaan het balie personeel van de radiologie en de MRI laboranten zo min mogelijk te terroriseren; dat is niet altijd gelukt... Bedankt dat jullie bijna altijd een spoedplekje voor ons konden regelen! Etienne Lemaire en Henk Schoenmakers bedankt voor de hulp met de MR-protocollen. Het secretariaat Radiologie vormden probleemloos onze gezellige administratieve life-line met de vakgroep Radiologie. Ook een blijk van dank aan Frans, Arno, Marc G. en Herman, ze hebben ons meerdere keren uit de digitale brand geholpen.
Fons Kessels, je stond/staat altijd voor me klaar als ik weer eens binnen kwam vallen en alles meteen geregeld wilde hebben. Je kritische blik hebben enorm bijgedragen aan de artikelen die we samen hebben geschreven. Het feit dat we ook lang over andere zaken dan statistiek konden praten heb ik zeer zeker gewaardeerd. Ook wil ik graag Patty Nelemans bedanken voor alle statistische hulp tijdens mijn eerste artikel (hoofdstuk 2).
Prof. Dr. Joachim Wildberger, ons nieuw afdelingshoofd van de Radiologie, hoewel het proefschrift al ver vergevorderd was toen u ons kwam versterken, heeft u toch nog met uw nieuwe inzichten kunnen bijdragen aan dit proefschrift. Ik hoop dan ook op een prettige samenwerking in de toekomst.
Ons rectumteam is natuurlijk niet compleet zonder Elleke Dresen. Heel leuk dat we onze promotiedag samen kunnen combineren. Dat we ook samen in opleiding zijn

maakt het allemaal alleen maar nog leuker. Ik verheug mij dan ook op de komende jaren.
Zo kom ik bij de "nieuwe" aanwinsten van het rectumteam Doenja Lambregts en Monique Maas. Ik ben blij met zulke goede opvolgers. Ik ben benieuwd welke interessante ontdekkingen we samen nog gaan doen.
Een blijk van dank ook aan mijn collega's op de "werkvloer" en speciaal: Suzanne, Nils, Marlies, Jos, Jaap, Mark L., Robbert-Jan, Carolien, Rianne, Frank, Walter, Eline, Gerrit en Dave. Robbert N., je hebt een geweldige drive zowel op het werk als op de golfbaan. Jammer dat je al zo snel klaar was met je promotie!

Johan, ontzettende paranimf, we hebben maar weinig woorden nodig om elkaar te begrijpen. Je bent een echte vriend, zoals Plutarchus het bedoelt heeft. Ook Maarten S. en Freek horen zeker in dit rijtje thuis. Ik mag mij gelukkig prijzen met zulke goede vrienden met hun aanstekelijke enthousiasme voor de medische wetenschap.
Mijn lieve ouders, Peter en Renée, jullie liefdevolle opvoeding, onvoorwaardelijke steun en vertrouwen, hebben mij staat gesteld dit proefschrift met zoveel plezier te schrijven.
Liza, grote zus van me, jij verstond me al voordat ik kon praten. Wat moet ik hier dan nog opschrijven? Fantastisch dat we allebei een wetenschappelijk pad volgen. We gaan zeker een artikel samen schrijven. Ik kijk nu al uit naar jouw promotiefeest!
Lieve Henrike, jouw impact op mij, en dus ook dit proefschrift, laat zich niet vangen in enkele regels van simpel zwart inkt. Je mooie glimlach relativeert moeiteloos, binnen een fractie van een seconde, de meest drukke dag. Ik ben ontzettend trots op ons en ik verheug me dan ook op onze toekomst samen.